UCL Université catholique de Louvain

Faculty of Bioengineers

Effects of silver nanoparticles on oxidative stress and Nrf2 pathway in an *in vitro* model of intestinal epithelium cells

Presented by Audrey Leurquin

Jury composition:

Promotor:	Emeritus Professor Yves-Jacques Schneider (UCL/IBST)
Co-promotor:	Professor Melissa Page (UCL/IBST)
Lectors:	Professor René Rezsöhazy (UCL/IBST)
	Assist. Professor Konstantinos Grintzalis (DCU)

Graduation thesis submitted for the obtention of the Bioengineer diploma: agronomical sciences

AGRO LOUVAIN

Academic year : 2017-2018

Acknowledgments

First of all I would like to thank my promoter, Yves-Jacques Schneider, for his precious advice, guidance and knowledge. Thank you also for your availability throughout this thesis and during its drafting despite your busy schedule.

My special thanks go to Madeleine Polet who supervised and guided me throughout this year and without whom this master's thesis would not have been possible. Thank you Madeleine for your patience and kindness as well as for your help and relevant advice during the writing of this thesis. Many thanks also to Laurie Laloux for always being available when I had questions or doubts.

I would also like to express my gratitude to Melissa Page, René Rezsöhazy and Konstantinos Grintzalis for having accepted to be part of my jury and taking the time to evaluate this work.

My thanks also go to all members of the BNTE lab for their warm welcome and integration into their team after the change of lab.

Warmest thanks to my family and friends for their infallible support and encouragement during this work as well as throughout my studies. Special thanks to Donika Kastrati, a very good friend to whom I could confide and share unforgettable moments at the lab.

Finally, I thank all the people who helped, one way or another, to the realisation of this thesis.

Abstract

Considering the very interesting physicochemical properties of nanomaterials, it is not surprising that during the last few years, nanomaterial applications expended exponentially. Among nanoparticles, silver nanoparticles (AgNPs) are the most commonly used in consumer products, mainly because of their antimicrobial properties. AgNPs are already incorporated in many products of the food sector such as food packaging materials, antimicrobial sprays and even dietary supplements. These applications could lead to abnormally high oral exposure for the consumer.

Many authors have demonstrated AgNPs toxicity towards various biological systems. Furthermore, there is still a huge lack of knowledge concerning the mechanisms of toxicity related to AgNPs and the contribution of Ag^+ involved in AgNPs toxicity. Therefore, this work was devoted to study AgNPs and Ag^+ effects on oxidative stress and the related cellular responses. In order to do so, monocultures of Caco-2 cells were used. They are indeed a widely used *in vitro* model of the human intestinal epithelium.
First of all, the ability of AgNPs and Ag^+ to generate reactive oxygen species (ROS) and induce oxidative stress was evaluated by performing an NBT assay. A significant increase in ROS production was observed for both AgNPs and Ag^+ with a nano-specific effect. The second part of this thesis was to determine the impact of AgNPs on enzymatic activity of several oxidative stress-related enzymes (CAT, GR, GP and GST). Unfortunately, we were not able to detect any significant changes in these enzymatic activities after 3h incubation with 15 µg/ml AgNPs. Thirdly, we studied the impact of AgNPs/Ag^+-induced ROS generation on Nrf2 signalling pathway by performing an ELISA quantification of HO-1, which is an Nrf2 specific gene target. Nrf2 is the major pathway involved in protecting cells from oxidative stress, through the induction of antioxidant-responsive genes. Surprisingly, we did not measure any significant effect on HO-1 production.
Finally, the effect of AgNPs on inflammation was evaluated, along with the potential implication of the Nrf2 signalling pathway. Indeed, preliminary work at the lab indicated that the pro-inflammatory response related to AgNPs was not due to activation of the NF-κB pathway. The alternative Nrf2 pathway was therefore studied to explain the production of the inflammatory marker IL-8 measured by ELISA. According to our results, Nrf2 does not seem to be involved in IL-8 production following AgNPs treatments.

In conclusion, although AgNPs were not cytotoxic at the studied concentrations, we have observed an increased ROS production. Numerous studies confirm our results regarding ROS production, but in contrast to our observations, suggest the implication of the Nrf2/HO-1 signalling pathway to explain the cellular responses related to the AgNPs-induced ROS production. Furthermore, AgNPs seem to induce a pro-inflammatory response through IL-8 upregulation. However, it remains unclear which pathways are involved.

Table of contents

Acknowledgments ..... **I**

Abstract ..... **II**

Table of contents ..... **III**

List of figures ..... **IV**

List of abbreviations ..... **V**

Part I: Introduction **1**

1. Nanotechnologies **1**

1.1. Sources of nanometer sized particles 1

1.2. Definition of nanomaterials 2

1.3. General properties of NPs 3

1.4. Sectors of application 4

1.5. Risk exposure to AgNPs 5

1.6. Sources of ingested NPs 6

1.7. Release of AgNPs and Ag^{+} from food packaging 9

2. The gastrointestinal tract **10**

2.1. General overview 10

2.2. Histological structures of the small intestine 11

2.3. *In vitro* model of the intestinal barrier 14

2.4. Fate of ingested NPs 17

2.5. Release of Ag^{+} by AgNPs 19

3. Mechanism of toxicity **23**

3.1. AgNPs induced oxidative stress 23

3.2. Cellular response against oxidative stress 24

3.3. Cellular damage resulting from oxidative stress and AgNPs 25

3.4. The Keap1-Nrf2 signalling pathway 26

3.5. Interleukins-8 and 6 (IL-8 and IL-6) 28

Part II: Material & methods **30**

1. Cell culturing **30**

1.1. Flask culturing 30

1.2. Subcultures 31

1.3. Plate culturing 32

1.4. Transwell™ polycarbonate inserts 33

2. Chemicals **34**
2.1. Silver nanoparticles 34
2.2. Silver nitrate 34
2.3. *In vitro* inflammatory cocktail 34
3. Assays on fully differentiated Caco-2 cells **35**
3.1. Nitro Blue Tetrazolium salt (NBT) assay 35
3.2. Enzymatic tests 36
3.3. HO-1 quantification 38
3.4. IL-8 and IL-6 quantification 41
3.5. Transepithelial electric resistance (TEER) 43
4. Statistical analysis **44**
Objectives **45**
Part III : Results **46**
1. AgNPs and Ag^+ solutions 46
2. Nitro Blue Tetrazolium salt (NBT) assay 47
3. Enzymatic tests 49
4. HO-1 quantification 49
5. IL-8 and IL-6 quantification 54
6. Transepithelial electrical resistance (TEER) 57
Part IV: Discussion **59**
1. AgNPs-induced oxidative stress 60
2. Enzymatic activity 61
3. HO-1 as Nrf2 gene target 63
4. AgNPs, ROS and inflammation 65
Part V: Conclusion and perspectives **67**
References **69**
Abstract **79**

List of figures

Figure 1: Common sources of NPs in the environment. 1
Figure 2: Relationship between primary NPs, aggregation and agglomeration. 3
Figure 3: Various applications and properties of AgNPs. 4
Figure 4: Potential exposure pathways from the expected normal use of consumer products, grouped by major NMs composition categories. 6
Figure 5: Applications of nanotechnology in the food industry. 8
Figure 6: Organisation of the digestive system 10
Figure 7: Large circular folds, villi and microvilli of the small intestine. 11
Figure 8: Organisation of the intestinal wall 12
Figure 9: Different cell types found in the intestinal epithelium 13
Figure 10: *In vitro* cell models 16
Figure 11: Illustration of a transwell™ insert system. 16
Figure 12: Fate of food-related ENMs in the GIT. 17
Figure 13: Schematic illustration of possible consequences arising from NP incubation in physiological fluids 18
Figure 14: Schematic illustration and characteristics of hard and soft coronas. 18
Figure 15: Representation of Ag^{+} release from AgNPs 20
Figure 16: Schematic representation of the predicted processing of AgNPs in the human stomach .. 21
Figure 17: Particle transport across epithelial cells. 21
Figure 18: Schematic transverse sections of a Peyer's patch lymphoid follicle and overlying (FAE) follicle-associated epithelium (A) Specialised antigen sampling M cells (B) 22
Figure 19: Possible uptake process and mechanism of cytotoxicity induced by AgNPs 23
Figure 20: Complete and incomplete reduction of molecular oxygen: production of specific reactive oxygen species by single electron additions 23
Figure 21: Representation of the relationship between antioxidant enzymes, GSH and GSSG. 24
Figure 22: Proposed mechanism of nanosilver toxicity 25
Figure 23: Molecular mechanisms of the Keap1–Nrf2 pathway in stress response 26
Figure 24: Glutathione synthesis 27
Figure 25: Heme oxygenase-1 pathway and resulting bioactive products 28
Figure 26: AgNPs toxicity through amplification loops between oxidative stress and inflammation .. 29
Figure 27: Culture flask with 75 cm2 growth area, containing culture medium. 30
Figure 28: Side view of the hemocytometer counting chamber 31
Figure 29: (A) Haemocytometer grid visualised under the microscope consisting of 9 large squares (B) Counting system to ensure accuracy and consistency. 32
Figure 30: 24-well plate for cell culturing with culture medium. 33
Figure 31: Schematic illustration of a Transwell^{TM} insert 33
Figure 32: NBT assay reaction and formation of a blue compound. 36
Figure 33: Representation of the timeline for enzymatic tests 36
Figure 34: Organisation of the different treatments for the HO-1 assay. 39

Figure 35: Enzyme linked immunosorbent assay (ELISA) principle. 39
Figure 36: LDH detection mechanism 40
Figure 37: BCA protein assay principle. 40
Figure 38: BCA calibration curve allowing the determination of protein concentration in samples.... 41
Figure 39: Different treatments applied on Transwell™ inserts. 42
Figure 40: (A) Measurement of the transepithelial electrical resistance in Caco-2 cells located in transwell^{TM} inserts (B) Epithelial voltohmmeter equipement..... 43
Figure 41: Different positive controls tested for the NBT assay. 48
Figure 42: NBT assay results for AgNPs and Ag^{+} treatments..... 48
Figure 43: Potential HO-1 activators: MG-132 and tBHQ 51
Figure 44: LDH cytotoxic assay for the different positive controls 51
Figure 45: HO-1 quantification after exposure to different concentrations of trigonelline and in conditions of pre-or co-incubation 52
Figure 46: HO-1 ELISA quantification after 3h treatment with: HBSS, AgNPs, tBHQ or Cocktail and with or without a 1h pre-incubation period with trigonelline. 53
Figure 47: HO-1 ELISA quantification after 3h treatment with: HBSS, Ag^{+}, tBHQ or Cocktail and with or without a 1h pre-incubation period with trigonelline..... 53
Figure 48: Secreted IL-8 contents after 3h incubation for each treatment.. 55
Figure 49: Secreted IL-8 contents after 21h recovery period for each treatment.. 56
Figure 50: Transepithelial electrical resistance (TEER) values after 3h incubation with different treatments.....57

List of abbreviations

AB: antibody
AG: antigen
Ag^+: silver ion
AgCl: silver chloride
AgNO3: silver nitrate
ANOVA: ANalysis Of Variance
AP-1: activator protein-1
AgNPs: silver nanoparticles
ARE: antioxidant response element
ARN: ribonucleic acid
ATP: adenosine triphosphate
BCA: bicinchoninic acid
BSA: bovine serum albumin
CAT: catalase
CuOOH: cumen hydroperoxide
DNA: deoxyribonucleic acid
DMEM: dulbecco modified Eagle's minimal essential medium
DMSO: dimethyl sulfoxide
ELISA: enzyme linked immunosorbent assay
ENM: engineered nanomaterials
FAD: flavin adenine dinucleotide
FAE: follicle associated epithelium
FBS: fetal bovine serum
GALT: gut-associated lymphoid tissue
GCL: glutamate-cysteine ligase
GIT: gastrointestinal tract
GP: glutathione peroxidase
GR: glutathione reductase
GSH: glutathione
GSSG: glutathione disulfide
GST: glutathione S-transferase
HO-1: heme oxygenase 1
H_2O_2: hydrogen peroxide
HBSS: Hank's balanced salt solution
IFN: interferon
ILs: interleukins
Keap1: Kelch ECH associating protein 1
LDH: lactate dehydrogenase
LPS: lipopolysaccharides
M-cell: microfold cell
NAC: N-acetyl-L-cysteine
NAD(P)H: nicotinamide adenine dinucleotide (phosphate)
NaOH: sodium hydroperoxide
NBT : nitro blue tetrazolium
NEAA: non essential amino acids
NF-κB: nuclear factor κB
NPs: nanoparticles
NQO1: NAD(P)H quinone oxidoreductase 1
Nrf2: nuclear factor erythroid 2–related factor 2
$O_2^{\cdot -}$: superoxide anion
$OH^{\cdot}$: hydroxyl radical
PBS: phosphate buffer solution
PI3K: phosphatidyl inostitol 3-kinase
RIPA: radioimmunoprecipitation assay
ROS: reactive oxygen species
SD: standard deviation
SEM: standard error of the means
SOD: superoxide dismutase
tBHQ: tert-Butylhydroquinone
tBuOOH: tert-Butylhydroperoxide
TNFs: tumor necrosis factor

Part I: Introduction

1. Nanotechnologies

1.1 Sources of nanometer sized particles

We have been exposed to nanometer sized particles for many ages. Indeed, nanoparticles (NPs) can be found everywhere in our environment because there are a variety of sources of NPs (Fig. 1). Firstly, naturally occuring NPs are the ones produced by volcanic fumes and other geological phenomena (Smita *et al.*, 2012).

Anthropogenic NPs compose the second category and are the ones formed during events involving human intervention. They can either be produced accidentally by humans or intentionally for their new properties (Lanone & Boczkowski, 2010).

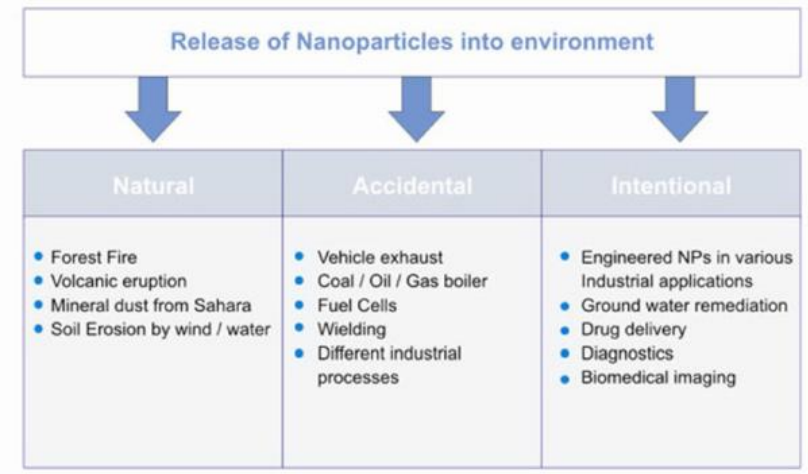

Figure 1: Common sources of NPs in the environment (Smita et al., 2012).

Naturally occurring NPs can be found in animals, plants as well as from geological origin (Rauscher *et al.*, 2014). Indeed, within the nanoscale, we can name the proteins, DNA (diameter of the double helix) but also many viruses. An example in the animal kingdom is that of insects. They have nanostructures in their eyes (corneal nipples) enabling them to absorb light more efficiently. The nanoscale nipple pattern on moth eyes has inspired new anti-reflective coatings for solar cells. Another surprising example are nanoscaled chitin multilayers in butterfly wings that can scatter light, acting as a diffraction grid and inducing iridescence (Shahan, 2012).

Similarly, plants have been an inspiration for the creation of new surfaces and films. The most known example is the wax nanocrystals present in the lotus leaves providing a hydrophobic water-repellent layer (Leydecker, 2012). This property has been used to create self-cleaning surfaces and even paints (StoColor Lotusan, 2018).

The last source of naturally occurring NPs is through geological phenomena. Earth's crust, oceans and atmosphere are considered as the largest distributors of naturally occurring NPs. Aerosols coming from dust storms, volcanic emissions and forest fires are the largest source of environmental NPs (Smita *et al*., 2012).

Accidental nanomaterials are usually described in the literature as by-products occurring as a result of combustion or industrial processes. We can distinguish three major sectors producing these unwanted particles (Lanone & Boczkowski, 2010):

- industrial sector: construction, demolition, processing of concrete and mining;
- transport sector: diesel and engine exhaust produced by incomplete combustion;
- domestic activities: cooking, coal/oil/gas boiler, heating, domestic biomass burning, smoking and also municipal waste incineration.

Lastly, engineered nanomaterials (ENMs) are intentionally produced nanomaterials for their special properties. ENMs present great opportunities for industrial growth in many different sectors of the society.

Nanotechnology is a rapidly evolving field, production volumes and market applications are strongly increasing. Analysts expect that markets will grow considerably in the near future. This could be worrying because it is inevitable that during the use of the related products, ENMs are released in the air, water and soil. Since the annual release of ENMs into the environment cannot be accurately estimated, concerns are raising about their impact on the environment and human health (Smita *et al*., 2012). Therefore, the development of risk assessment programs has become a task of a great relevance. This master thesis will be exclusively devoted to ENMs and especially to silver nanoparticles (AgNPs).

1.2 Definition of nanomaterials

There are plenty of different definitions for nanomaterials but the most widely used is probably the definition formulated by the European Commission. They defined the term 'nanomaterials' in an attempt to create a uniform interpretation for identifying materials using particle size as the only metric. The definition is used to classify materials as a 'nanomaterial' for legislative and policy purposes (Rauscher *et al*., 2014). The EC wanted the definition to achieve consistent application across all legislation (Bergeson & Hutton, 2017).

The European Commission recommends since October 2011 the following definition of the term 'nanomaterial' (2011/696/EU).

"*A nanomaterial is a natural, incidental or manufactured material containing particles, in an unbound state or as an aggregate or as an agglomerate and where, for 50 % or more of the particles in the number size distribution, one or more external dimensions is in the size range 1 nm- 100 nm.*"

The recommendation further specifies the following terms: 'particle', 'agglomerate' and 'aggregate' (Fig. 2).

(a) 'particle' is a minute piece of matter with defined physical boundaries; (b) 'agglomerate' is a collection of weakly bound particles or aggregates where the resulting external surface area is similar to the sum of the surface areas of the individual components; (c) 'aggregate' is a particle comprising of strongly bound or fused particles.

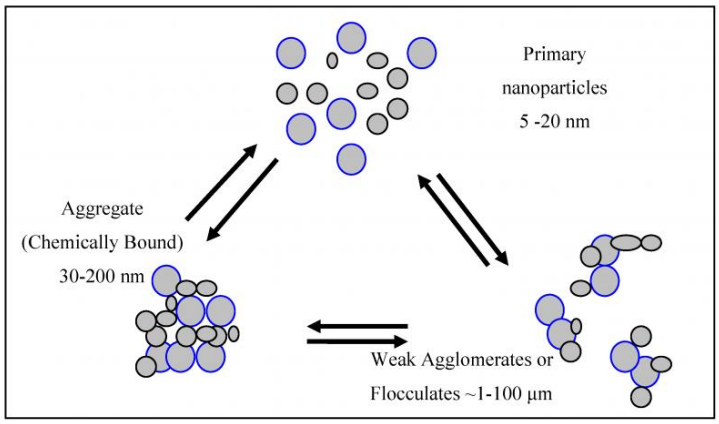

Figure 2: Relationship between primary NPs, aggregation and agglomeration (Egerton, 2014).

According to the International Organisation for Standardization (ISO), a nanoparticle can be defined as a nano-object with all three external dimensions in the nanoscale. The latter being the size range going from approximately 1 nm to 100 nm.

1.3 General properties of NPs

NPs are engineered for their special properties. Complete characterization of NPs may include measurements of size distribution, shape, solubility, surface area, state of dispersion, surface chemistry, and other physico-chemical properties (Park *et al*., 2011).

Because of their small size and the very high surface to volume ratio, NPs usually have a very elevated reactivity potential as well as new properties (Nel *et al.*, 2006). NPs are situated at a bridge between bulk materials and atomic or molecular structures. Therefore, their physicochemical features differ substantially from those of their respective bulk materials (Smita *et al*., 2012). They have exceptional features such as increased strength, chemical reactivity, conductivity and optical sensitivity. Furthermore, while bulk materials have constant physical properties regardless of their size, nano-scale sized particles often have size-dependent properties. NPs have a large proportion of energetically unstable atoms on their surface that are readily available for reaction (Buzea *et al*., 2007).

Although these new properties seem very interesting at first glance, we should question the safety of these particles when they come into contact with biological systems and the environment. They could lead to possible undesirable results and harmful interactions, with the potential to generate toxicity. This is all the more worrying given that their small size confers greater particle mobility both in the environment and the body (Buzea *et al.*, 2007).

Furthermore, once NPs are released in the environment, very little is known about their fate. It has already been proven that NPs have the ability to accumulate in various environmental matrices (e.g., air, water, soil and sediments) but also in various organisms such as blue and green algae, fish and others (Smita *et al*., 2012).

1.4 Sectors of application

Since NPs have unique physical and chemical properties, it is not surprising to find them in various areas of society such as in electronics, medicine, textiles, health care, food, agriculture, cosmetics and many others (Chen & Schluesener, 2008).

Nanomaterials are increasingly incorporated into consumer products. In 2014, 1814 products containing nanotechnology are already available in the market were archived. These products can be grouped under eight different consumer goods categories: goods for children, appliances, food and beverages, electronics, cross-cutting, automotive, home and garden and finally health and fitness. This last category includes the largest listing of products with nanotechnologies (42% of the listed products) especially in the subcategory of personal care products, which includes products such as toothbrushes, lotions and hairstyling tools (Vance *et al*., 2015).

On a mass basis, titanium dioxide (TiO_2), silicon dioxide and zinc oxide are the most produced nanomaterials worldwide. While the annual global production of AgNPs is estimated at 320 tons, representing only 2% of the annual production of titanium dioxide, they are the most widely used in terms of the number of products containing these particles. The reason for this popularity is their well-documented antimicrobial properties.

Some more specific applications for AgNPs are represented on figure 3. Due to its strong antibacterial activity, nanosilver is included in various consumer products: cosmetics, health care, water disinfectants, drug carrier, textiles, room sprays, food packaging materials, food supplements but also medical devices.

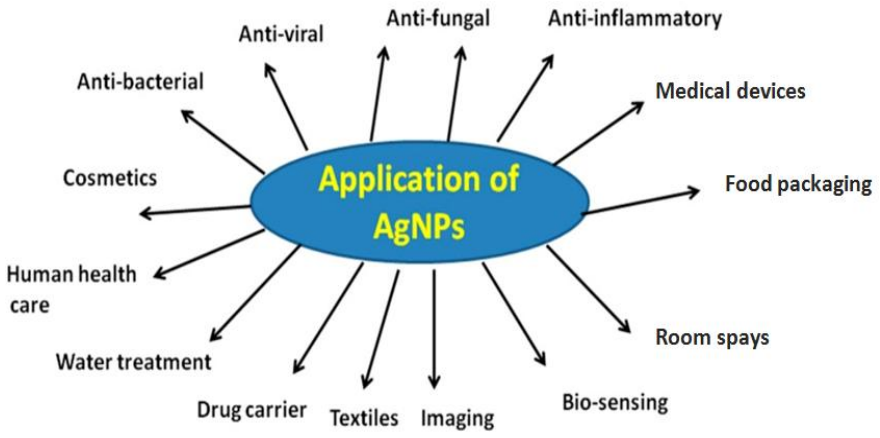

Figure 3: Various applications and properties of AgNPs (Zhang *et al*., 2016).

1.5 Risk exposure to AgNPs

The assessment of exposure to silver nanomaterials in consumer products is very complex. Indeed, consumer risk exposure depends on the formulation, application and route of exposure of products containing nanosilver. For each product these criteria vary and have to be evaluated to assess the potential risk of exposure (Table 1).

The exposure depends first of all on the characteristics of formulation such as the concentrations of AgNPs in the product, the size and form in which it is present (free particles, aggregates, agglomerates or coating) but also the possibility for release or leakage of AgNPs or Ag^+ from the product. Unfortunately, the availability of these data is very limited at the moment. The reported levels of silver release from consumer products are non consistent from one study to another, this is probably due to differences in the methodology used. Another very important characteristic of formulation is the way the nanomaterials are incorporated into the product. Free NPs are released more quickly than NMs that are integrated into larger structures or fixed in a matrix (SCENIHR, 2009).

Concerning the application of the products, the most critical feature is whether the release of AgNPs occurs through direct contact (liquids and spray) or indirect contact via leaching of particles out of the product. Products containing free NPs with direct human exposure are considered to have the highest potential risk (e.g. food supplements or sunscreen products). Apart from that, event duration and frequency can also be taken into account. Finally, the route of exposure is also very important for the risk assessment. Inhalation via sprays for example is considered to have the highest risk followed by oral exposure (food supplements or leaching from food packaging) and finally dermal exposure (cosmetics and personal care products). Interestingly, inhaled NPs can end up in the GIT through mucosal clearance. In other words, oral exposure can also be a consequence of inhalation.

Table 1: Characteristics to determine AgNPs risk exposure (adapted from SCENIHR, 2009).

Formulation	• concentrations of AgNPs in the product • size of NPs and form in which it is present • probability of release of AgNPs or Ag^+ from the products • location of the nanomaterial in the products (free particles/ particles fixed in a matrix)
Application	• direct contact (e.g. liquids, sprays); indirect contact (release NPs during wear and tear) • event duration • frequency of event
Exposure route	• inhalation • dermal • oral

When we look at the number of products within each type of exposure pathway, we can see that the most represented category is exposure through dermal contact, especially for metal NPs (Fig 4). Indeed, many applications consist of a solid products containing NMs on their surface or liquid products with NMs suspensions that are meant to be applied on the skin (cosmetics). The second most frequent route of exposure is through inhalation of NPs (sprays). Finally, 16% of the products contain NPs that may be ingested (e.g. food supplements, additives).

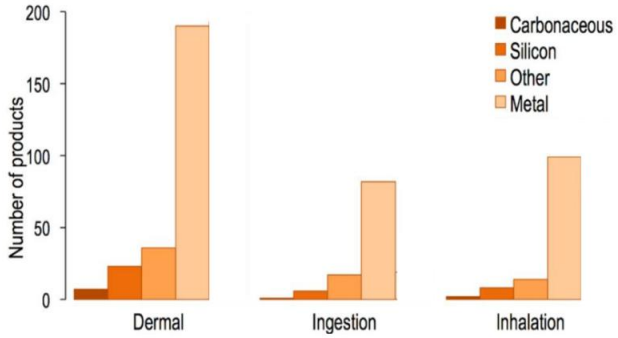

Figure 4: Potential exposure pathways from the expected normal use of consumer products, grouped by major NMs composition categories (Vance *et al.*, 2015).

1.6 Sources of ingested NPs

Nanotechnologies are applied throughout all phases of food production, thus covering many aspects, such as food security, disease treatment, packaging materials, delivery systems, bioavailability and new materials for pathogen detection (Bouwmeester *et al.*, 2009).

NPs have a wide range of benefits to the food sector including: new tastes, textures and sensations, improved nutritional value, increased absorption and bioavailability of nutrients, improved packaging, traceability and security of food products (Chaudry *et al.*, 2008). Food production can be divided in three different categories: agricultural production, food processing and food preservation and packaging.

Agricultural production

NPs can be used in pesticides (nano-sized agro-chemicals) to increase efficiency compared to conventional formulations. Consequently, residues of these products might be present on food products and be ingested by consumers (Sekhon, 2010).

Another application is the use of NPs for water cleaning purposes. Aluminum oxide NPs can adsorb pollutants and are therefore used for water remedia tion methods (Ravindhranath & Ramamoorty, 2017). Studies have also shown that nanoscaled iron particles are very effective for the detoxification of environmental contaminants and can be used for environmental remediation. These NPs are then found in the environment and contamination of the crops cannot be excluded, resulting in potential consumer exposure (Bouwmeester *et al.*, 2009).

Food processing and functionalized foods (Fig 5.)

Nanotechnologies are applied in food production tools and machinery as coatings or as nano-sieves for the filtration of beer or milk for example (Sekhon, 2010). Carry-over of NPs to food is expected to be negligible for food processing applications (Chaudry *et al*., 2008).

NPs can also be found inside food products as food additives or ingredients. Nanostructured food ingredients appear on the markets with the claims that they offer improved taste, texture, color and consistency. We can find low-fat nanostructured mayonnaise or ice creams that are supposed to be as ‘‘creamy’’ but less calorific as their alternatives (Sekhon, 2010).

Concerning inorganic food additives, the permitted ones are: silicon dioxide, magnesium oxide and titanium dioxide. Silver is being increasingly marketed as a health supplement and taken orally as aqueous dispersions of colloidal silver. While colloidal silver has been banned since 2010 as a food supplement in the European market, it remains available on the web (Chaudry *et al*., 2008).

Another major area of functionalized food is through nanodelivery systems for bioactive compounds. Nanodelivery encompasses different techniques such as nanoencapsulation, nanoemulsion, nanoliposomes and many others. With nanoencapsulation, food additives (polyphenols, vitamins, antioxidants and other bioactive compounds) are entrapped into nanostructures for various purposes. Most frequently they are made in order to improve their bioavailability by enhancing their solubility, protecting these bioactive components against destructive environment of the digestion process and elevating the permeation in small intestine (Katouzian & Jafari, 2016; Hu *et al.*, 2017).

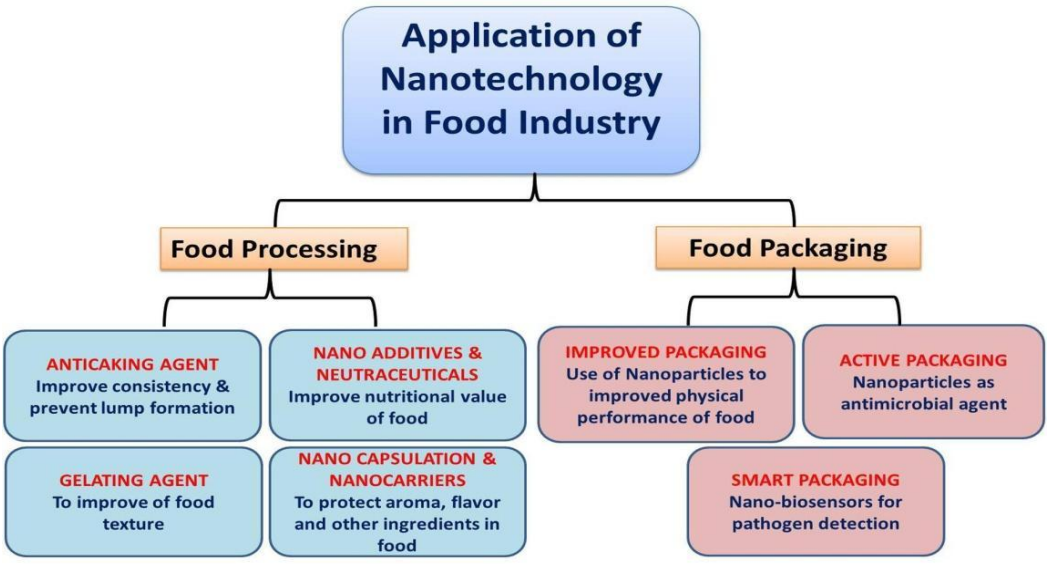

Figure 5: Applications of nanotechnology in the food industry (Trepti *et al*., 2017).

Preservation and packaging (Fig 5.)

NPs can be integrated in food contact materials for many purposes (Fig 5):

- to **lengthen shelf-life**: this will be the most important application of nanotechnologies in the food area for the future (Chaudhry *et al*., 2008).
- to **improve packaging properties**: flexibility, mechanical strength, gas barrier properties, moisture stability, thermal resistance and recycling properties. (e.g., silicate NPs, nanocomposites, magnesium- and zinc-oxide) (Trepti *et al*., 2017).
- use of **"active" packaging** releasing NPs with antimicrobial functions into the food. Nano- sized metals, especially silver, inhibit the growth of microorganisms allowing longer preservation. They are also incorporated in domestic refrigerators, kitchenware and tableware to prevent microbial growth (Trepti *et al*., 2017).
- **''Intelligent'' food packaging** consitisting of incorporating nanosensors to report the condition of the food and thus ensuring food safety and traceability throughout transport and storage. Nanosensors are able to monitor changes in temperature, pH, moisture, gas composition, contamination/spoilage by microorganisms and detect the presence of degradation products of the food commodities (Fuertes 2016). These changes are detected by the indicators and transformed into a response, usually through colorimetric indicators, which can be easily measured and correlated with the freshness of food (Carbone *et al*., 2016).

1.7 Release of AgNPs and Ag^+ from food packaging

The global market for active and intelligent packaging has an annual growing rate of 8% and will probably double between 2011 and 2021 (Fuertes *et al*., 2016). The main risk of this new packaging is unwanted contamination of the food. Indeed, since the food is in direct contact with NPs, migration into the food cannot be excluded. Actually, nanosilver from 'active' packaging must migrate to the food surface to some extent in order to be effective and improve shelf-life. Therefore a compromise must be made between the level of migration and the antimicrobial activity (Fernandez *et al*., 2010). In the EU, EFSA provided an upper limit of Ag migration from food packaging. Recommendations are not to exceed 50 µg Ag/kg in food (EFSA, 2009).

Several studies demonstrate the migration of silver present in food packaging materials, to the food itself. This migration is affected by multiple factors including (i) temperature, (ii) duration of exposure, (iii) concentration gradient, (iv) position of the NPs in the packaging material, (v) interaction between the nanoparticle and the material and (vi) the nature of the food (Roger & Hagen, 2016). The highest migration of silver was observed for the acidic food simulant and reached the value of 5.7 µg Ag/kg, which is still below the maximum migration limits stated by the EU legislation. Silver release occurred predominantly in ionic form, but AgNPs were also released (12%). After the first contact with food stimulants (repeated use), silver migration decreased considerably (Goetz *et al.*, 2013). In another study, researchers suggested that this silver release was due to two different migration mechanisms. The first one being the release of free AgNPs and Ag^+ from the coatings. The other mechanism is the oxidative dissolution of AgNPs into Ag^+ (Echegoyen & Nerín, 2013). Even though the majority of the migration studies found levels of migration of ionic silver below the EU specific migration limit of 50 µg Ag/kg food, there are also several studies, in which migration exceeded this limit. This indicates that new food packaging products containing nanosilver must be studied individually. There is also a need to investigate the impact on health following chronic exposure to these AgNPs (Addo *et al.* 2015).

Since AgNPs are widely used throughout the food sector, they can therefore be ingested and come into contact with our intestinal cells. Because of the fact that only few studies describe the effects of AgNPs on the intestinal epithelium, we chose to investigate the impact of AgNPs on an *in vitro* model of intestinal cells.

2. The gastrointestinal tract

2.1 General overview

The gastrointestinal tract is an organ system that performs the main stages of food processing: ingestion, mechanical, chemical and enzymatic decomposition into absorbable size molecules and finally the elimination of remaining waste by feces (Campbell *et al*., 2012). It extends from the mouth to the anus and includes successively oesophagus, stomach, small intestine and large intestine. The complete human digestive system also takes into account the accessory organs of digestion: tongue, salivary glands, pancreas, liver and gallbladder (Fig. 6) (Raven *et al.*, 2014; Ciappellano, 2016).

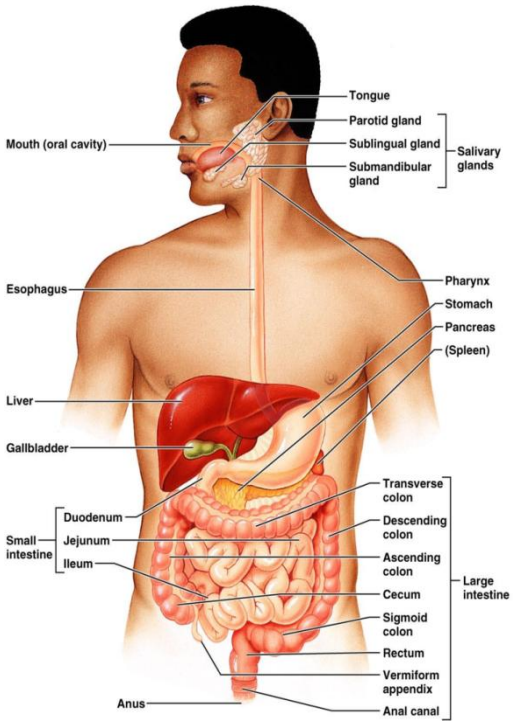

Figure 6: Organisation of the digestive system (Cummings, 2006).

The major feature of the small intestine is its huge absorption surface caused by numerous folds, villi and microvilli. The small intestine is composed of three parts: the duodenum, the jejunum and finally the ileum. The first section, the duodenum, is a short structure of 20-25 cm long. Its main function is to receive the chyme from the stomach together with pancreatic juice and biliary secretions. Thanks to the secretions of the accessory glands but also to the secretions of the intestinal wall itself (mucus, bicarbonate, digestive enzymes), most of the enzymatic hydrolysis of food is carried out in the small intestine. The digestive enzymes break down proteins and carbohydrates while bile emulsifies fats into micelles that can be partially hydrolysed and absorbed (Raven *et al*., 2014; Ciappellano, 2016).

The jejunum, between the duodenum and the ileum, is the main nutrient absorption site of the small intestine and measures about 2.5 m long. The final section of the small intestine is the ileum of about 3 m long. Its function is mainly to absorb vitamin B12 and bile acids through very specific mechanisms. It can also absorb the remaining products of digestion.

The large intestine has a length of 1.6 m and consists of the cecum, the rectum and the anal canal. It is less specialized than the small intestine for the digestion and absorption of nutrients because the surface area of its epithelium is much inferior due to a lack of folds and villi. Its main functions are to reabsorb water, minerals or other residual compounds as well as the by products of the metabolism of the many bacteria that it hosts (e.g. short chain fatty acids, vitamin K, vitamin B and folic acid) (Campbell *et al*., 2012).

The gastrointestinal tract contains many bacteria that play an important role in the immune system. Additionally, the intestinal epithelium itself plays a crucial role in defence against external threats since it acts as a selectively permeable barrier (Eurell, 2004).

2.2 Histological structures of the small intestine

The intestinal absorption surface is impressively increased contrasted with the surface of a simple cylinder. The mucosal layer is specially adapted to provide a large surface area in order to maximize the absorption of nutrients through the presence of large circular folds, intestinal villi but even more due to microvilli on the apical side of enterocytes (Fig 7). These multiple folds increase the absorptive surface up to 300 m^2 (Raven *et al*., 2014).

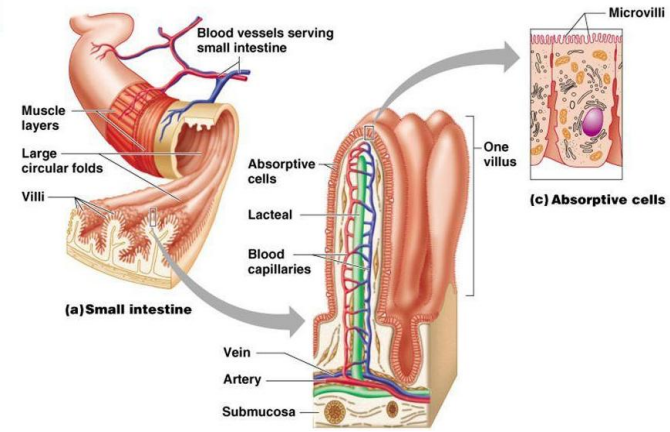

Figure 7: Large circular folds, villi and microvilli of the small intestine (Cummings, 2003).

The walls of the small intestine are made of four different tissue layers surrounding the intestinal lumen. Looking from the center to the outside we find: the mucosa, the submucosa, the muscularis externa and finally the serosa (Fig. 8) (Eurell, 2004).

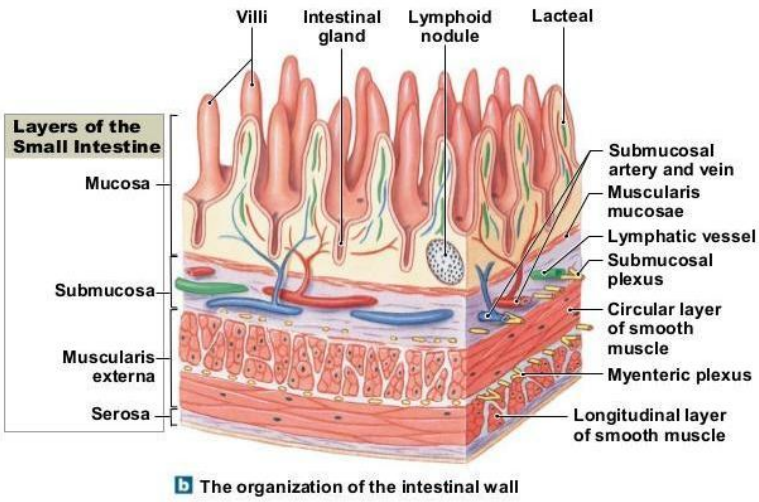

Figure 8: Organisation of the intestinal wall (Pearson, 2013).

2.2.1 The mucosa

The mucosa is the most inner layer, in direct contact with the intestinal lumen, and is composed of an epithelium that covers a connective tissue called *lamina propria*. Both are separated with a basement membrane. The lamina propria, which has a rich vascular and lymphatic network, absorbs the digestion products. Between the villi of the mucosa, we can find glands called crypts of Lieberkühn. They are composed of paneth cells that secrete intestinal juice but they also contain stem cells. Underneath these crypts we find a thin layer of smooth muscle, the *muscularis mucosae*.

The intestinal epithelium is composed of a single layer of different cell types and creates a physical barrier. The cells of this monolayer are joined together by tight junctions that contribute to the impermeability of the membrane. The two main functions of this epithelium are absorbing nutrients and water and providing a barrier against harmful substances.

Different cell types can be distinguished in the intestinal epithelium as is illustrated by figure 9. The distribution of these cells varies throughout the intestines but the enterocytes remain the most numerous ones (Bourlioux *et al*., 2003; Eurell, 2004; Raven *et al*., 2014).

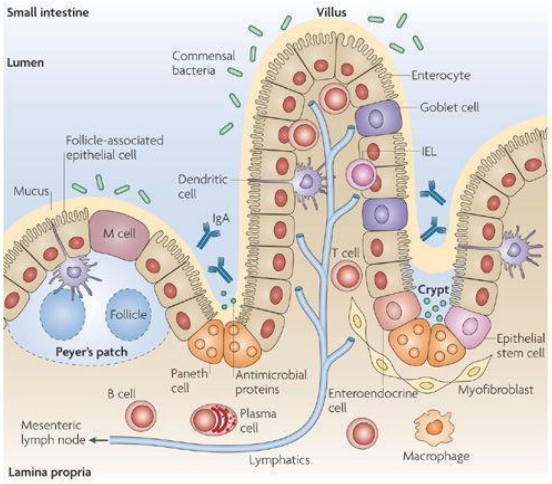

Figure 9: Different cell types found in the intestinal epithelium (Abreu *et al.*, 2010).

Enterocytes: these polarized cells are arranged in a monolayer and are specialized in the absorption of nutrients at the apical level and their release to the blood and lymphatic capillaries. They are the most common cells in the intestinal epithelium (90% of the cells). Their apical side has microvillosities and form the brush border whose role it is to increase the absorptive surface (Bourlioux *et al.*, 2003; Ciappellano, 2016). Enterocytes are also involved in the delivery of secretory immunoglobulin A (IgA) from the blood to the intestinal lumen.

Goblet cells: the major function of goblet cells is the production of mucus, a viscous fluid composed of highly glycosylated proteins (mucins) suspended in electrolyte solutions (Shroyer & Kocoshis, 2011). This mucus forms a protective gel-like layer over the surface epithelium and protects against bacterial invasion. It is the first defence line of the gastrointestinal tract and interacts with the immune system. The main functions of mucus are limiting the number of bacteria that can reach the epithelium, protecting against shear stress and shielding the intestinal mucosa from peptic digestion and chemical damage. Recent studies have shown that goblet cells can acquire antigens from the intestinal lumen and deliver them to dendritic cells (Hooper, 2015; Pelaseyed *et al.*, 2014).

Entero-endocrine cells: these cells regulate the process of digestion by acting on the intestinal mobility and digestive secretions through the secretion of intestinal hormones such as secretin, GIP (glucose-dependent insulinotropic polypeptide) and CCK (cholecystokinin) (Shroyer & Kocoshis, 2011).

Paneth cells: these cells are located at the bottom of the intestinal crypts and secrete antimicrobial peptides (lysozyme and defensins). They have an important role in intestinal host defence and homeostasis since they are part of the enteric innate immunity (Bevins & Salzman, 2011).

M-cells or Microfold cells (so called because of the presence of microfolds at their surface): M-cells are specialized epithelial cells forming part of the follicle-associated epithelium (FAE) that overlies the Peyer's patches and samples the intestinal lumen. M-cells have the ability to capture antigens from the lumen and transcytose them across the gut epithelium. Antigens are delivered to antigen-presenting cells located in a subepithelial pocket, such as dendritic cells. This leads to the induction of immune responses (des Rieux *et al.*, 2006).

2.2.2 The submucosa

This layer is composed of relatively thick connective tissue, containing blood and lymphatic vessels whose role it is among others to support the mucosa. The absorbed elements pass through the mucosa and are picked up to the blood vessels of the submucosa. Chylomicrons, for their part, are absorbed by lymphatic vessels and reach the bloodstream later. This layer also links the mucosa to the underlying smooth muscles of the muscularis externa. Within the submucosa, we can also find cells of the nervous system. These cells allow the regulation of different gastrointestinal activities and the transmission of information between the digestive and nervous system. They are located in the submucosal plexuses of Meissner. They work in a complementary way with the myenteric plexus to produce peristaltic waves and increase digestive secretions (Campbell, 2012).

2.2.3 The muscularis externa

The muscularis externa contains two layers of smooth muscles with a different orientation. The inner layer is the circular layer of smooth muscles while the outer layer is disposed in a longitudinal way. This disposition of muscular fibers ensures the progression of the food bolus by contraction (peristalsis) in the oral-aboral direction (Bourlioux *et al.*, 2003; Shroyer & Kocoshis, 2011; Ravel *et al.*, 2014).

2.2.4 The serosa

The serosa is the outermost layer of the intestine. It is a smooth membrane formed by a thin layer of cells and their secretion product. The secreted fluid, called serous fluid, forms a loose connective tissue that reduces friction from the movement of the muscularis. All the previous layers of the small intestine are encompassed by the serosa (Shroyer & Kocoshis, 2011; Campbell, 2012).

2.3 *In vitro* models of the intestinal barrier

Since the purpose of this thesis is to study the effects of AgNPs on intestinal cells, it was essential to have an *in vitro* model of the intestinal epithelium at our disposal. We opted for a cell line originating from a human colon adenocarcinoma: Caco-2 cells. This model has been extensively used over the last years as a model of the intestinal barrier and is considered to be the golden standard (Fröhlich & Roblegg, 2012).

The parental cell line obtained from a human colon adenocarcinoma, undergoes in culture a process of differentiation that leads to the formation of a confluent monolayer of mature cells. Although they originate from colonocytes, the cells develop many characteristic features of enterocytes lining the small intestine. This model is widely used to study intestinal drug absorption across the intestinal epithelium (Artursson & Karlsson, 1991). Caco-2 cells spontaneously differentiate and exhibits signs of both structural and functional similarities with intestinal enterocytes e.g.:

Structural (des Rieux *et al.,* 2007; Sun *et al.*, 2008; Ciappellano, 2016):

- Monolayer with functional tight junctions
- Polarized monolayer with distinct basolateral and apical membranes
- Presence of brush border microvilli at the apical membrane (Wilson *et al.*, 1990).

Functional:

- Expression of typical transporters for amino acids, bile acids, carboxylic acids, etc.
- High enzymatic activity of brush border associated enzymes (sucrase-isomaltase, lactase, amino-peptidase N, dipeptidylpeptidase IV and alkaline phosphatase.) (Chantret *et al.*, 1988)
- Formation of domes which are typical of transporting epithelial monolayers (Pinto *et al.*, 1983)

Thanks to these special features, Caco-2 cells have been of great utility in intestinal absorption studies. They have the ability to model human absorption characteristics and this explains why Caco-2 is the most commonly used intestinal permeability model (Osakwe, 2016). Other advantages are the high reproducibility and long-term viability of the Caco-2 model. Finally, this model is well characterized, easily maintained and enables to perform qualitative and quantitative transport studies across an epithelial layer (Wilson *et al*., 1990).

However, the Caco-2 model also presents certain limitations: culture-related conditions as well as the different Caco-2 cell lines used in different laboratories make it extremely difficult to compare results (Sambuy *et al.*, 2005). Furthermore, Caco-2 monocultures don't represent the complexity of a whole system and are therefore unable to predict accurately adverse effects as the human body does. As Osakwe has nicely formulated: "The whole intact system encompassing the natural physiological environment, comprising discrete functions that integrate into a network of functions could not be recapitulated in the *in vitro* systems, which is critical to identify toxicity." (Osakwe, 2016). Therefore, the translation of information obtained from the Caco-2 monolayer to *in vivo* requires more sophisticated modelling approaches. Different complex models have been developed to approach the physiology of the human body. These models are based on the use of different cell types in co-cultures (Fig.10).

A commonly used model is the co-culture of two human cell lines, Caco-2 and HT29-MTX. These mucus-producing cells (goblet-type cells), have been incorporated into an *in vitro* cell culture model and renders a physiologically realistic mucus layer that gives more accurate predictions (Mahler *et al.*, 2009). Another example of a co-culture model is the use of Caco-2 cells along with Raji B cells to stimulate differentiation of M-cells. Indeed, the presence of Raji B cells triggers the differentiation of some Caco-2 cells into M-cell like cells. This model can play a crucial role in the development of targeted oral vaccines through M-cells (des Rieux *et al.,* 2007; Skalska *et al.,* 2010). Finally, we can combine these two approaches to obtain a triculture model with enterocyte like cells, goblet like cells and M-cell like cells (Ciappellano, 2016).

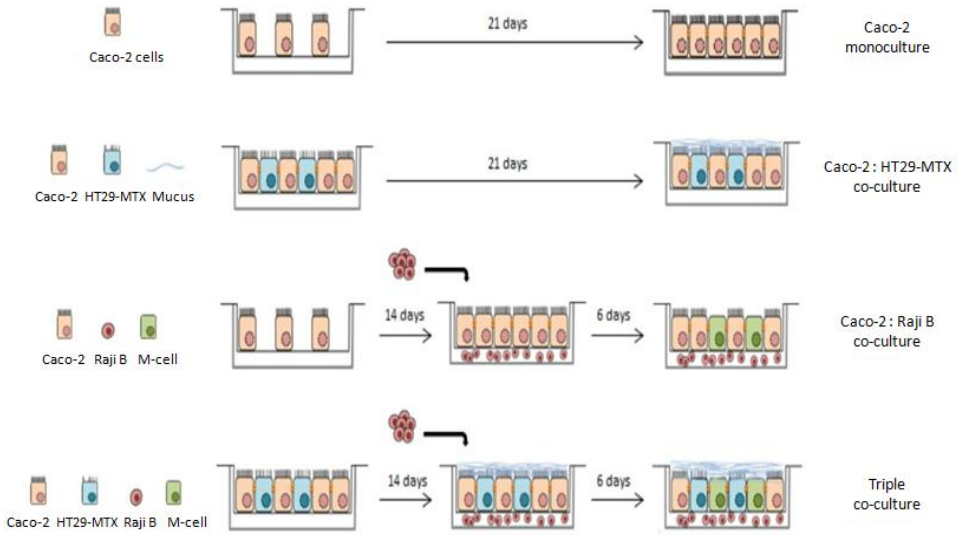

Figure 10: *In vitro* cell models (Araújo & Sarmento, 2013).

However, increasing the number of cell types also increases: the complexity of the model, the costs associated with parallel cultures and makes the interpretation of the data more complicated. This is why we opted for an improved model of Caco-2 monolayer by using transwell™ inserts that enable a differentiation between apical and basolateral media (Fig. 11). Having two distinct compartments allows kinetic events in the monolayer, including paracellular transport and influx/efflux on apical and basolateral membranes.

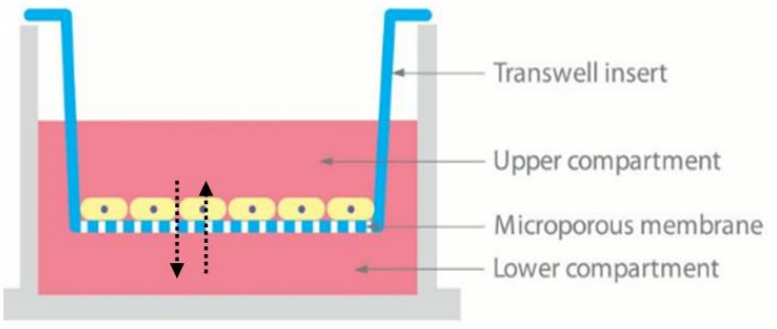

Figure 11: Illustration of a transwell™ insert system (Corning Permeable Support Systems).

2.4 Fate of ingested NPs

Human exposure to ENMs present in food and food contact materials occurs mainly through oral ingestion. Since we possess a specialized epithelium with a huge surface that is able to absorb a maximum amount of nutrients, there may be questions about the absorption of unwanted particles such as AgNPs. However, there is currently not much information regarding metabolism/biotransformation of ENMs upon oral administration. This raises several concerns, especially considering the small sizes of ENMs that may enter the food chain undetected, accumulate within tissues and be taken up by individual cells (Fig. 12) (Martirosyan *et al.*, 2014).

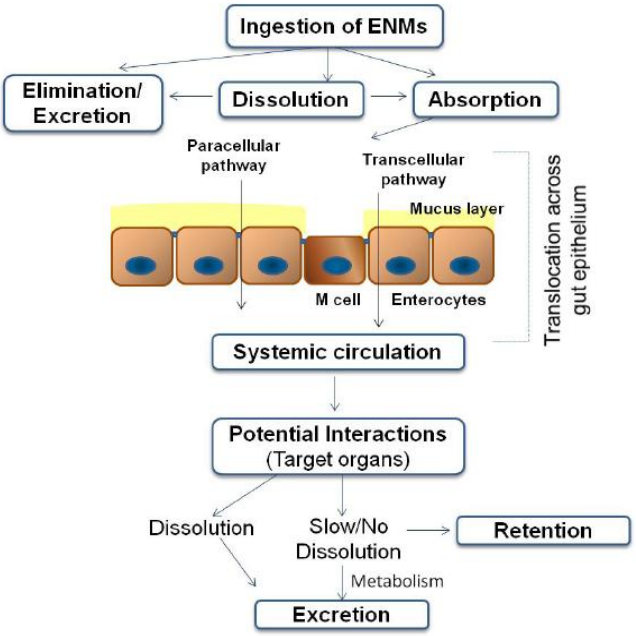

Figure 12: Fate of food-related ENMs in the GIT (Martirosyan *et al.*, 2014).

When NPs are ingested, they enter our body and are subjected to the digestive processes in the GIT. Throughout the GIT, their physicochemical properties change as a result of their interaction with food, digestive enzymes, electrolytes and intestinal microbiota. Since physicochemical characteristics are key determinants of their distribution throughout the body, these interactions will determine their toxicity. Among all parameters characterising NPs, it seems that size, aggregation/agglomeration state and surface coating are the most critical for their toxicity. For example, it is known that surfactants added to prevent agglomeration drastically change chemical reactivity and thus affect their cytotoxicity (Park *et al.*, 2011). NPs undergo different types of changes when they are in contact with biological media as they interact with their components. The major consequences of these interactions are represented on figure 13 (Urban *et al.*, 2016).

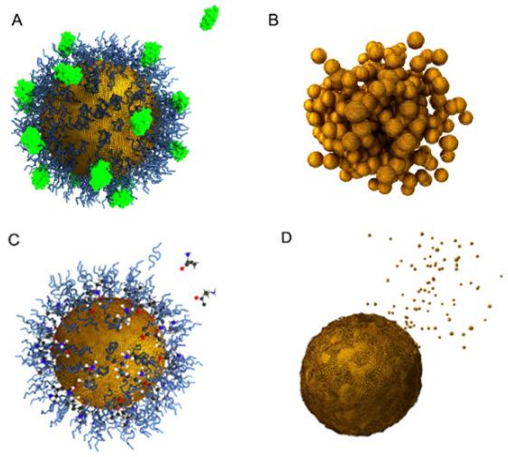

Figure 13: Schematic illustration of possible consequences arising from NP incubation in physiological fluids: (A) formation of protein corona; (B) NP aggregation; (C) removal of ligands; (D) NP dissolution (Urban *et al*., 2016).

A) Firstly, the interaction of NPs with proteins can result in the formation of a corona. Hard coronas are characterized by a tightly bound protein layer on the particle surface, formed by proteins with a high affinity. As a result, this leads to slow exchange rates (*i.e*., several hours) of proteins composing the NPs surface. On the contrary, soft coronas are composed of lower affinity proteins thus forming a weakly associated layer with rapid exchange *(i.e.,* several minutes) (Fig. 14). There is evidence that distinct protein components in combination with size and/or surface curvature of AgNPs may yield a unique "protein corona signature ". The cellular and biochemical responses will depend on that unique corona signature (McShan *et al*., 2014; Duran *et al.*, 2015; Urban *et al.*, 2016). Therefore, it is generally accepted that the protein corona, rather than the NP itself, defines the biological identity of NPs. This corona can act as a carrier for the particles and influence for example their absorption across the GIT that could lead to unpredictable effects (Martirosyan *et al.,* 2014; Urban *et al.*, 2016).

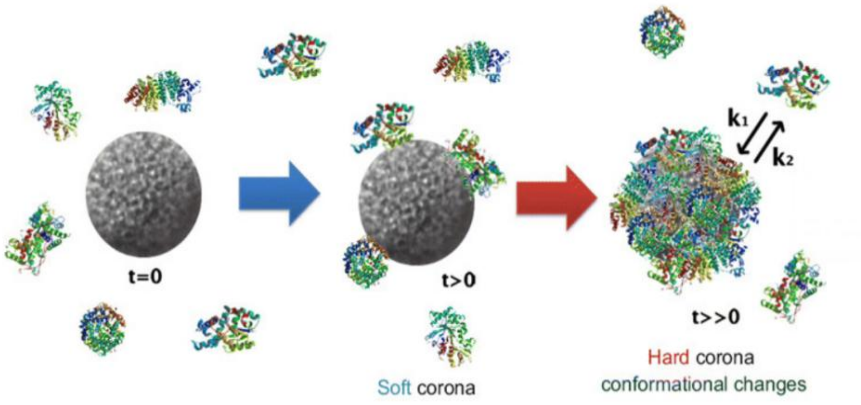

Figure 14: Schematic illustration and characteristics of hard and soft coronas (Duran *et al*., 2015).

B) Secondly, nanoparticle interaction with physiological fluids can induce aggregation. Aggregation refers to the inter-particular adherence that leads to the formation of large and irregular clusters of particles. It is mainly due to displacement of the coating agents by molecules found in biological fluids (e.g., water and inorganic ions) making the particles unstable and thus promoting aggregation.

C) Thirdly, when AgNPs are located in biological media, certain biomolecules present in the media can remove the surface-coating agent from NP. Indeed, the AgNPs ligands (e.g., citric acid, amino acids, cetyl trimethylammonium bromide (CTAB), and sodium dodecyl sulphate (SDS)), are non covalently attached to AgNPs and can thus be displaced by biological macromolecules. Some studies have shown that thiol-containing molecules such as cysteine can remove ligands at physiological concentration. As a result, AgNPs become unstable leading to changes in the profile of adsorbed protein.

D) Finally, AgNPs can undergo oxidative dissolution when they are in contact with molecular oxygen. Silver atoms on the surface of nanosilver, can be oxidized to silver oxide, which in turn can interact with the media to release Ag^+. This process can occur in the environmental media, biological media, as well as inside the cell. Thus, AgNPs can be seen as a source of Ag^+ through this slow-release process. The main factors influencing oxidative dissolution of AgNPs are particle related properties (e.g., size, shape and surface coating), but also matrix related characteristics, such as dissolved oxygen, temperature, pH and the presence of proteins. For example, a study has shown that increasing bovine serum albumin (BSA) concentrations resulted in increasing dissolution rates of AgNPs because of the high affinity of BSA for Ag^+. This, however, did not increase AgNPs toxicity as the dissolved Ag^+ were adsorbed onto the BSA molecules (Ostermeyer *et al.*, 2013).

2.5 Release of Ag^+ by AgNPs

Multiple studies have revealed that AgNPs are responsible for the release of silver ions. The initial release of Ag^+ is most likely due to Ag^+ already present in the stock dispersion within the coating layer on the NPs surface (Fig. 15). This coating layer has a significant importance since it is responsible for the dispersion and redox stability. After this initial release of Ag^+, another mechanism occurs. The zero-valent silver at the surface of the particles may be oxidized to Ag^+ by dissolved oxygen. Since this oxidative dissolution occurs at a slower rate it is responsible only for the long-term release of Ag^+. Therefore, scientists propose that rapid initial Ag^+ release was attributable to the desorption of Ag^+ from NPs surfaces and not from further release due to later oxidation processes (Köser *et al.*, 2017).

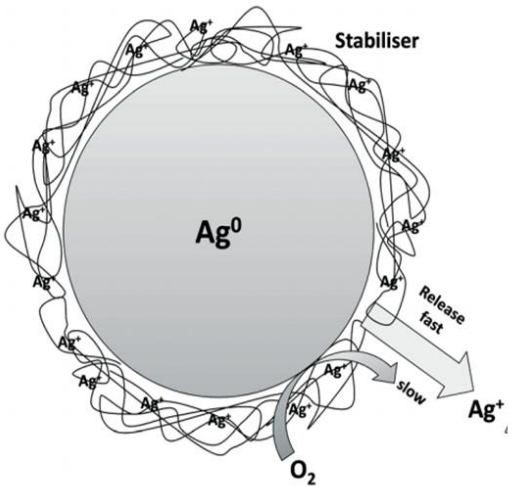

Figure 15: Representation of Ag^+ release from AgNPs (Köser *et al*., 2017).

There is also a general consensus on the fact that the chemical form of silver has implications for its toxicity. For example, the antimicrobial effect of AgNPs is considered to be due to the release of Ag^+ via a Trojan-horse-type mechanism. According to this mechanism, NPs are internalized within cells and are then ionized leading to the release of toxic ions (Park *et al*., 2010; Hsiao *et al*., 2015). Smaller AgNPs, which have greater mobility and surface area compared to larger particles, have higher dissolution rates, leading to higher cellular toxicity and oxidative stress. It is therefore necessary to consider the speciation of silver and the amount of Ag^+ released in order to understand its contribution to the toxicity of AgNPs. It is very difficult to determine what portion of the toxicity is caused by the nano-form and what is from the ionic form (McShan *et al*., 2014).

The surface oxidation rate is closely related to the AgNPs surface coating but also to the interaction with nucleic acids, lipid molecules and proteins present in biologic media. Media components, such as chloride and proteins, control the available dissolved Ag^+ by precipitation and complexation. Ag^+ have a high affinity for organic molecules with low molecular weight, especially thiol-containing compounds such as cysteine or glutathione (McShan *et al*., 2014).

Under highly acidic conditions, as can be found in the stomach, AgNPs can dissolve and generate free Ag^+ that will precipitate with chloride present in the stomach (Fig. 16). This AgCl is essentially insoluble and is known to bind to silver surfaces and facilitate in AgNPs aggregation by aiding in the formation of interparticle AgCl bridges (Axson *et al*., 2015). Since smaller AgNPs have larger surface areas, they also have higher dissolution rates that lead to increased Ag^+ concentration. In turn, this gives rise to greater AgCl precipitation and aggregation.

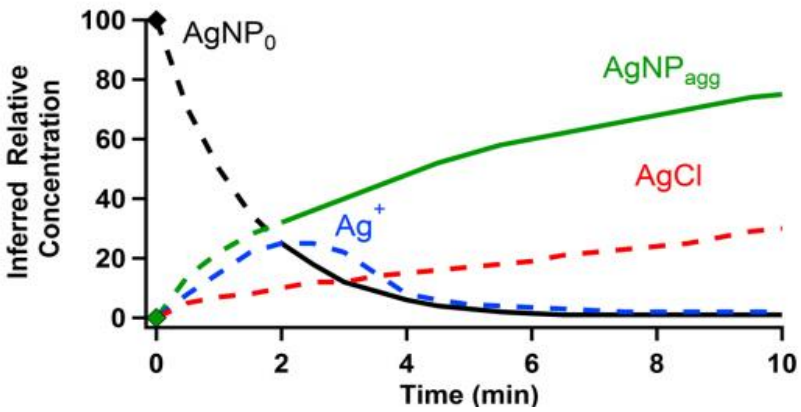

Figure 16: Schematic representation of the predicted processing of AgNPs in the human stomach (Axson *et al*., 2015).

Another *in vitro* digestion study has shown that in the stomach, AgNPs dissolve in Ag^+ but that these are mainly bound to the digestive matrix or are present as nanosized salts. Only 19% of the ions have been found to be free dissolved ions and/or silver soluble complexes (Bove *et al*., 2017).

Once the remaining particles have reached the intestinal epithelium, they are confronted with the mucosal layer that acts as a selective barrier. While most of the AgNPs are eliminated from the body via the feces, some remain in the gut lumen, where they can interact with the intestinal surface or with microbiota (Javurek *et al*., 2017). Another, even smaller fraction even manages to cross the intestinal epithelium. Particles with low solubility in digestive fluids are paid more attention due to their bigger potential to cross the GIT. As stated by the Scientific Committee on Emerging and Newly Identified Health Risks (SCENIHR, 2009), free and low solubility ENMs such as AgNPs are a priority concern for human and environmental safety.

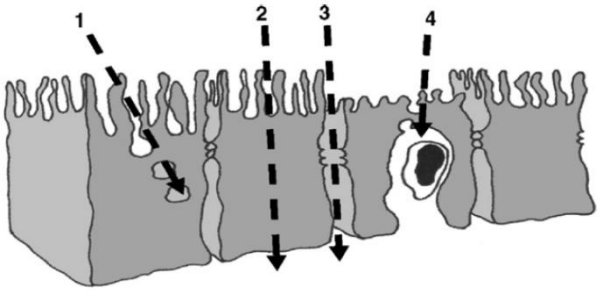

Figure 17: Nanoparticle transport across epithelial cells (des Rieux *et al*., 2006).

NPs can cross the intestinal epithelium through various pathways as can be seen on figure 17. Theoretically, NPs could be transported by enterocytes (1) after being taken up by endocytosis and released by exocytosis. Another possible pathway is through passive diffusion through enterocytes (2). NPs can reach the basal pole by paracellular transport between the tight junctions connecting neighboring cells (3). Finally, specialised cells such as M-cells can also be involved in the transport of NPs (4). Even though all those pathways are in theory possible, some are more realistic than others.

There is evidence that particle translocation can occur across enterocytes, but because of their low endocytic activity, the amount of particles translocated via this route is usually low. The paracellular pathway and passive diffusion pathway through enterocytes also seem to be rare (Fröhlich & Roblegg, 2012).

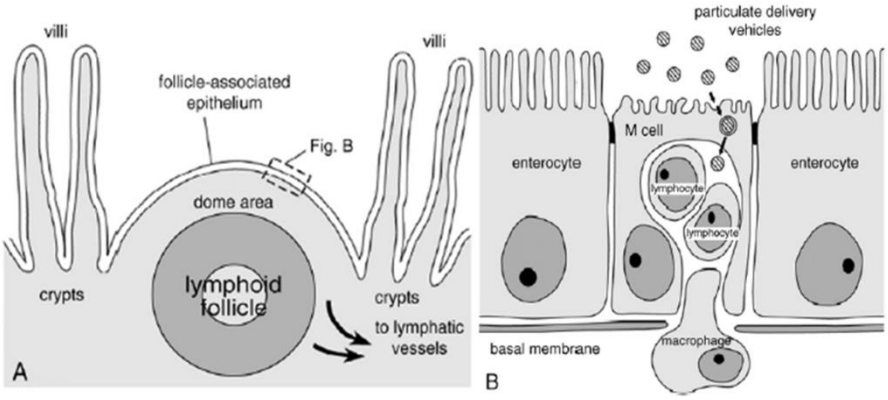

Figure 18: (A) Schematic transverse sections of a Peyer's patch lymphoid follicle and overlying (FAE) follicle-associated epithelium (B) Specialised antigen sampling M-cells (des Rieux *et al*., 2006).

It is generally believed that particle translocation via transcytosis in M-cells of Peyer's Patches is more frequent (Fig. 18). This is not surprising considering that M-cells are adapted to absorb large range of materials (Martirosyan *et al*., 2014). However, since there are vastly more enterocytes than M-cells, enterocytes could still play a large role in NPs transport across the epithelium. Transport of AgNPs through the transcellular pathway depends on physicochemical properties of particles such as; size, surface charge, surface hydrophobicity, presence/absence of ligands but it also depends on the physiology of the GI tract (Bouwmeester *et al*., 2011). It is generally agreed that nanoparticle transcytosis increases when their size decreases. This could be explained by the fact that bigger particles are better retained in the mucus layer than smaller ones, which therefore can cross the mucus layer and reach the cells faster (Georgantzopoulou *et al*., 2016).

Once these particles have crossed the epithelium, they reach systemic circulation and can be distributed to secondary target organs (e.g., liver, spleen, brain, kidney and testes) where they can cause functional and/or structural impairment (Mao *et al*., 2018). In addition to the problems linked to crossing the intestinal barrier and the following systemic invasion, we must also consider the effects of AgNPs on the intestinal barrier itself. AgNPs are suspected to cause inflammation and oxidative stress of the digestive tract, thus affecting the integrity of the intestinal barrier (Martirosyan *et al*., 2014). This thesis will investigate the impact of AgNPs exposure on intestinal cells and more particularly on cellular responses related to oxidative stress.

3. Mechanism of toxicity

The toxicity of AgNPs is closely related to its biotransformation, including surface oxidation, release of silver ions and interaction with macromolecules. The form in which silver is presented also strongly influences its toxicity. Because of the lack of efficient techniques to measure AgNPs dissolution in cells, there is always a challenge to distinguish which portion of the toxicity is from the ionic form and which is from the AgNPs form of silver.

3.1 AgNPs-induced oxidative stress

It is generally admitted that the main mechanism of AgNPs toxicity results from the generation of reactive oxygen species (ROS) that lead to oxidative stress and finally causes damage to cellular components. On one hand, AgNPs can act from the outside of the cells by interacting with membrane proteins and activating signalling pathways that generate ROS, leading to the inhibition of cell proliferation. On the other hand, AgNPs can also enter cells and cause mitochondrial dysfunction leading to mitochondrial stress resulting in oxidative stress (Fig. 19) (Bressan *et al*., 2013; AshaRani *et al.,* 2009).

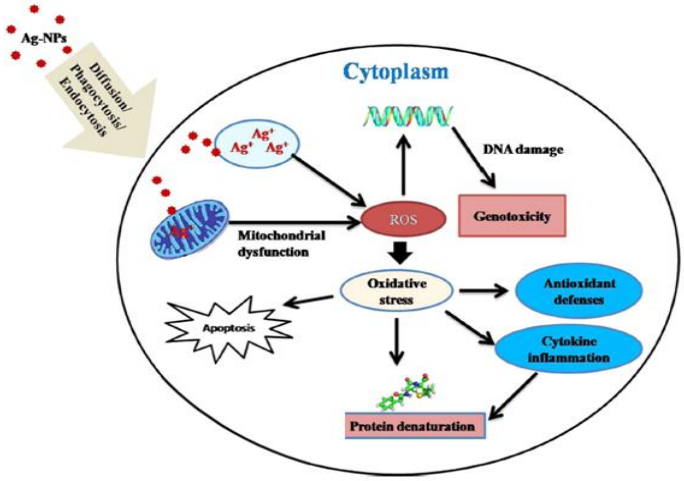

Figure 19: Possible uptake process and mechanism of cytotoxicity induced by AgNPs (Akter *et al*., 2017).

ROS are chemical species that are produced as by-products of cellular oxygen metabolism, which occurs in mitochondria. The main source of ROS is through electron leakage during the electron transport chain. The final electron acceptor (O_2) is therefore only partially reduced leading to ROS instead of H_2O (Fig. 20).

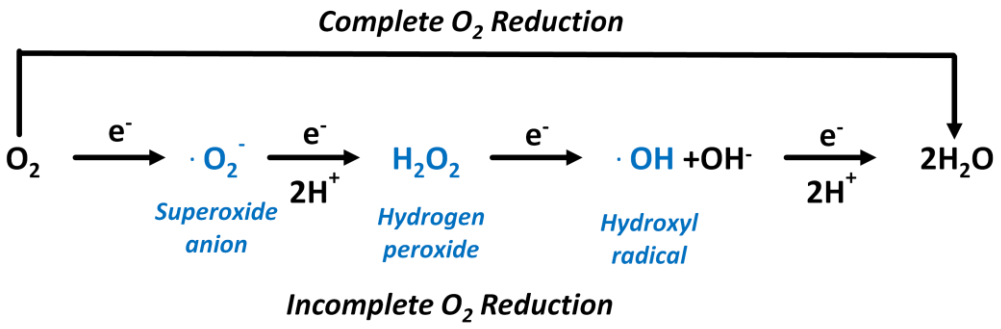

Figure 20: Complete and incomplete reduction of molecular oxygen: production of reactive oxygen species by single electron additions (Bartz & Piantadosi, 2010).

Numerous agents including AgNPs can induce significant generation of ROS. The main ROS include the superoxide anion ($O_2^{\cdot-}$), hydrogen peroxide (H_2O_2) and the hydroxyl radical ($OH^{\cdot}$). The abnormal accumulation of ROS is called oxidative stress and can lead to serious cellular damage including DNA damage and apoptotic cell death. Oxidative stress occurs when ROS production exceeds the capacity of cellular antioxidant defence systems. Since ROS are highly reactive, they tend to react quickly and impose oxidative damage on indispensable biomolecules. For example, ROS can alter DNA bases and cause strand breaks, which ultimately results in DNA damage. Organisms have therefore developed various antioxidant defence systems for protecting their cells against ROS (Sinha *et al.*, 2013).

3.2 Cellular response against oxidative stress

Cells have developed a range of proteins to detoxify ROS and repair oxidative damage to DNA, lipids and proteins. Among the antioxidant enzymes, we can find enzymes such as superoxide dismutases (SOD), glutathione peroxidases (GP), catalase (CAT), glutathione S-transferase (GST) and glutathione reductase (GR). Other, non enzymatic factors, such as glutathione (GSH) and glutathione disulfide (GSSG) have also an important role in ROS detoxification (Fig 21).

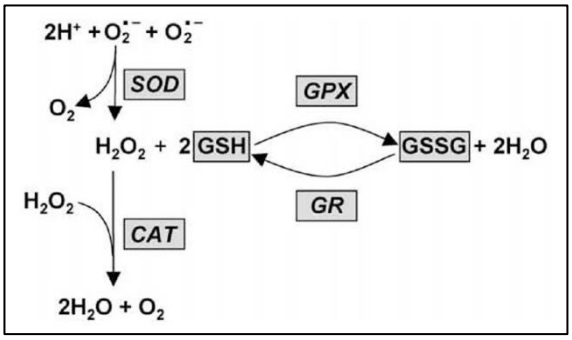

Figure 21: Representation of the relationship between antioxidant enzymes, GSH and GSSG (Borowicz *et al.*, 2016).

Firstly, SOD scavenges superoxide anion and converts it into O_2 and H_2O_2. The resulting H_2O_2 can be transformed by 2 different enzymes. The first one, CAT, converts H_2O_2 into H_2O and O_2 whereas GP needs GSH as cofactor to transform H_2O_2 into H_2O. GR, on the other hand, regenerates GSH from its oxidized form (GSSG). GSH is one of the major endogenous antioxidant scavengers that is able to bind and reduce ROS. Maintaining a sufficient GSH pool is therefore critical in order to ensure a decent defence system for cell survival. GSH can also act on its own and scavenge free radicals through direct chemical reactions. It has been proven that GSH can interact with metal ions, including Ag^+. Hence, it could bind directly to Ag^+ as a response against oxidative stress. GST has also the ability to catalyse the conjugation of GSH to a wide variety of electrophilic substances such as; drugs, toxins and products of oxidative stress. Therefore, GST plays an important role in preventing oxidative damage.

3.3 Cellular damage resulting from oxidative stress and AgNPs

Usually, the processes causing AgNPs toxicity involve; ROS generation through mitochondrial dysfunction, depletion of antioxidant defence systems and damage to different cellular components. In turn, ROS generation can lead to lipid peroxidation, protein carbonylation and DNA oxidation (Fig. 22). AgNPs can also directly interact with proteins, DNA and cell membranes causing significant damage. The cytotoxic effects of AgNPs are dependent on their concentration, size and duration of exposure (Akter *et al.*, 2017).

3.3.1 Protein damage

Because of the high affinity of silver for sulphur groups, an important toxicity mechanism for AgNPs is their interaction with proteins. As a result, they can cause protein conformational changes or even protein damage with a loss of function. AgNPs also interact with glutathione and antioxidant enzymes as they contain sulphur groups, leading to a decreased activity. Protein depletion through sulfhydryl group binding promotes apoptosis. Therefore, a main cytotoxic effect of AgNPs is apoptosis-mediated cell death (Akter *et al.*, 2017; McShan *et al.*, 2014).

3.3.2 DNA damage

AgNPs can directly or indirectly affect DNA, ultimately causing apoptosis. AgNPs can tightly bind DNA and alter its conformation. Interaction of AgNPs with DNA also leads to cell cycle (G1) arrest and completely blocks the S phase, therefore inducing apoptosis (Zhang *et al.*, 2016). AgNPs-induced ROS overproduction causes; DNA damage through oxidation of DNA bases, DNA strand breaks and mutations. This leads to increased genotoxicity by DNA damage.

3.3.3 Cell membrane damage

AgNPs may cause alteration of membrane permeability, which ultimately induces apoptosis. According to a study performed on a fibroblast cell line, AgNPs induced actin depolymerization in the cytoskeleton leading to cell membrane damage. This enabled calcium influx and induced intracellular calcium overload, which caused ROS overproduction and mitochondrial membrane potential variation. As a result, apoptosis caused cell death (Cheng *et al.*, 2013). Exposure to AgNPs also alters the membrane permeability of barrier cells including intestinal cells (McShan *et al.*, 2014).

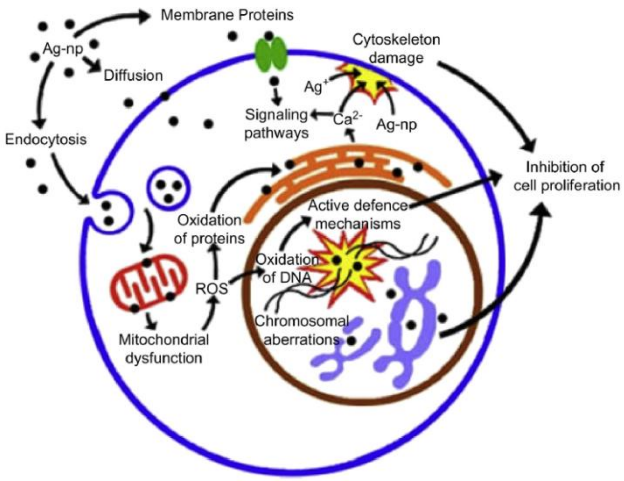

Figure 22: Proposed mechanism of nanosilver toxicity (McShan *et al.*, 2014).

3.4 The Keap1-Nrf2 signalling pathway

The nuclear factor erythroid 2–related factor 2 (Nrf2) is another defensive pathway that plays an important role in preventing cellular stress. Nrf2 is the major pathway involved in protecting the cell from oxidative stress, through the induction of antioxidant-responsive genes and genes of the phase II detoxifying enzymes (Fig. 23) (Taguchi *et al.*, 2011).

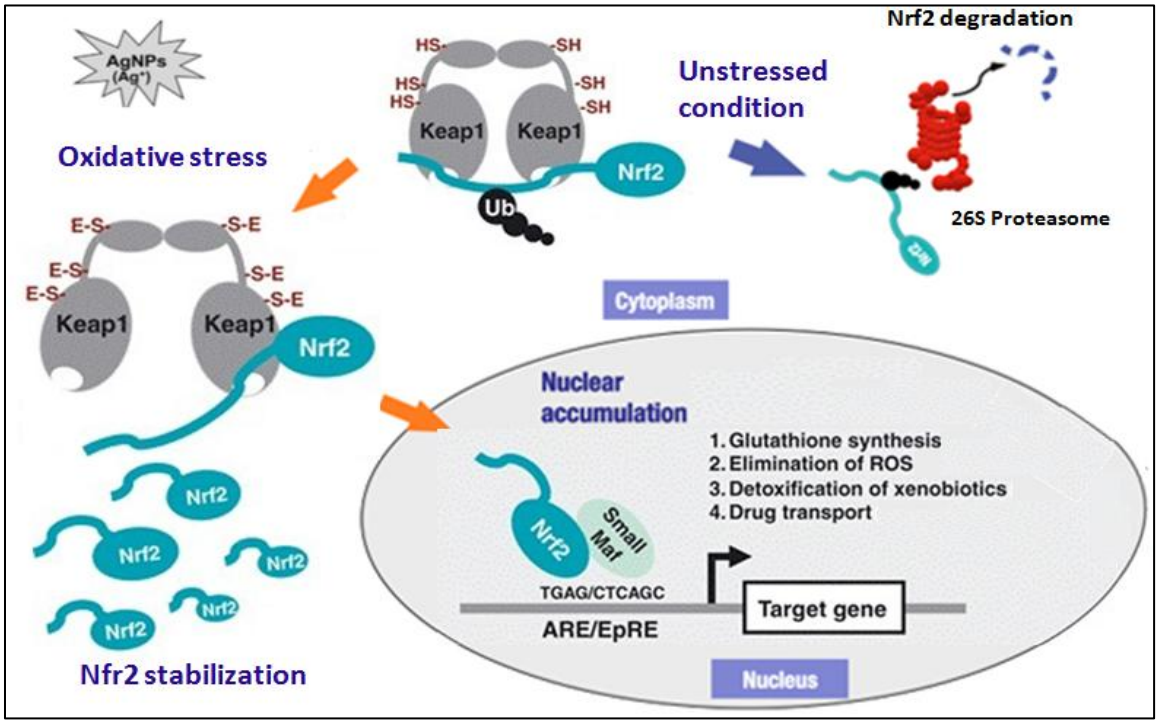

Figure 23: Molecular mechanisms of the Keap1–Nrf2 pathway (Taguchi *et al.*, 2011).

There are two key signalling proteins within this pathway (Fig 23.). The first one being the transcription factor Nrf2 (nuclear factor erythroid 2-related factor 2) that binds to antioxidant response element (ARE) in target genes. The second very important protein is Keap1 (Kelch ECH associating protein 1). Its function is to repress Nrf2 by binding to it and promoting its degradation by the ubiquitin-proteasome system. Keap1 is a protein with many cysteine residues that enable it to act as a sensor, detecting changes in cellular redox state. Under normal conditions, Nrf2 is bound to Keap1 protein and is therefore degraded by a proteasome. On the contrary, an increase in intracellular ROS leads to an increase in the oxidation or conjugation of Keap1 cysteines, causing a conformation change of Keap1 and the release of Nrf2. This dissociation enables the translocation of Nrf2 into nucleus, where it heterodimerises with small masculoaponeurotic fibrosarcoma (Maf) proteins which in turn facilitates the binding of Nrf2 to the ARE and promotes the expression of Nrf2 target genes such as antioxidant and phase II enzymes that restore redox homeostasis.

Some well known Nrf2 gene targets are: superoxide dismutase (SOD), catalase (CAT), glutathione-S-transferases (GST), glutathione peroxidase (GP), glutamate-cysteine ligase (GCL), NAD(P)H quinone oxidoreductase 1 (NQO1) and heme oxygenase 1 (HO-1) (Xiong *et al.*, 2015; Kansanen *et al.*, 2013). Each of these enzymes is involved in the removal of ROS and participate to restore the redox balance. The role of the four first enzymes was already explained above.

Glutathione (GSH) is a tripeptide composed of glutamate, cysteine and glycine. Glutamate cysteine ligase (GCL) catalyses the first and rate-limiting step in the formation of the cellular antioxidant glutathione (Fig 24). Glutamate and cysteine are ligated to form γ-glutamylcysteine (γ -GC). The second step is carried out by glutathione synthetase (GS), which ligates glycine to γ -GC to form GSH (Franklin *et al.*, 2009; Krejsa *et al.*, 2010).

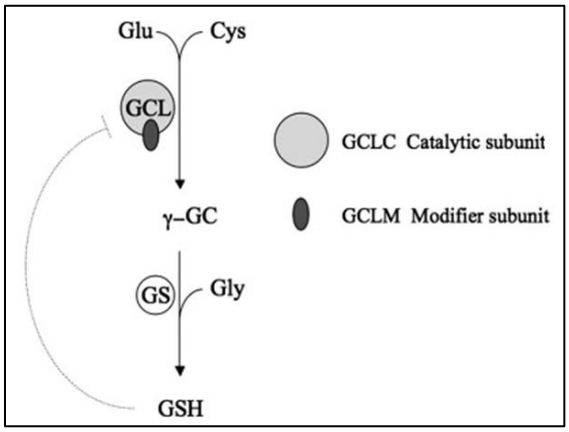

Figure 24: Glutathione synthesis (Franklin *et al*, 2009).

NAD(P)H quinone oxidoreductase 1 (NQO1), is an FAD containing quinone reductase that catalyses the 2-electron reduction of quinones. This double reduction of quinones to hydroquinones is considered to be a detoxification process since it prevents the formation of highly reactive semiquinones than can lead to the formation of ROS. Indeed, semiquinones have the propensity to donate the excess electron to molecular oxygen, thereby generating superoxide anion. In addition to its function as quinone reductase, NQO1 also has superoxide scavenging activity, although being less efficient than SOD (Siegel *et al.*, 2012; Vredenburg *et al.*, 2014).

Finally, the activation of Nrf2 influences the generation of cytoprotectors such as heme oxygenase 1 (HO-1). HO-1 catalyses the first and rate-limiting step in heme degradation. However, HO-1 is not only induced by its heme substrate but also by non-heme inducers such as heavy metals, cytokines and many others (Fig. 25). HO-1 can neutralize ROS by degrading heme into equimolar quantities of Fe^{2+}, biliverdin and carbon monoxide (Choi *et al.*, 1996; Kim *et al.*, 2013). These products attenuate AgNPs-induced cellular stress, especially biliverdin that is converted into bilirubin by biliverdin reductase and that has antioxidant properties. Tissue protection is achieved by the three bioactive products acting as anti-apoptotic, anti-oxidant or anti-inflammatory factor (Aueviriyavit *et al.*, 2014, Loboda *et al.*, 2016).

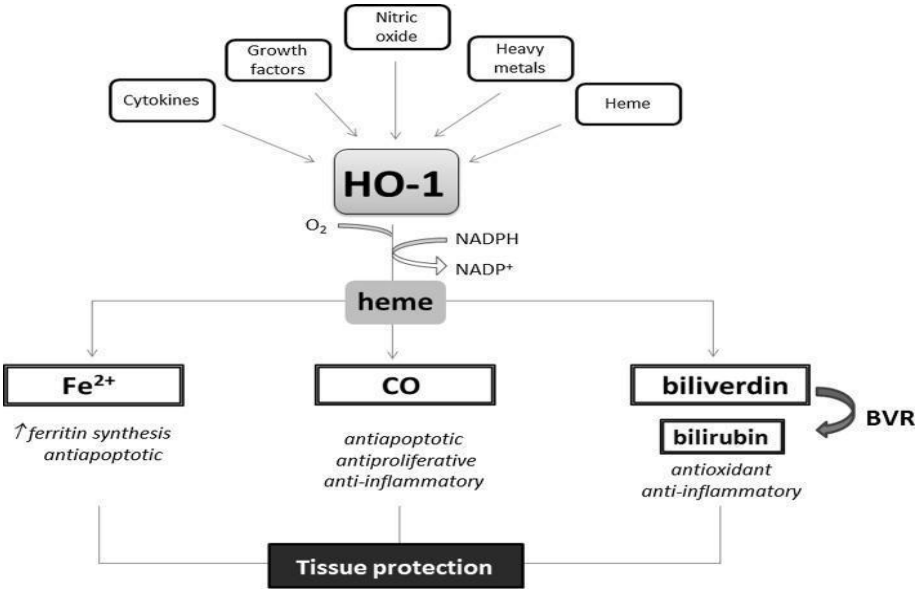

Figure 25: Heme oxygenase-1 pathway and resulting bioactive products (Loboda *et al.*, 2016).

3.5. Interleukins-8 and 6 (IL-8 and IL-6)

In addition to defending cells against oxidative damage, emerging evidence suggests that Nrf2 is also involved in controlling inflammatory responses. It has been proven that continued oxidative stress can lead to chronic inflammation. Indeed, in inflammatory cells, ROS contribute to the expression of a variety of different inflammatory cytokines (Kobayashi *et al.*, 2013).

Excessive ROS activate various inflammatory signalling pathways such as the NF-κB (nuclear factor kappa B) pathway, which in turn induces the expression of various pro-inflammatory cytokines among which interleukin 6 (IL-6) and interleukin 8 (IL-8). Consequently, Nrf2 exerts indirect anti-inflammatory effects through ROS detoxification but also direct effects by regulating the expression of inflammation-associated genes (Wardyn *et al.*, 2015). For example, Nrf2 activates ATF3 (activating transcription factor 3) gene expression by binding to AREs in its promoter, this ATF3 will in turn repress the expression of the pro-inflammatory cytokine IL-6, which will finally results in anti-inflammatory effects.

Furthermore, it has already been proven that both IL-6 and IL-8 promoter regions contain a functional antioxidant response element (ARE) that can be targeted by Nrf2 (Zhang *et al.*, 2005; Wruck *et al.*, 2011). Whether Nrf2 stimulates or inhibits the expression of pro-inflammatory cytokines IL-6 and IL-8 is controversial and will be discussed later.

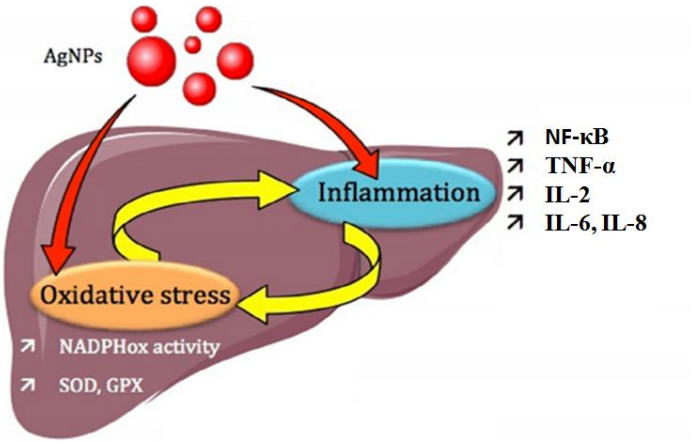

Figure 26: AgNPs toxicity through amplification loops between oxidative stress and inflammation (Gaillet *et al.*, 2015).

As already mentioned above, oxidative stress caused by AgNPs can trigger inflammatory reactions through the activation of transcription factors such as NF-κB thus leading to the release of cytokines including tumor necrosis factor-α (TNF-α) and IL (interleukins)-1, IL-2, IL-6 and IL-8. On the other hand, these pro-inflammatory cytokines enhance the expression and activity of NADPH oxidase, resulting in oxygen radical production (Joo *et al.*, 2015). Therefore, the interaction of Nrf2 and inflammatory cytokines, could lead to amplification loops between oxidative stress and inflammation (Fig. 26). The understanding of the amplification loops may help to unravel the mechanisms of AgNPs toxicity causing DNA damage and cell death (Gaillet *et al.*, 2015).

Part II: Material & methods

1. Cell culturing

As already detailed in point 2.3 of the introduction, the *in vitro* model of the small intestine used during this master's thesis consists of Caco-2 cells originating from a cell line isolated from a human colon adenocarcinoma. The line used during this work is derived more particularly from the clone 1 cell line supplied by Dr. M. Rescigno from Milano-Bicocca University (Italy) and were used from "passage" 10 to 30.

1.1. Flask culturing

Caco-2 cells were grown in flasks of 75 cm^2 (Fig. 27) or 175 cm^2 (Corning Incorporated, New York, NY) containing a minimal culture medium called Dulbecco modified Eagle's minimal essential medium (DMEM) that contains 4.5 g/l glucose (Lonza, Verviers, BE). This minimal medium was supplemented with 10 % (v/v) fetal bovine serum (FBS), 1% (v/v) non-essential amino acids (Lonza), 1% (v/v) L-glutamine 200 mM in a 0.85 % NaCl solution (Lonza) and finally 1% (v/v) of a mixture of penicillin-streptomycin antibiotics (Lonza). Thus, the resulting mixture, called culture medium hereafter, contains all the elements necessary for the maintenance and development of the cells. In order to mimic the conditions of the human body, Caco-2 cells were cultured at 37°C under 10% (v/v) CO_2 and under a water-saturated atmosphere. These incubation conditions remained the same during the entire study. Flask culturing was conducted to reach 90 to 100 % confluence within 7 days, after what a "passage" served to carry out the next subculture.

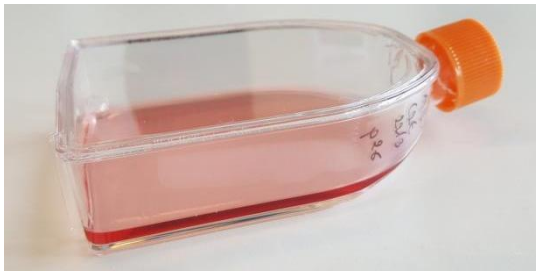

Figure 27: Culture flask with 75 cm2 growth area, containing culture medium (Corning).

1.2. Subcultures

In order to perform a subculture, the Caco-2 cell layer was rinsed with phosphate buffered saline (PBS) to eliminate dead or unfixed cells and to wash away the remaining culture medium that could lead to the inactivation of the trypsin. For the next step, the cell layer was detached from the flask with a trypsin–EDTA 0.05% mixture (Lonza) that was incubated during 5 to 10 min. Detached cells were then suspended in culture medium to stop the action of the trypsin. A cell count of this suspension is then carried out to determine to volume of suspension that has to be used to inoculate the new flask or to start a plate culture.

The counting is performed by diluting 20µl of the cell suspension twice with Trypan blue (Lonza), a blue dye that highlights the dead cells. Trypan blue is a tetrasodium salt that penetrates into cell membranes. The principle of the test is based on the differential exclusion of the dye. It enters all cells but only the living cells can actively expel it, thus remaining colourless. After the staining, 20µl of this homogenized mixture is placed between a Bürker chamber (containing a counting grid) and a cover glass (Fig. 28). The assembly is then observed under a microscope and the number of living cells (not stained) contained in 3 randomly chosen large squares are counted (Fig. 29A). It should be noted that only cells within the large square and those crossing the edge on two out of the four sides were counted as it is illustrated in figure 29B, where the cells on the bottom and right sides were not considered.

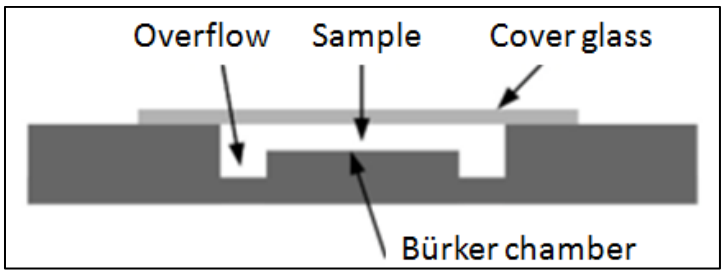

Figure 28: Side view of the hemocytometer counting chamber (Microbehunter).

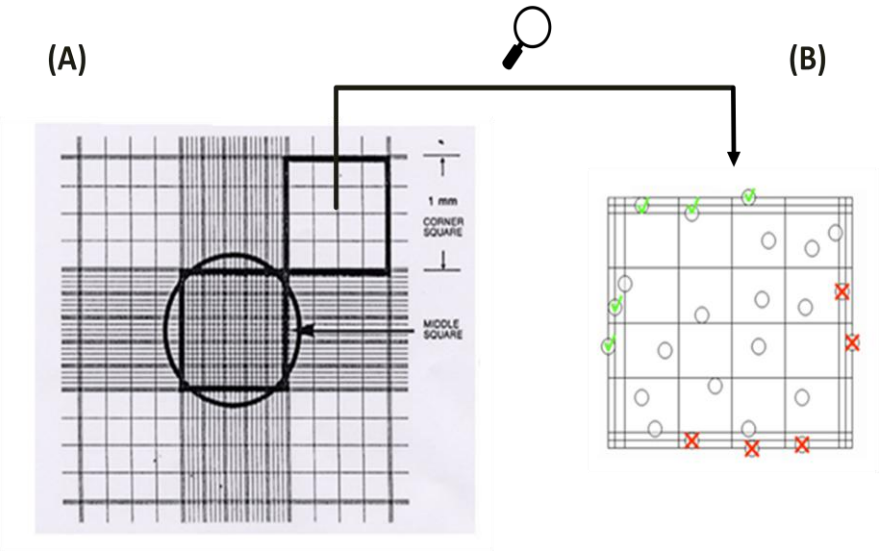

Figure 29: (A) Haemocytometer grid visualised under the microscope consisting of 9 large squares (B) Counting system to ensure accuracy and consistency (Phe-culturecollection).

The formula below makes it possible to estimate the cell density from the number of living cells counted. The 10^4conversion factor is used to express the cell density within 1ml. Once the cell density is known, 10 000 cells/cm^2 were transferred along with fresh culture medium in a new culture flask to reach confluence after 7 days.

$$Cell\ density\ (cells/mL\ ) = \frac{(number\ of\ living\ cells\ x\ dilution\ factor(2) x\ 10^4)}{number\ of\ counted\ large\ squares\ (3)}$$

1.3. Plate culturing

Plate cultures are used to perform experiments that require exposure of cells to multiple conditions. After counting the cell density of the suspension obtained from the flask, we added the right amount of culture medium to the suspension to adjust the cell density to 63 000 cells/cm^2. Caco-2 cells were then inoculated on 24 or 48-well polystyrene plates or on 12-insert plates (Corning). The culture media (DMEM) were changed every 2 or 3 days to ensure cell survival. Cells were fully differentiated 21 days after inoculation and the experiments could then be performed.

1.3.1 24 and 48-well plates

The plates that had to be inoculated were first pre-treated with collagen 1% (v/v) in PBS for 1 hour at 37°C to promote cell attachment. After rinsing the wells with PBS, cells were seeded at 63 000 cells/cm^2. Experiments were performed after 21 days differentiation in either 24-well plates for HO-1 assays or 48-well plates for NBT and enzyme activity assays. Only the 24 central wells of 48 well plates were used to avoid a too important evaporation of the culture medium at the periphery.

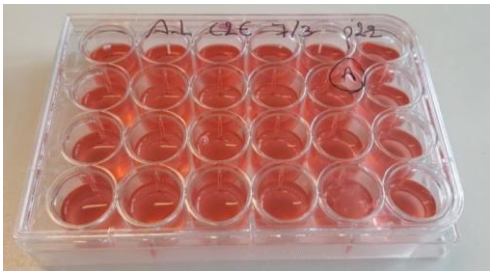

Figure 30: 24-well plate (Corning) for cell culturing with culture medium.

1.4. Transwell™ polycarbonate inserts

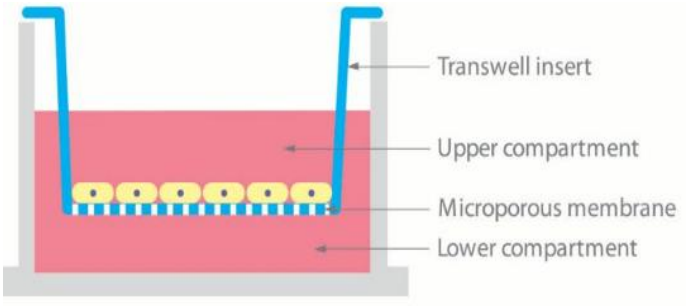

Figure 31: Illustration of a Transwell™ insert (Corning Permeable Support Systems).

Caco-2 cells were grown on 12-well plate inserts (Costar Transwell Permeable Supports, Corning), consisting of a microporous membrane that divides the well into two compartments. This membrane is made of polycarbonate and has pores with a diameter of 0.4 µm (Fig 31).

The first compartment, the apical compartment, mimics the intestinal lumen whereas the basal compartment mimics the blood circulation. The plates are inoculated at the apical compartment at 63 000 cells/cm^2 (corresponding to 70 000 cells/well). Culture medium was added both on the apical (0.35 ml) and the basolateral compartment (1.5 ml). The experiments were performed 21 days later, on fully differentiated cells. Plates with Transwell™ inserts were used for experiments regarding the inflammatory markers IL-8 and IL-6.

2. Chemicals

In order to create the different AgNPs and Ag^+ treatments that were added on cells during the experiments, Hank's Balanced Salt Solution (HBSS, Lonza, Verviers, BE) was used as solvent. Indeed, according to previous work, HBSS strongly limits interaction between and AgNPs or Ag^+, unlike other solutions such as DMEM (Master's thesis Massart I., 2016). Moreover, HBSS is the simplest culture medium since it maintains pH and osmotic balance as well as providing essential inorganic ions and glucose to the cells. However, chloride anions contained in HBSS medium will likely interact with Ag^+ to form AgCl.

2.1. Silver nanoparticles (AgNPs)

Silver nanoparticles (NM-300K, Joint Research Center repository, Ispra, IT) were characterized by the manufacturer for having an average diameter of 15 nm and 90% of the particles have a diameter < 20 nm. They were suspended in an aqueous solution (1 016 µg/ml) and form a colloidal suspension. This aqueous suspension, called "dispersant", is composed of non-ionic surfactants (4% (v/v) polyoxyethylene sorbitan mono-laurate (Tween 20) and 4% (v/v) polyoxyethylene-glycerol-trioleate), which stabilizes and limits particle aggregation. A certain volume of this suspension of AgNPs was weighed and was diluted in MilliQ water (Merck Millipore, Darmstadt, DE) to obtain a stock solution (300 µg/ml) from which the solutions used in the tests were diluted successively in MilliQ water. These solutions were added on cells in HBSS to obtain the final concentrations ranging from 1.5 to 15 µg /ml. Previous work has shown that this range of concentrations was not cytotoxic (Master's thesis Massart I., 2016). In the case of plates with Transwell™ inserts, incubation solutions were placed in the apical side to mimic oral exposure.

2.2. Silver nitrate (source of Ag^+)

The $AgNO_3$ (> 99.5%, Sigma-Aldrich, Steinheim, DE) was solubilized in milliQ water to obtain a stock solution (3mg/ml of Ag^+). From this stock solution, the $AgNO_3$ solutions used during the tests were obtained by serial dilutions in milliQ water. These were diluted directly on cells in the HBSS to reach the final non cytotoxic concentrations ranging from 0.15 to 1.5 µg/ml of Ag^+. In the case of plates with Transwell™ inserts, incubation solutions were placed in the apical compartment to mimic oral exposure.

2.3. *In vitro* inflammatory cocktail

An inflammatory cocktail was applied on Caco-2 cells in order to reproduce *in vivo* inflammatory conditions that lead to the activation of the NF-κB pathway as described in Van de Walle *et al.* (2010). The inflammatory cocktail consisted of 50 ng/mL tumor necrosis factor α, 25 ng/mL interleukin-1β, 50 ng/mL interferon-γ and 1 µg/mL lipopolysaccharide all provided by Sigma-Aldrich. For inserts, lipopolysaccharide was placed in the apical chamber while the other components were added in the basolateral compartment.

3. Assays on fully differentiated Caco-2 cells

These assays aimed at studying whether AgNPs and Ag^+ induce oxidative stress and cellular responses to it. In order address this question, we performed a first assay estimating the ability of AgNPs and Ag^+ to induce the production of ROS. In addition, various assays determined the activity of cellular enzymes that are able to reduce oxidative stress. Enzymes that were analyses were: catalase, glutathione reductase, glutathione peroxidase and glutathione-S-transferase. In order to determine the activation of Nrf2 pathway following oxidative stress, we performed HO-1 quantification by ELISA. Finally, we also quantified IL-8 and IL-6 cytokines in order to determine if their production can be explained by the Nrf2 pathway.

3.1. Nitro Blue Tetrazolium salt (NBT) assay

This assay aimed at studying whether AgNPs and Ag^+ induce oxidative stress in Caco-2 cells. The assay was performed on 48-well plates, 3 weeks after inoculation, so that the cells were fully differentiated. This assay measures the production of ROS in cells via the formation of blue crystals of formazan.

Treatments

We first exposed cells to the different treatments (HBSS, AgNPs, Ag^+, tBuOOH) during 3 hours. In this test, HBSS represents our negative control whereas tert-Butylhydroperoxide (tBuOOH) served as a positive control that is known to induce ROS. We tested two different positive controls at two different concentrations: tBuOOH (0.8 – 1.6 mM) and Cumen hydroperoxide (0.1- 0.2 mM) but we decided to use tBuOOH at 1.6 mM since it induced the highest response for the NBT assay. Finally, different concentration of AgNPs (1.5 - 5 -10 -15 µg/ml) and Ag^+ (0.15 - 0.5 -1- 1.5 µg/ml) were tested on cells.

After the 3 hours incubation period with these different treatments and after rinsing the wells, the soluble tetrazolium reagent was placed on cells for another 3 hours. This yellow reagent is absorbed by the cells and is located in their cytosol where it can be reduced by ROS and form a blue compound (Fig. 32). After rinsing the wells again, we added the extraction solution composed of dimethyl sulfoxide (DMSO) and sodium hydroxide (NaOH) whose role was to dissolve and extract the blue crystals. Finally, 200µl of each well were transferred into a 96-well plate to read the absorbance at 680 nm, enabling the quantification of ROS present in the cells.

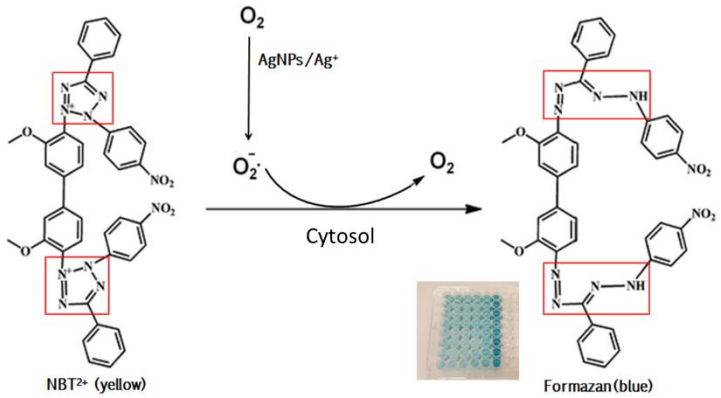

Figure 32: NBT assay reaction and formation of a blue compound.

3.2. Enzymatic tests

We performed enzyme activity assays in order to see if AgNPs induced a change in the activity of enzymes involved in reducing oxidative stress. For all enzymatic tests, we exposed cells to either HBSS or AgNPs (15µg/ml) for 3h. After the 3h incubation period, variable recovery periods (0h, 3h, 6h, 15h or 21h) in culture medium were applied (Fig. 33). Enzymatic tests were performed on cellular extracts obtained after the different recovery periods.

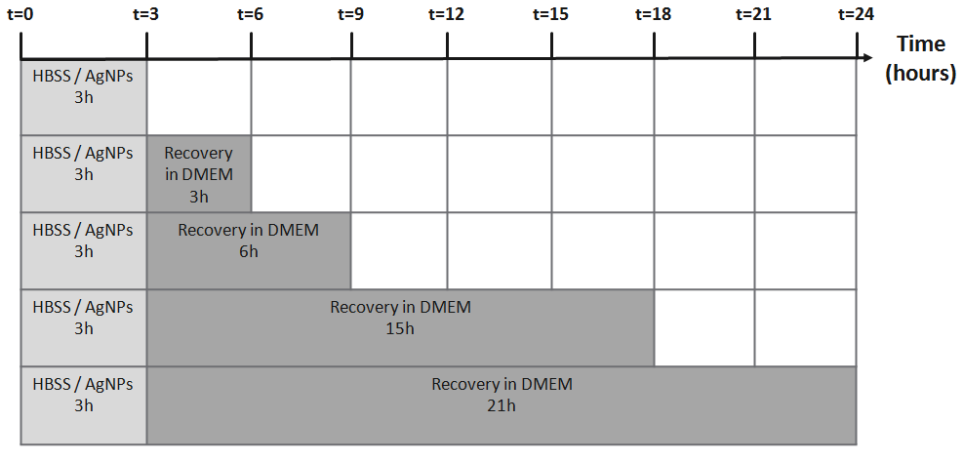

Figure 33: Representation of the timeline for enzymatic tests.

Enzyme activity assays were performed as described in Martirosyan *et al.,* 2016;

- Catalase (CAT) activity was determined by measuring the kinetics (every 20 sec for 10 min) of hydrogen peroxide (H_2O_2) decomposition at 240 nm in 50 mM phosphate buffer, pH 7.2.

$$2\,H_2O_2 \xrightarrow{CAT} O_2 + 2\,H_2O$$

- Glutathione reductase (GR) activity was measured by kinetics of NAD(P)H consumption in the presence of oxidized glutathione (GSSG), monitored at 340 nm.

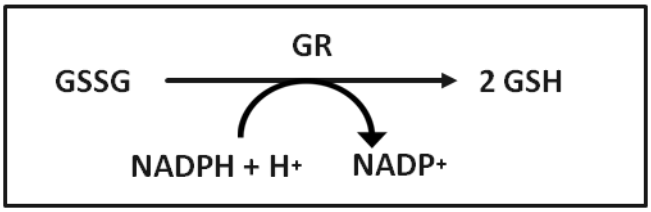

- Glutathione-S-transferase (GST) activity was assayed by the kinetics of the formation of the S-(DNP)GS complex by the reaction of GSH with 1-chloro-2,4-dinitrobenzene (CDNB) at 340 nm.

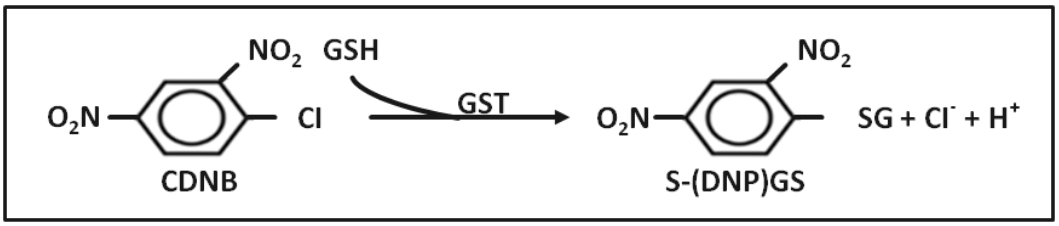

- Glutathione peroxidase (GP) activity was quantified by continuous kinetics of the consumption of NAD(P)H measured at 340 nm by coupling its reaction with GR consumption of GSSG, generated by the GP.

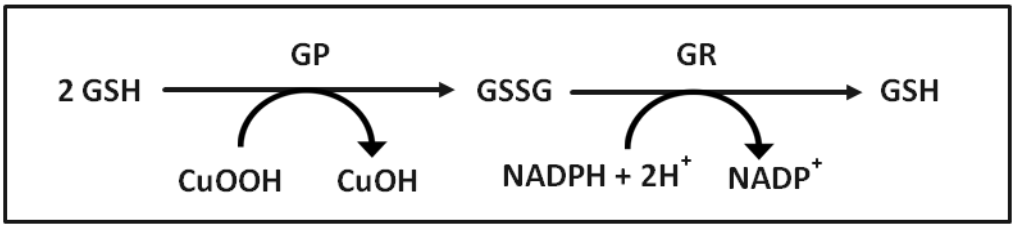

Bradford protein assay

Total protein content was quantified for each cellular extract by performing a Bradford assay. The principle of this assay is that the binding of protein molecules to Coomassie Brilliant Blue (CBB) dye under acidic conditions results in a color change from brown to blue. This method actually measures the presence of the basic amino acid residues, arginine, lysine and histidine, which contributes to formation of the protein-dye complex. Serial dilutions of BSA protein standard were made ranging from 5 to 50 µg/ml in order to establish the BSA standard curve that will allow total protein quantification. The absorbance was measured at 610 nm.

3.3. HO-1 quantification

Furthermore, we wanted to determine whether AgNPs and Ag^+ induce the activation of the Nrf2 pathway. The HO-1 protein, a known target of Nrf2, was quantified by performing an Enzyme linked immunosorbent assay (ELISA).

Trigonelline, an Nrf2 inhibitor, was used in order to verify if AgNPs and Ag^+ act through the Nrf2 pathway. Trigonelline (N-methylnicotinic acid) is an alkaloid derived from coffee beans, which acts by destabilising Nrf2 and therefore inhibiting Nrf2 activity (Bollong *et al.*, 2015). On the other hand, tert-Butylhydroquinone (tBHQ) was used as positive control for Nrf2 activation. TBHQ alters the redox status in the mitochondrial compartment leading to mitochondrial oxidative stress resulting in Nrf2 activation.

Trigonelline efficiently decreased tBHQ-induced Nrf2 activity in pancreatic carcinoma cell lines (No *et al.*, 2014). Furthermore, it was also able to block the expression of HO-1 in hepatocellular carcinoma cells confirming its ability to act as an Nrf2 inhibitor (Xiaofang *et al.*, 2015).

Treatments

Preliminary tests were performed in order to:

(I) verify that trigonelline inhibits the production of HO-1,

(II) determine the concentration of trigonelline to use,

(III) check that the used concentrations are not cytotoxic via an LDH test and

(IV) choose whether to pre-incubate or co-incubate with trigonelline.

From these pre-tests we decided to pre-incubate with trigonelline at the concentration of 1 µg/ml that was proven not to be cytotoxic (<10% necrosis).

Concerning the Nrf2 activator, different conditions were tested: (tBHQ 50-200 µM; MG-132 50 µM). Since tBHQ 200 µM induced the highest HO-1 response, it was therefore selected for the actual test. This concentration of tBHQ also had a negligible toxicity on Caco-2 cells.

For the actual assay, fully differentiated Caco-2 cells in 2 different 24-well plates were used. In order to determine the effects of trigonelline (Nrf2 inhibitor) on the production of HO-1 by cells exposed to AgNPs and Ag^+, we performed a 1h pre-incubation period with trigonelline 1µM (Plate 2) in HBSS. After the trigonelline treatment, both plates were rinsed with HBSS and the different treatments (Fig. 34) (tBHQ 200µM; AgNPs 1.5-5-15 µg/ml; Ag^+ 0.15-0.5-1.5 µg/ml; HBSS and Cocktail) were applied and incubated 3 h at 37 °C. The solvent used for all the solutions was HBSS and the total volume present in each well was 600 µl.

After the 3h incubation, the wells were rinsed with HBSS and the Caco-2 cell layer was collected in 500 µl radioimmunoprecipitation assay (RIPA) buffer added with a protease inhibitor pellet (cOmplete, Sigma-Aldrich). After sonication (170W, 5 min) and centrifugation (6260 g, 5 min), the total amount of protein in cell extracts was quantified through BCA assay and HO-1 was quantified through ELISA.

Plate 1: without pre-incubation with trigonelline					
tBHQ	tBHQ	tBHQ	Ag^+ 0.15	Ag^+ 0.15	Ag^+ 0.15
AgNPs 1.5	AgNPs 1.5	AgNPs 1.5	Ag^+ 0.5	Ag^+ 0.5	Ag^+ 0.5
AgNPs 5	AgNPs 5	AgNPs 5	Ag^+ 1.5	Ag^+ 1.5	Ag^+ 1.5
AgNPs 15	AgNPs 15	AgNPs 15	HBSS	HBSS	HBSS
/	/	/	Cocktail	Cocktail	Cocktail

Plate 2: with 1h pre-incubation with trigonelline					
tBHQ+ trigo	tBHQ+ trigo	tBHQ+ trigo	Ag^+ 0.15 + trigo	Ag^+ 0.15 + trigo	Ag^+ 0.15 + trigo
AgNPs 1.5 + trigo	AgNPs 1.5 + trigo	AgNPs 1.5 + trigo	Ag^+ 0.5 + trigo	Ag^+ 0.5 + trigo	Ag^+ 0.5 + trigo
AgNPs 5 + trigo	AgNPs 5 + trigo	AgNPs 5 + trigo	Ag^+ 1.5 + trigo	Ag^+ 1.5 + trigo	Ag^+ 1.5 + trigo
AgNPs 15 + trigo	AgNPs 15 + trigo	AgNPs 15 + trigo	/	/	/

Figure 34: Organisation of the different treatments for the HO-1 assay.

ELISA for HO-1 quantification

The HO-1 dosage required an enzyme linked immunosorbent assay, commonly named ELISA. The sandwich immunocapture principle is illustrated in figure 35. First of all, the plate was covered with specific capture ABs (coating buffer) and incubated overnight at room temperature (RT). The day of the assay, several steps were executed separated each time by several rinses using wash buffer. After blocking with bovine serum albumin (BSA), samples and standards containing HO-1 AGs were incubated for 1h at RT. During this step, the HO-1 AGs were being captured by the complementary ABs in solid phase. After rinsing the wells various times with wash buffer, secondary detection ABs were added for another 1h incubation at RT. The secondary ABs enable the detection of the captured AGs since they contain labelled ABs recognising another epitope of the AGs. In this case, ABs are coupled with biotin, which is the binding site for the horseradish peroxidase enzyme coupled with streptavidin. The next step consisted of adding for 30 min the horseradish peroxidase enzyme coupled with streptavidin the allows the transformation of the 3,3',5,5'-tetramethylbenzidine (TMB) substrate in a coloured product. Finally, the reaction was stopped after 30 min with HCl (1M) and the absorbance was read at 450 nm (corrected at 570 nm) using a spectrophotometer. Using the calibration curve, the amounts HO-1 (pg/well) were determined. The detection limit of this assay is 0.049 ng/ml.

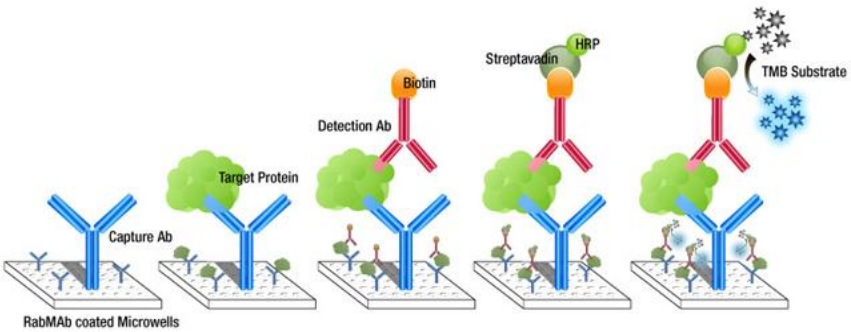

Figure 35: Enzyme linked immunosorbent assay (ELISA) principle.

Lactate dehydrogenase (LDH) assay

The LDH assay is a colorimetric test indicative of cellular integrity. The measurement is directly proportional to the amount of necrosis. Since lactate dehydrogenase (LDH) is an exclusively cytosolic enzyme, an increased enzymatic activity measured in the culture medium indicates an alteration of membrane permeability and makes it possible to estimate cell death (Fig. 36). The LDH leakage in dead or damaged cells allows the conversion of lactate in pyruvate and regenerates NADH from NAD^+ and H^+. In turn, NADH enables the conversion of the tetrazolium salt in formazan. The resulting formazan absorbs maximally at 492 nm and can be measured quantitatively at 490 nm with a 650 nm reference wavelength. The LDH assay was used to check that the different treatments applied on Caco-2 cells were not inducing cytotoxic effects.

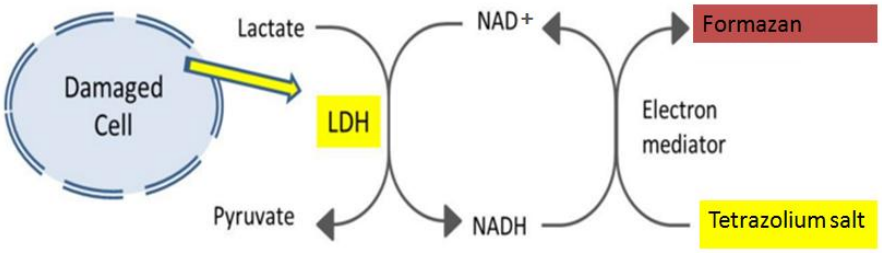

Figure 36: LDH detection mechanism (Dojindo).

BCA assay principle

The bicinchoninic acid (BCA) protein assay is used for the quantification of total protein in a sample. The BCA stock solution contains among others bicinchoninic acid and copper (II) sulfate pentahydrate in a highly alkaline solution (pH 11.25). The BCA assay relies on two major reactions (Fig. 37). Firstly, the peptide bonds in protein reduce Cu^{2+} to Cu^+. This reduction is caused by four amino acid residues including cysteine or cystine, tyrosine, and tryptophan that are present in protein molecules. As a consequence, the amount of reduced Cu^{2+} is proportional to the amount of protein present in the solution. The second reaction consists of two molecules of bicinchoninic acid that chelate with Cu^+, forming a purple-colored complex that strongly absorbs light at a wavelength of 562 nm.

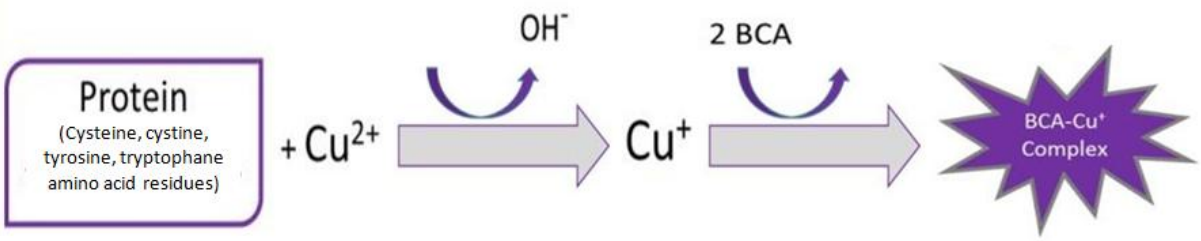

Figure 37: BCA protein assay principle (BQC kit).

BCA assay methodology

The first step of this assay consists of preparing standard solutions (in RIPA buffer) of known protein concentration. BSA standards were used for the calibration curve with concentrations in the range of 200-2000 µg/ml. 25µL of samples (diluted if necessary) was mixed with 200µL of BCA working reagent (according to the manufacturer's instructions) and incubated at 37 °C for 30 min. The absorbance was read at 562 nm and correlated to the protein concentration using the calibration curve (Fig. 38). BCA assay was performed on cellular extracts collected during HO-1, IL-8 and IL-6 tests to determine total protein content.

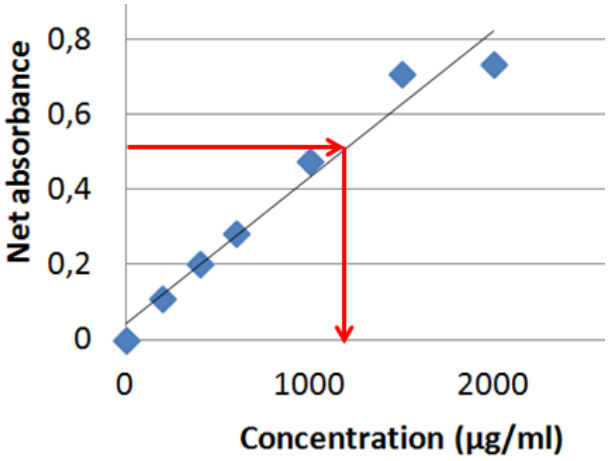

Figure 38: BCA calibration curve allowing the determination of protein concentration in samples.

3.4. IL-8 and IL-6 quantification

Previous analysis at the laboratory showed an increased IL-8 production after AgNPs and Ag^+ treatments. Furthermore, they could not conclude that this inflammatory cytokine was produced by the NF-κB pathway. Therefore, we wanted to investigate whether this IL-8 production could be due to the Nrf2 pathway as a response to oxidative stress induced by AgNPs and Ag^+. In addition to IL-8, we also quantified IL-6 production.

Treatments

Tests were performed on fully differentiated Caco-2 cells in Transwell™ inserts. After equilibration for 30 min in HBSS and a trigonelline pre-incubation treatment for some of the wells, cells were incubated with different treatments for 3 h as described in figure 39. In the apical chamber, we applied 350µL of tBHQ, AgNPs, cocktail or HBSS, each diluted in HBSS whereas the basolateral chamber contained 1.5mL of HBSS.

After the 3 h incubation, media on both sides of the inserts were collected and replaced by culture medium during 21 h at 37 °C, hereafter called the "recovery period". After this final recovery period, the extracellular media were again collected and stored at -20°C until the day of the dosage. Cells were also collected in 200µl of RIPA buffer, added with a protease inhibitor pellet (cOmplete) and were sonicated (170 W, 5 min) followed by a centrifugation (6260 g, 5 min). They were used for the BCA assay to quantify the total amount of protein.

Interestingly we also measured the transepithelial electrical resistance (TEER) after the 3h incubation period with the different treatments to assess the monolayer permeability that could be affected by AgNPs.

Plate 1: without pre-incubation with trigonelline			
tBHQ	AgNPs 1.5	AgNPs 5	AgNPs 15
tBHQ	AgNPs 1.5	AgNPs 5	AgNPs 15
/	/	/	AgNPs 15

Plate 2: with 1h pre-incubation with trigonelline			
tBHQ + trigo	AgNPs 1.5 + trigo	AgNPs 5 + trigo	AgNPs 15 +trigo
tBHQ + trigo	AgNPs 1.5 + trigo	AgNPs 5 + trigo	AgNPs 15 +trigo
tBHQ + trigo	AgNPs 1.5 + trigo	AgNPs 5 + trigo	AgNPs 15 +trigo

Plate 3: with or without trigonelline		
HBSS	Cocktail	Cocktail +trigo
HBSS	Cocktail	Cocktail +trigo
HBSS	Cocktail	Cocktail +trigo

Figure 39: Different treatments applied on 30 Transwell™ inserts. The different conditions consist of: either 3h incubation with (tBHQ 200µM-AgNPs 1.5-5-15 µg/ml-Cocktail–HBSS), or a 1h pre-incubation with trigonelline 1 µg/ml followed by the 3h incubation.

ELISA for IL-8 and IL-6 quantification

Both IL-8 and IL-6 quantifications were performed by ELISA, very similarly to HO-1, according to the manufacturer's instructions. After coating the wells with specific capture ABs, the plates were incubated overnight at 4°C. Free sites were blocked with assay diluent containing serum. Then, samples and standards containing AGs (target protein) were loaded and incubated for 2h at RT. During this step, the AGs are being captured by the complementary ABs in solid phase. After rinsing the wells various times with wash buffer, the working reagent, containing both detections ABs and the horseradish peroxidase coupled with streptavidin, was added and incubated for 1h at room temperature. After that, the TMB substrate was added for 30 min allowing the formation of a coloured product. Finally, the reaction was stopped with HCl (1M) and the absorbance was read at 450 nm (corrected at 570 nm) on a spectrophotometer. Using the calibration curve, the amounts IL-8 and IL-6 (pg/well) were determined.

3.5. TransEpithelial Electric Resistance (TEER)

TEER measures the transepithelial electrical resistance of the cellular monolayer, expressed in Ωcm^2 and reflecting the degree of passage of ions through the epithelium. A difference in electrical resistance reflects a variation in paracellular permeability. Paracellular passage is considered to be the limiting factor for solutes transport since the resistance of the apical and basolateral membranes, as well as that of intercellular spaces, is negligible. The tight junctions limit a large part of the paracellular passage by allowing an important cohesion between cells. They are responsible for the epithelium impermeability and are crucial to ensure barrier properties of intestinal cells. We can evaluate the integrity and functional closure of these tight junctions by measuring the electrical resistance of the cell layer. If the integrity of the tight junctions is compromised, the resistance decreases allowing ions to pass more easily through the epithelium. TEER was evaluated after the 3h incubation period with the different treatments to determine the influence of AgNPs on tight junction integrity.

Protocol TEER measurement

After exposing the cellular monolayer for 3h at 37 °C to the different treatments, the TEER was measured (by Epithelial voltohmmeter, WPI, Sarasota, FL) by placing a first electrode (Millipore, Millicell-ERS, Billerica, MA) in the apical medium, another one in the basolateral medium (Figure 40). The values were expressed as a percentage of TEER values measured for the HBSS control.

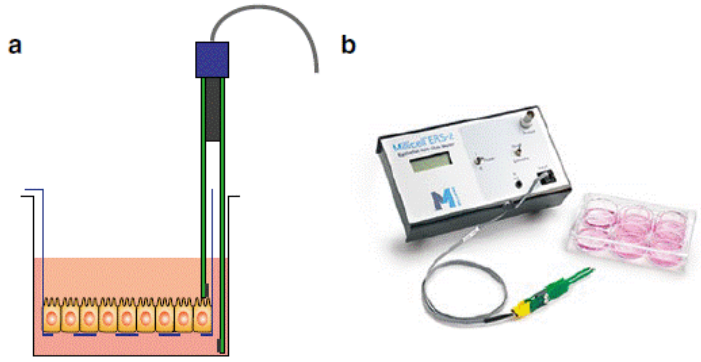

Figure 40: (A) Measurement of the transepithelial electrical resistance in Caco-2 cells located in transwell™ inserts (B) Epithelial voltohmmeter equipement (Ebrary).

4. Statistical analysis

In order to draw relevant conclusions that are supported by statistical analysis, each experimental condition had to be repeated. Therefore, most of the tests described above have been repeated in a similar manner on different dates. These biological repetitions included on each date a certain number of samples treated with the same condition, called replicates.

All statistical analysis was performed using JMP13 of SAS Institute Inc. First of all, the normality of the data distribution (by Shapiro-Wilk) and the equality of variances (by Levene) were verified. These two conditions determine which comparison test was the most accurate in order to confirm if the differences between the data coming from various treatments were significantly different than the control (HBSS treatment).

When data had a normal distribution and equal variances, ANOVA-1 could be applied to verify if at least one of the treatments resulted in a significant difference. If this was the case, Dunnet's method was used to carry out a multiple step-comparison that compared each treatment to the control.

If the data followed a normal distribution, but the variances were not equal, a more robust ANOVA (Welch ANOVA) had to be applied. Treatments were compared individually to the control by the simple Student test. However, the significance threshold had to be modified according to the Bonferroni correction by reason of the multiple treatment comparison. All data were expressed as mean ± SEM (standard error of the means). Differences were considered statistically significant when the probability p*value < 0.05 or in case of Bonferroni, $p ** value < \frac{0.05}{\#treatments - 1(control)}$.

Objectives

AgNPs are the nanoparticles found in the highest number of consumer products because of their interesting physicochemical properties. They are already integrated in many products of the food processing sector due to their specific antimicrobial properties. Applications go from food packaging materials to antimicrobial sprays and even to dietary supplements. AgNPs can therefore be ingested and come into contact with our digestive tract.

However, several *in vivo* and *in vitro* studies demonstrate that AgNPs can cause toxic effects. Moreover, the mechanisms of action of AgNPs remain largely unknown as well as the fraction of AgNPs toxicity related to the release of Ag^+. Because of their ever-increasing use in the food sector, many questions are raised about their safety on intestinal cells, which are the first protective barrier after ingestion. In order to evaluate the risks to which consumers are exposed, it is imperative to carry out additional investigation.

The objective of this thesis is therefore to contribute to the deepening of the knowledge concerning AgNPs, more particularly to study the impact of AgNPs on oxidative stress and inflammation.

In the present study, Caco-2 cells have been used as an *in vitro* model of human intestinal epithelial cells. The experiments aimed at studying the effects of AgNPs and Ag^+ in order to:
(I) evaluate the ability of AgNPs and Ag^+ to generate ROS and induce oxidative stress;

(II) study the impact of ROS generation on the Nrf2 signalling pathway by quantifying HO-1, a Nrf2 specific gene target;

(III) determine the possible implication of Nrf2 pathway in the increased IL-8 production.

The experiments were performed by NBT assay for ROS quantification and by ELISA for the HO-1 and IL-8 quantification.

Part III: Results

The role of AgNPs and Ag^+ on oxidative stress and Nrf2 pathway was investigated using Caco-2 cells. Nrf2 is one of the major pathways involved in protecting cells from oxidative stress, through the induction of several antioxidant-responsive genes. We performed a first assay estimating the ability of AgNPs and Ag^+ to induce the production of ROS. In addition, various assays determined the activities of cellular enzymes that are able to reduce oxidative stress. Enzymes that were analysed were: catalase, glutathione reductase, glutathione peroxidase and glutathione-S-transferase. In order to determine the activation of the Nrf2 pathway following oxidative stress, we performed an HO-1 quantification by ELISA. Indeed, HO-1 is known to be a specific gene target of the Nrf2 transcription factor. Finally, we also quantified two cytokines, *i.e.* IL-8 and IL-6, in order to determine if their production can be related to the activation of the Nrf2 pathway. Previous research conducted at the lab was unable to prove that NF-κB pathway was responsible for the production of IL-8, which is why we are now studying the potential involvement of Nrf2.

As described in Part II: Materials & methods, treatments mainly consisted of AgNPs/ Ag^+ in the presence or absence of trigonelline pre-incubation. In each experiment, treatments were applied on cells for 3 h at 37 °C. As a reminder, trigonelline acts by destabilising Nrf2 and therefore inhibits Nrf2 activity. Pre-treatment with trigonelline was applied to some wells for experiments involving Nrf2 (HO-1 and IL-8/IL-6). Indeed, under these conditions Nrf2 should be inhibited, which allows us to determine the possible implication of Nrf2 in the observed responses.

1. AgNPs and Ag^+ solutions

As explained in Part I: section 2.5, AgNPs solutions contain a certain amount of Ag^+ that can be released after desorption of Ag^+ from AgNPs surfaces. A long term release of Ag^+ can also occur through oxidative dissolution of AgNPs. This raises the need for characterization of the soluble silver fraction in AgNPs suspensions in order to distinguish which fraction of the observed effect might be caused by Ag^+. A study conducted with AgNPs similar to ours demonstrated an average Ag^+ content of 7% in AgNPs solutions (Van der Zande *et al.*, 2014). We therefore took this fact into account and decided to compare AgNPs treatments with solutions containing 10% Ag^+ in order to be able to determine any nano-specific effect. We suspect that our AgNPs solutions contain even less than 10% Ag^+ since we keep them safe from heat and light, which reduces long term AgNPs dissolution.

We decided to use non-cytotoxic concentrations for the experiments. Based on different cytotoxicity assays previously performed at the laboratory, we opted for the following concentrations: 1.5-5-10-15 µg/ml AgNPs and 0.15-0.5-1-1.5 µg/ml for Ag^+.

In order to obtain those solutions, a certain volume of AgNPs suspension was weighed and diluted in MilliQ water to obtain a stock solution (300 µg/ml) from which the solutions used in the tests were diluted successively in MilliQ water. These solutions were finally added on the cells in HBSS during the experiments to obtain the final concentrations ranging from 1.5 to 15 µg /ml. Regarding Ag^+ solutions, we used $AgNO_3$ in powder form as a source of Ag^+. The $AgNO_3$ was solubilized in milliQ water to obtain a stock solution (3 mg/ml of Ag^+). We performed serial dilutions of this stock solution in milliQ water after finally diluting them on the cells contained in the HBSS to reach the final and non cytotoxic concentrations ranging from 0.15 to 1.5 µg/ml of Ag^+.

We chose HBSS to dilute the AgNPs and Ag^+ solutions during the experiments because HBSS is the simplest culture medium. It is used to maintain pH and osmotic balance as well as providing essential inorganic ions and glucose to the cells. In addition, HBSS strongly limits the interaction of AgNPs and Ag^+ with constitutive elements of the medium as might be the case for more complex media containing serum (Master's thesis Vandenkerckhove J., 2015; Master's thesis Massart I, 2016). However, chloride anions contained in HBSS medium could most likely interact with Ag^+ to form AgCl.

2. Nitro Blue Tetrazolium salt (NBT) assay

The NBT assay was used to determine the capacity of different treatments to induce oxidative stress in Caco-2 cells, as this reagent is oxidized by reactive oxygen species to form blue crystals of formazan. It was performed on 48-well plates, 3 weeks after inoculation, so that the cells were fully differentiated.
We first exposed the cells for 3h to the different treatments (HBSS, AgNPs, Ag^+, tBuOOH). After that, the soluble tetrazolium reagent was placed on the cells for another 3 hours. This yellow reagent is absorbed by cells and is located in their cytoplasm where it can be reduced by ROS and form a blue compound. The blue crystals were then extracted with a solution composed of DMSO and NaOH. Finally, the absorbance was read at 680 nm, enabling the quantification of ROS that were present in the cells.

Protocol elaboration

In order to verify that the NBT response was effectively due to an increased ROS production, we needed to have a positive control that is known to induce ROS. We tested two different positive controls at two different concentrations: tert-Butyl hydroperoxide (tBuOOH 0.8 - 1.6 mM) and Cumen hydroperoxide (CuOOH 0.1- 0.2 mM) based on similar experiments performed in the lab. According to figure 41, CuOOH at 0.2 mM and tBuOOH at 1.6 mM induced the production of ROS in Caco-2 cells. Based on these results, we decided to use tBuOOH at 1.6 mM since it induced the highest response for the NBT assay.

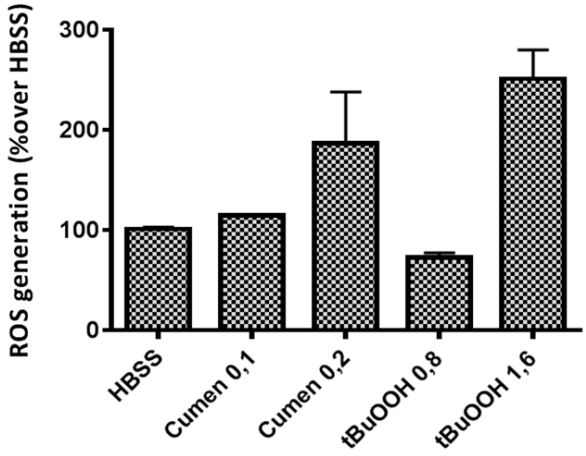

Figure 41: Different positive controls tested for the NBT assay: tBuOOH (0.8-1.6 mM) and CuOOH (0.1- 0.2 mM). Results are expressed as a percentage of the absorbance over the absorbance of cells treated with HBSS, the negative control. Values (mean ± SEM) come from one repetition with three replicates per condition.

Results for the NBT assay

As a reminder, the NBT assay aims at measuring the capacity of AgNPs and Ag^+ to induce reactive oxygen species (ROS) in Caco-2 cells through the formation of blue crystals of formazan. The obtained results are shown on figure 42.

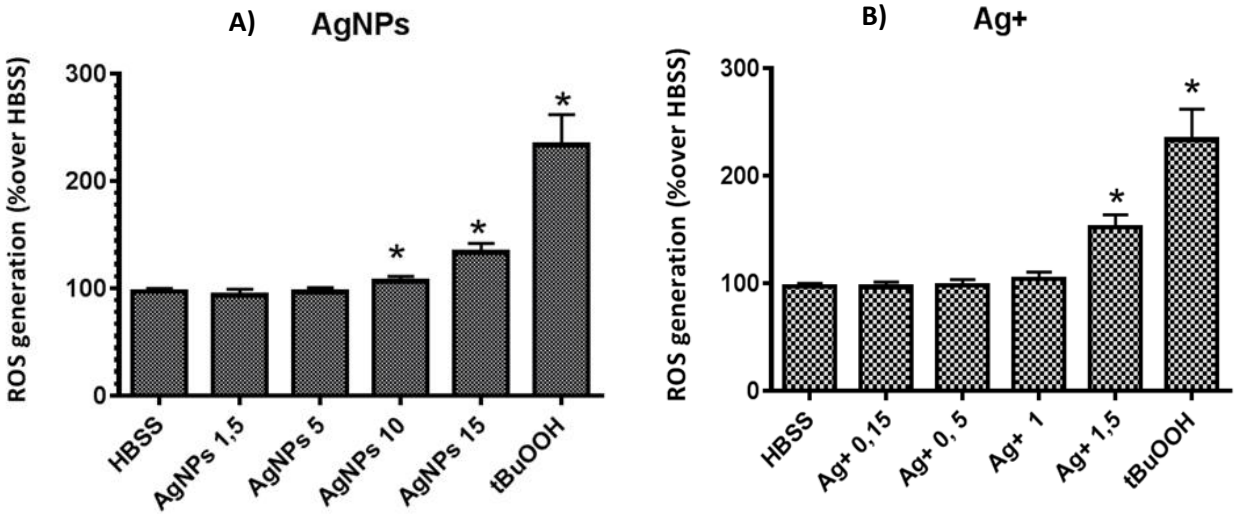

Figure 42: NBT assay results for AgNPs (A) and Ag^+ (B) treatments. ROS generation is expressed as a percentage of the absorbance over the absorbance of cells treated with HBSS, the negative control. Values (mean ± SEM) come from three repetitions with three replicates per condition. Asterisks show values significantly different from the control (HBSS).

According to figure 42 (A) representing the absorbance of the AgNPs and tBuOOH (positive control) treatments compared to the HBSS (negative control), we can see that there is a significant difference between AgNPs (10 and 15 µg/ml) and the HBSS treatments. This confirms that AgNPs induce ROS in Caco-2 cells.

The same conclusion can be drawn for the Ag^+ treatments (Fig. 42 (B)) where only the highest concentration (Ag^+ 1.5 µg/ml) induced a significantly different response compared to HBSS.

Interestingly, we can also detect a nano-specific effect on ROS production. Indeed, according to the literature only 10% maximum of Ag^+ can be released from AgNPs. The AgNPs (10 µg/ml) treatment was significantly different from the HBSS control, whereas the Ag^+ (1 µg/ml) treatment was not, suggesting that the ROS production can not only be explained by the release of Ag^+ from AgNPs.

For both tests the tBuOOH was significantly different than the HBSS treatment, confirming its capacity to induce oxidative stress.

3. Enzymatic tests

Preliminary tests to measure oxidative stress related enzymes did not show any significant effect on enzymatic activity (results not shown). We suspect that the sensitivity of the tests was not sufficient to detect differences. We therefore did not perform enzymatic tests with enough repetitions to be able to draw conclusions. However, other studies have been able to study the effects of AgNPs on enzymatic activity of various oxidative stress related enzymes and those studies will be talked about in the discussion.

4. HO-1 quantification

In order to determine if the AgNPs-induced oxidative stress increased the Nrf2 pathway, we quantified HO-1 protein through ELISA. Nrf2 is one of the major pathways involved in protecting cells from oxidative stress, through the induction of several cytoprotective genes such as HO-1. Indeed, the HO-1 gene is a known Nrf2 target and its response is supposed to increase when Nrf2 signalling pathway is activated. For this experiment, trigonelline was used as an Nrf2 inhibitor, whereas tert-Butylhydroquinone tBHQ was used as positive control for Nrf2 activation. Trigonelline is an alkaloid derived from coffee beans that acts by destabilising Nrf2 and therefore inhibiting Nrf2 activity. On the other hand, tBHQ alters the redox status in the mitochondrial compartment leading to mitochondrial oxidative stress resulting in Nrf2 activation.

Approximately half of the wells containing fully differentiated Caco-2 cells were pre-incubated for 1h with trigonelline (Nrf2 inhibitor) 1µM in HBSS, in order to determine the involvement of Nrf2 on HO-1 production by cells exposed to AgNPs and Ag^+.

After the trigonelline treatment for half of the wells, all the 48 wells were rinsed with HBSS and the different treatments (HBSS; AgNPs 1.5-5-15 µg/ml; Ag^+ 0.15-0.5-1.5 µg/ml; tBHQ 200 µM or Cocktail) were applied and incubated for 3h at 37 °C. Finally, the Caco-2 cell layer was collected in a buffer containing protease inhibitors. The cell layer was stored at -20°C after sonication (170 W, 5 min) and centrifugation (6260 g, 5 min) until the day of the HO-1 quantification through ELISA.

Protocol elaboration

Before performing the actual tests, we had to perform some preliminary tests in order to choose which Nrf2 activator to use and to determine the experimental conditions for the incubation with trigonelline.

Concerning the Nrf2 activator, different conditions were tested to induce HO-1 production: (tBHQ 50-200 µM; MG-132 50 µM). MG-132 treatment leads to the non-toxic proteasome inhibition, which in turn leads to increased Nrf2 accumulation and nuclear translocation. As a result, MG-132 should increase the levels of HO-1 through Nrf2 signalling pathway (Dreger *et al.*, 2009; Sheng *et al.*, 2017). On the other hand, tBHQ alters the redox status in the mitochondrial compartment leading mitochondrial oxidative stress resulting in Nrf2 activation (Imhoff & Hansen, 2010).

As observed for several proteins after AgNPs treatments, sometimes the amount produced after the 3h exposure is not sufficient to observe significant differences compared to the control. It is therefore frequent to establish a second incubation period in culture medium without AgNPs, called recovery period, to allow cells to produce higher amounts of protein as a response to AgNPs. For convenient reasons, the recovery period has been established at 21h. The secreted HO-1 was quantified either after 3h incubation with the treatments or after 3h incubation with the treatments followed by an additional 21h recovery period.

According to figure 43, the 3h treatment with tBHQ (200 µM) was retained as positive control for the HO-1 tests since it induced the highest HO-1 response. Furthermore, there will not be an additional 21h recovery period since HO-1 levels were higher immediately after the 3h incubation with the treatments.

In order to estimate the possible toxicity of these treatments on Caco-2 cells, we quantified the cytoplasmic lactate dehydrogenase (LDH) enzyme in the extracellular medium. Triton-X was used as positive control for this LDH test since it is highly toxic. Results are presented in figure 44 and are expressed as percentage over the positive control. Since the arbitrary limit of 10% of necrosis is not reached, the cytotoxic effects of the 3h treatment with tBHQ 200 µM are considered to be negligible.

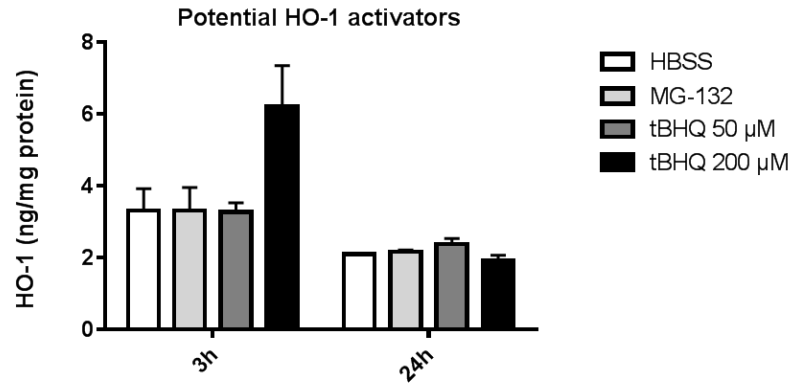

Figure 43: Potential HO-1 activators: MG-132 (50 µM), tBHQ (50 µM) and tBHQ (200 µM) either after a 3h incubation on Caco-2 cells or after a 3h incubation followed by a 21h recovery period in DMEM. Results are normalized by the total amount of protein quantified by BCA assay. Values (mean ± SEM) were assessed by ELISA and come from one repetition with three replicates per condition.

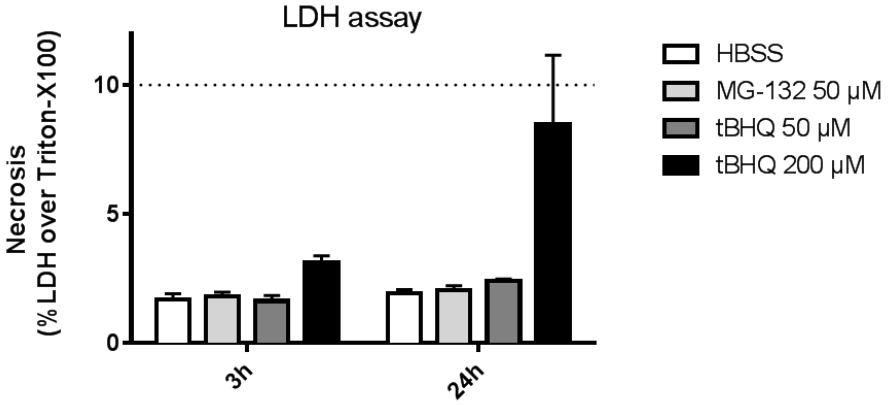

Figure 44: LDH cytotoxic assay for the different potential HO-1 activators either after a 3h incubation on Caco-2 cells or after a 3h incubation followed by a 21h recovery period in DMEM. Results are expressed as percentage of LDH released by cells incubated with Triton-X. Values (mean ± SEM) come from one repetition with three replicates per condition.

On the other hand, experimental conditions for the trigonelline incubation needed to be tested in order to:

(I) verify that trigonelline inhibits the production of HO-1;

(II) determine the concentration of trigonelline to be used;

(III) choose whether to pre-incubate or co-incubate with trigonelline.

For this inhibitor, we tried two different experimental conditions (pre-or co-incubation with tBHQ 200µM) and three different trigonelline concentrations (0.01-0.1-1 µM). Under pre-incubation conditions, trigonelline was added on cells for 1h after being removed and replaced by tBHQ for 3 additional hours. For the co-incubation conditions however, trigonelline was not removed after 1h and tBHQ was added together with the trigonelline that was already present.

The results of these tests are shown on figure 45. From the analysis of this graph, we opted for the highest concentration of trigonelline (1 µM) and choose to pre-incubate. Indeed, those were the conditions that induced the best HO-1 inhibition with a decreased HO-1 production of 42.5% compared to the control (HBSS with tBHQ 200 µM). The retained conditions were proven not to be cytotoxic (results not shown).

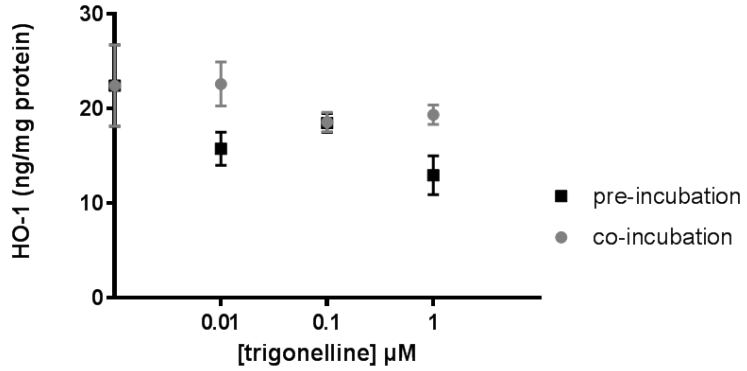

Figure 45: HO-1 quantification after exposure to different concentrations of trigonelline and in conditions of pre-or co-incubation. Results are normalized by the total amount of protein quantified by BCA assay. Values (mean ± SEM) come from one repetition with three replicates.

Results for HO-1 ELISA quantification

Results from the HO-1 ELISA quantification are shown on figures 46 for AgNPs and 47 for Ag^+. We were not able to detect a significant increase in HO-1 production after AgNPs or Ag^+ treatments compared to the HBSS control. Furthermore, tBHQ did not induce a significant increase in HO-1 production compared to HBSS, as it did during the protocol elaboration.

Similarly, the 1h pre-incubation with trigonelline (1 µM) did not result in the inhibition of HO-1 production observed during the elaboration of the protocol.

These two last observations might indicate that trigonelline and/or tBHQ did not induce the response they were supposed to induce. Especially since other studies were able to show HO-1 inhibition by trigonelline and activation by tBHQ (Xiaofang *et al.*, 2015; No *et al.*, 2014). Having repeatedly thawed trigonelline before use may have degraded its quality.

Finally, the inflammatory cocktail was applied in order to reproduce the *in vivo* inflammatory conditions that lead to the activation of the NF-κB pathway. The cocktail consisted of 50 ng/mL TNF-α, 25 ng/mL IL-1β, 50 ng/mL IFN-γ and 1 µg/mL LPS. This time, it is not surprising that we did not detect an HO-1 increase after the treatment with the inflammatory cocktail since HO-1 is a specific gene target of Nrf2 and not NF-κB. This result indicates that the inflammatory cocktail does not induce Nrf2.

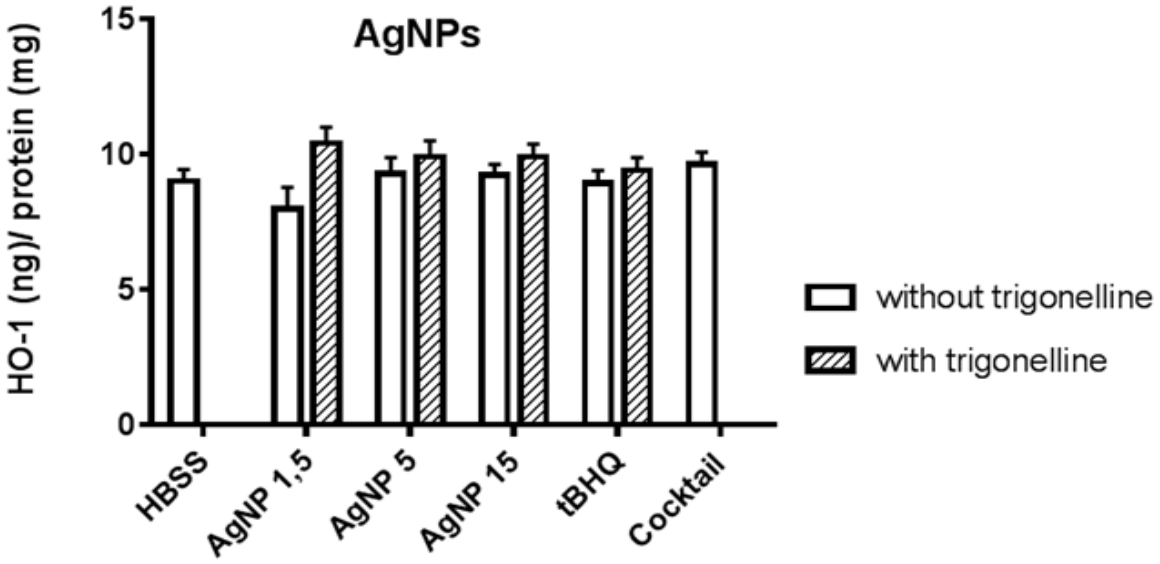

Figure 46: HO-1 ELISA quantification after 3h treatment with: HBSS, AgNPs 1.5-5-15 µg/ml, tBHQ, Cocktail and with or without a 1h pre-incubation period with trigonelline. Results are normalized by the total amount of protein quantified by BCA assay. Values (mean ± SEM) from this graph represent three independent repetitions with three replicates per condition.

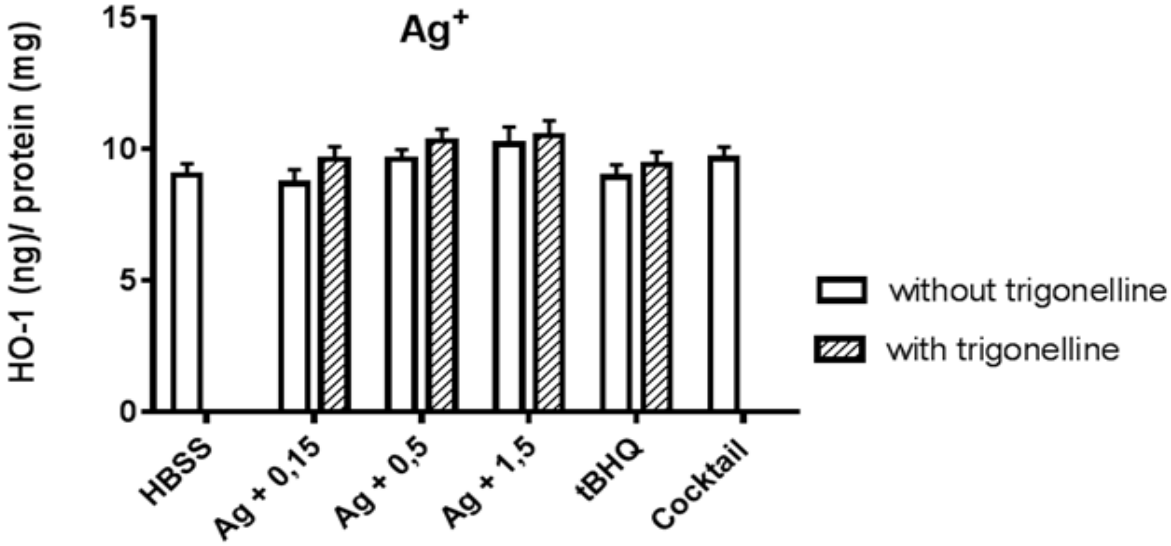

Figure 47: HO-1 ELISA quantification after 3h treatment with: HBSS, Ag+ 0.15-0.5-1.5 µg/ml, tBHQ, Cocktail and with or without a 1h pre-incubation period with trigonelline. Results are normalized by the total amount of protein quantified by BCA assay. Values (mean ± SEM) from this graph represent three independent repetitions with three replicates per condition.

5. IL-8 and IL-6 quantification

Previous analysis at the laboratory showed an increased IL-8 production after AgNPs and Ag^+ treatments. Nevertheless, they could not conclude that the production of this inflammatory cytokine was induced by the NF-κB pathway. Therefore, we would like to investigate whether this IL-8 production can be due to the Nrf2 pathway as a response to oxidative stress induced by AgNPs. In literature, it has already been proven that both IL-6 and IL-8 promoter regions contain a functional antioxidant response element (ARE) that can be targeted by Nrf2 (Zhang *et al.*, 2005; Wruck *et al.*, 2011). Furthermore, there is evidence that Nrf2 activation significantly increases the half-life of IL-8 mRNA resulting in higher levels of protein secretion (Zhang *et al*., 2005). In addition to IL-8, we also analysed IL-6 production.

Tests were performed on fully differentiated Caco-2 cells in Transwell™ inserts. A major advantage with this culture method is the physical separation between the apical and basolateral medium, which is closer to real conditions in the human body. After a 1h trigonelline pre-incubation treatment for some of the wells, all the cells were incubated with different treatments for 3h (HBSS, AgNPs, tBHQ or cocktail). Treatments were applied in the apical compartment to simulate oral exposure. After this 3h exposure to the different treatments, the extracellular media of each compartment of the inserts were collected and replaced by culture medium. Indeed, previous research at the laboratory showed that inflammatory mediators content such as IL-8 were low directly after the 3h treatment. Consequently, a second incubation period (recovery period) was established in culture medium without AgNPs to induce cells to produce a greater amount of inflammatory markers. For convenient reasons, the recovery period has been established at 21h (Master's thesis Vandenkerckhove J., 2015). After this final recovery period, the extracellular media in each compartment of the inserts were again collected and stored at -20°C until the day of the ELISA quantification. According to previous research at the lab, there was no interference between AgNPs solutions and ELISA quantification assay.

Caco-2 cell layers were also collected in a buffer containing protease inhibitors and were sonicated (170 W, 5 min) followed by centrifugation (6260 g, 5 min). The cellular extracts were used to quantify the total amount of protein in each well through BCA assay. Finally, we also measured the transepithelial electrical resistance (TEER) after the 3h treatments to assess monolayer permeability that could be affected by AgNPs.

Results for IL-8 ELISA quantification

The experiment was carried out in inserts and therefore enabled the distinction between the apical and basolateral IL-8 contents. The obtained results are shown in figure 48 for the 3h incubation period with the different treatments and on figure 49 after the 21h recovery period. IL-8 contents were normalized by the amount of total protein contained in the cellular extracts. Regarding the amounts of IL-6 produced, they were unfortunately below the limit of quantification of the ELISA assay, corresponding data are therefore not shown.

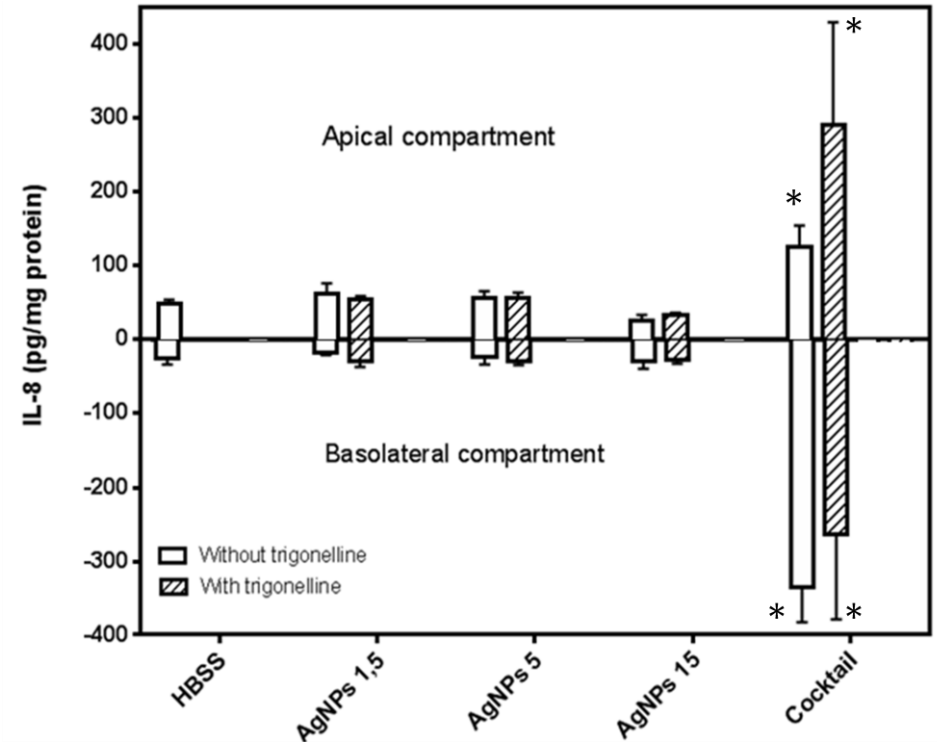

Figure 48: Secreted IL-8 contents after 3h incubation with the different treatments (HBSS, AgNPs and Cocktail). Some wells were pre-incubated for 1h with trigonelline. Results are normalized by the total amount of protein quantified by BCA assay. Values (mean ± SEM) were assessed by ELISA assay and come from three repetitions with three replicates per condition. Asterisks show values significantly different from the control (HBSS).

According to figure 48, which represents the IL-8 production after the 3h incubation period with the different treatments and with or without 1h pre-incubation with trigonelline, several observations can be made.

Regarding AgNPs treatments, there were no significant differences with HBSS control, although there appears to be a slight decrease in apical IL-8 production as AgNPs concentrations increase. Between AgNPs 1.5 µg/ml and AgNPs 15 µg/ml there is a 29% decrease in total amounts of secreted IL-8.

Secondly, the trigonelline treatment (Nrf2 inhibitor) does not appear to have any inhibitory effect on IL-8 production, which might indicate that IL-8 production is not related to the Nrf2 pathway. Another explanation could be that trigonelline did not work as it should have, as it seems to be the case in the aforementioned HO-1 assay.

Finally, since the inflammatory cocktail was applied on Caco-2 cells in order to reproduce the *in vivo* inflammatory conditions that lead to the activation of the NF-κB pathway, it is not surprising that it produced the highest response of the pro-inflammatory cytokine IL-8. Only the cocktail induced a significantly different response compared to HBSS. Indeed, total IL-8 content was 525% higher for the cocktail than for HBSS treatment.

The amounts of IL-8 formed after the 3h incubation period are relatively low compared to those quantified after the 21h recovery period (Fig. 49). Total amounts of secreted IL-8 for the AgNPs 15 µg/ml treatment increase from 55 pg IL-8/mg protein after 3h to 941 pg IL-8/mg protein after the recovery period, representing an increase of 1611%. For the cocktail, total values go from 456 pg IL-8/mg protein after 3h to 3290 pg IL-8/mg protein after the recovery period (621% increase).

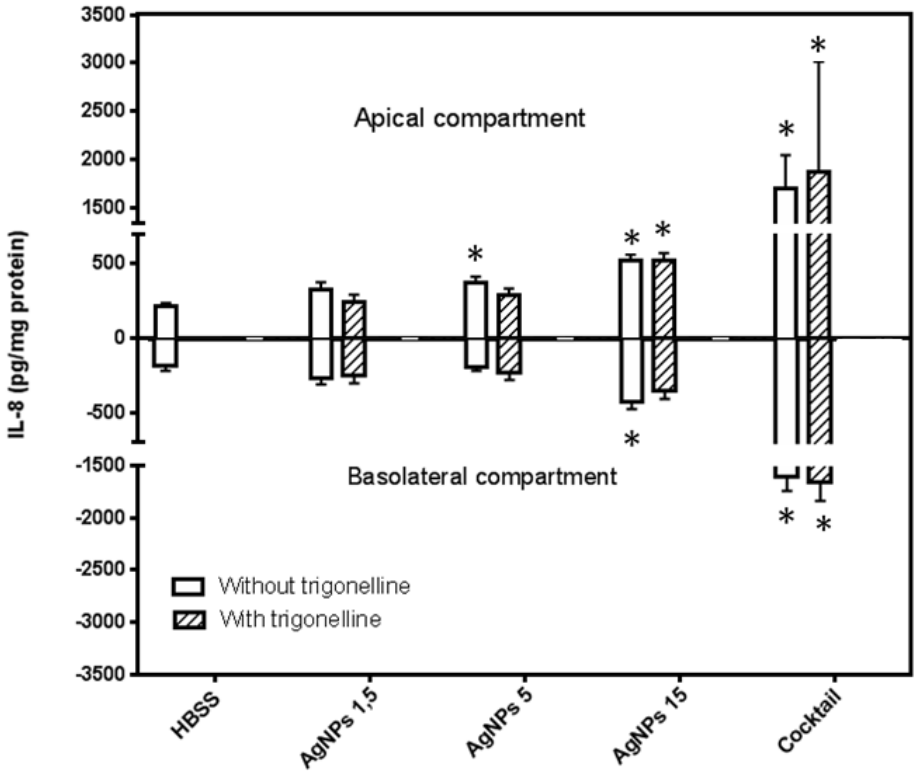

Figure 49: Secreted IL-8 contents after 21h recovery period for each treatment (HBSS, AgNPs and Cocktail). Some wells were pre-incubated for 1h with trigonelline. Results are normalized by the total amount of protein quantified by BCA assay. Values (mean ± SEM) were assessed by ELISA assay and come from three repetitions with three replicates per condition. Asterisks show values significantly different from the control (HBSS).

Figure 49 illustrates the IL-8 production after the 21h recovery period following the 3h incubation with the different treatments. Here again, several observations can be made. First of all, we can see that HBSS (control) induced the lowest total IL-8 production (385 pg IL-8/mg protein). Similarly to the previous figure, trigonelline did not have any inhibitory effect on IL-8 production suggesting that IL-8 production was not due to the Nrf2 pathway or that trigonelline did not exert its inhibitory effect on Nrf2. Thirdly, we can see that IL-8 production significantly increased with AgNPs concentrations, both in the apical and basolateral compartments. Total IL-8 content increased with 144% when we compare HBSS with AgNPs 15 µg/ml.

In accordance with figure 48, the cocktail produced the highest IL-8 response with a 755% increase compared to HBSS.

6. Transepithelial electrical resistance (TEER)

Increased paracellular permeability is an indicator of damage to the integrity of the intestinal barrier. We evaluated the potential effects of our treatments on the Caco-2 cell barrier integrity through the measurement of the transepithelial electrical resistance (TEER), which quantifies the movement of ions through the paracellular route. If the integrity of the tight junctions is compromised, TEER values decrease. TEER was evaluated after the 3h incubation with the different treatments by placing a first electrode in the apical medium and another one in the basolateral medium. Results are shown on figure 50 where values are expressed as a percentage of TEER values measured for the HBSS treatment.

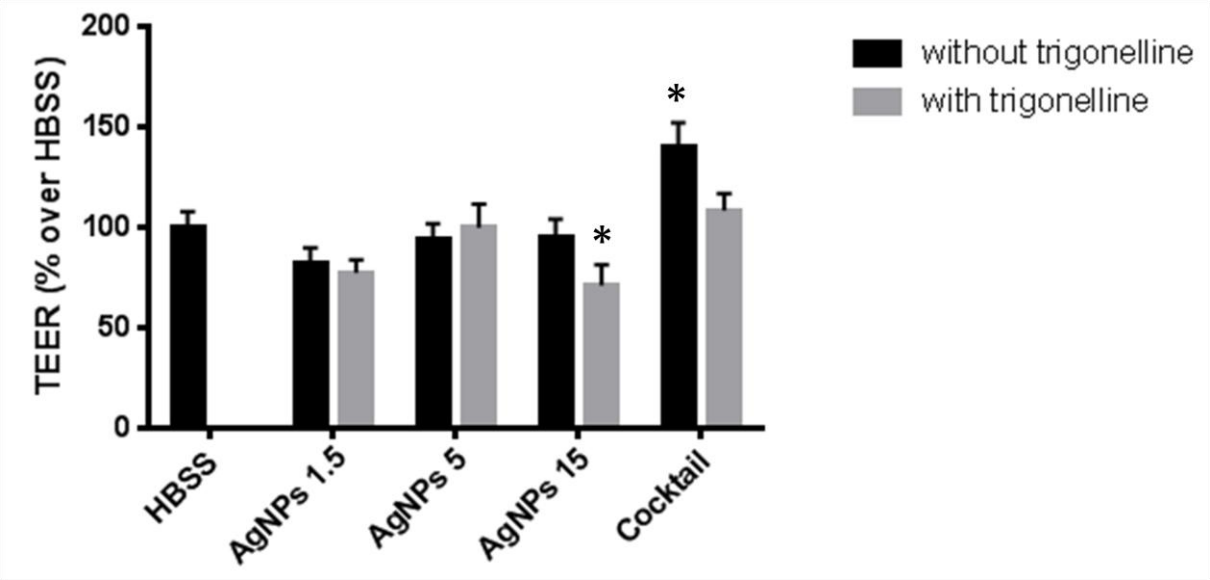

Figure 50: Transepithelial electrical resistance (TEER) values after 3h incubation with different treatments: HBSS, AgNPs and Cocktail. Some wells were pre-incubated for 1h with trigonelline. Results are expressed as a percentage of TEER values measured for the HBSS treatment. Values (mean ± SEM) were assessed by ELISA assay and come from three repetitions with three replicates per condition. Asterisks show values significantly different from the control (HBSS).

According to figure 50, TEER values were not affected significantly after 3h incubation with the two lowest AgNPs treatments, indicating that the paracellular permeability was not affected. A 29% decrease in TEER was observed for AgNPs 15 µg/ml with trigonelline pre-treatment compared to HBSS.

According to a study conducted by Martirosyan *et al.*, AgNPs (30 µg/ml) were shown to affect the intestinal epithelial barrier integrity, evidenced by decreased TEER values. Furthermore, after analysing two tight junction proteins, occluding and zonula occludens 1, they discovered that the continuity of both proteins was disrupted leading to the opening of TJs in the presence of AgNPs. The increased epithelial permeability induced by AgNPs treatment could be ROS mediated. ROS have been reported to activate the tyrosine kinase and phosphatidylinositol-3-kinase and alter the composition of the tight junctions, explaining the increased paracellular permeability (Martirosyan *et al.*, 2013).

On the other hand, our results suggest that the inflammatory cocktail, consisting of TNF-α, IL-1β, IFN-γ and LPS, increased the TEER with 40% which is equivalent to decreased paracellular permeability. However, according to the literature, TNF-α-induces tight junction disruption measured by a reduction in TEER (Leonard et al., 2010; Shen et al., 2017). A last study performed on Caco-2 cells showed a significant decrease of TEER after being exposed to a pro-inflammatory stimuli composed of LPS, IL-1β and IFN-γ, indicating compromised barrier properties (Luescher et al., 2017).

Part IV: Discussion

For several years, AgNPs have been introduced in various applications of the food sector and their incorporation is constantly increasing. It is therefore not surprising that we ingest, most often unconsciously, AgNPs particles of which a not insignificant fraction could be absorbed. However, there is currently not much information regarding biotransformation of AgNPs upon oral administration. This raises several concerns, especially considering their small sizes allowing them to accumulate within tissues and be taken up by individual cells (Martirosyan *et al.*, 2014). Several *in vivo* studies have shown that once these particles have crossed the intestinal epithelium, they reach systemic circulation and are distributed to various organs especially in the kidney, liver, spleen, brain, lung and testes where they could cause functional and/or structural impairment (Tang *et al.*,2009; Massarsky *et al.*,2014; Jarak *et al.*,2017; Mao *et al.*, 2018).

Many studies are establishing links between AgNPs exposure and observed toxic responses. Physicochemical characteristics such as size, aggregation/agglomeration state and surface coating are considered to be the most critical for their toxicity. In addition, it is known that surfactants added to prevent agglomeration drastically change chemical reactivity and thus also affect their cytotoxicity (Park *et al.*, 2011). Together with specific characteristics of AgNPs, interaction with the biological environment also causes changes that influence the toxicity of these particles. Indeed, interaction of AgNPs and biological media leads to the formation of a unique protein corona. The structure and composition of this protein corona depend on NPs properties (e.g. size, shape and surface charge), nature of the physiological environment (blood, interstitial fluid, cell cytoplasm, etc.) and the exposure duration. The cellular and biochemical responses including signalling, kinetics, transport, accumulation, and toxicity of AgNPs will depend on that unique corona signature (Martirosyan *et al.,* 2014; Urban *et al.*, 2016).

Oxidative dissolution of AgNPs in Ag^+ is also considered to have a major role in AgNPs toxicity. The main factors influencing oxidative dissolution of AgNPs are particle related properties (e.g., size, shape and surface coating), but also matrix related characteristics, such as dissolved oxygen, temperature, pH and the presence of proteins (Ostermeyer *et al.*, 2013; Köser *et al.*, 2017). There is also a general consensus on the fact that the chemical form of silver has implications for its toxicity. The antimicrobial effect of AgNPs is considered to be due to the release of Ag^+ via a Trojan-horse-type mechanism (Park *et al.*, 2010; Hsiao *et al.*, 2015). Smaller AgNPs, which have greater mobility and surface area compared to larger particles, have higher dissolution rates, thus leading to higher cellular toxicity and oxidative stress (Zhang *et al.*, 2016). It is therefore necessary to consider the speciation of silver and the amount of Ag^+ released in order to understand its contribution to the toxicity of AgNPs (McShan *et al.*, 2014).

1. AgNPs-induced oxidative stress

AgNPs exposure induces toxic mechanisms leading to non-specific oxidative stress through the production of reactive oxygen species (ROS). Indeed, once the AgNPs have managed to get inside the cells, both AgNPs and Ag^+ can interfere with mitochondrial activity leading to increased intracellular ROS. In turn, ROS could promote the oxidation of AgNPs and enhance the liberation of more Ag^+. Thus, AgNPs would cause a sustained ROS production and release of Ag^+, ultimately resulting in a series of adverse effects (Dawei *et al.*, 2013).

There is still a strong debate regarding whether AgNPs or Ag^+ induce toxicity in biological systems. Some previous studies suggest that Ag^+ is the actual species that accounts for the toxicity of AgNPs (Park *et al.*, 2010). However, *in vitro* work also indicates that AgNPs toxicity cannot only be explained by the release of Ag^+ by the particles (Kim & Ryu, 2013).
An AgNPs solution free of Ag^+ should be useful to distinguish the cytotoxic effects of the particles themselves from the dissolved ions. For this purpose, N-acetyl-L-cysteine (NAC) can be introduced into an AgNPs solution to bind with free Ag^+ with its sulfhydryl groups. In a study involving algae, the NAC treatment completely removed the inhibitory effects of Ag^+ and AgNPs on metabolic activity, suggesting that the toxicity of AgNPs was due to the release of Ag^+ (He *et al.*, 2012). However, this conclusion seems too easy. Indeed, the antioxidant properties of NAC can also be responsible for this protective effect. NAC is both a silver ion chelator and an antioxidant that scavenges ROS. The reduction of toxicity of both AgNPs and Ag^+ after addition of NAC could also prove the involvement of ROS in the observed toxicity (Reidy *et al.*, 2013). In other words, since the NAC treatment efficiently prevented AgNPs toxic effects, this could suggest that oxidative stress is primarily responsible for AgNPs cytotoxicity.
According to our results obtained from the NBT assay, we were able to detect an increased ROS production for AgNPs (10 and 15 µg/ml) and Ag^+ (1.5 µg/ml) treatments, confirming that AgNPs induce ROS in Caco-2 cells. Furthermore, because the ROS production upon AgNPs (10 µg/ml) exposure was significantly different from that in the HBSS control, whereas the treatment with Ag^+ (1 µg/ml) was not, this could suggest that at least some of the ROS production resulted from the presence of AgNPs. The response could not only be explained by Ag^+ release from AgNPs, suggesting a nano-specific effect on ROS production. Especially since we suspect that the AgNPs solutions that were used actually contained less than 10% Ag^+. Previous similar research conducted at the lab monitored intracellular ROS production by 2',7'-dichorofluorescein diacetate (DCFH-DA) staining on fully differentiated Caco-2 cells. They observed an increase in intracellular ROS generation for 3h treatments with AgNPs for concentrations starting from 45 µg/ml. Furthermore, they also concluded that Ag^+ release from AgNPs, contributed only partially to the oxidative stress upon exposure to AgNPs (Martirosyan *et al.*, 2014). These results are consistent with our observations although we detected an increase in ROS for lower AgNPs concentrations.

Several other studies confirm the results we obtained with the NBT assay and show that AgNPs induced oxidative stress cannot be explained solely by the release of Ag^+. AgNPs were found to generate more ROS than Ag^+, which indicates that ROS production is due to specific characteristics of AgNPs and responses can not only be attributed to Ag^+ release (Hsin *et al.*, 2008; Piao et al., 2011; Kim & Ryu, 2013; Georgantzopoulou *et al.*, 2016).

Other evidence is that NAC significantly decreased toxicity of Ag^+, but not AgNPs treatments, while addition of Trolox (ROS scavenger) to the treatment, efficiently decreased the oxidative stress related toxicity of both agents (Li *et al.*, 2017).

Several studies proved the involvement of mitochondria in AgNPs induced ROS production. Hsin *et al.*, performed a pre-treatment with cyanide that is known to inhibit the mitochondrial electron-transferring activity of cytochrome C oxidase. They found that the cyanide treatment inhibited the AgNPs-induced ROS generation confirming the involvement of mitochondria (Hsin *et al.*, 2008).

Other studies confirm the crucial role of ROS in AgNPs-induced toxicity. Several parameters indicate oxidative stress in tissues and cells, the first one being the level of lipid membrane peroxidation. It was found to be increased upon AgNPs treatment in a variety of mammalian cell types, such as in human Chang liver cells (Piao *et al.*, 2011) as well as in skin carcinoma and fibrosarcoma cells, when cells were challenged with concentrations of 6.25 µg/mL AgNPs (Arora *et al.*, 2008). Another indicator of oxidative stress is an increased amount of protein carbonylation in AgNPs-treated cells, including human colorectal carcinoma cells (Verano-Braga *et al.*, 2014) and Chang liver cells (Piao *et al.*, 2011). Finally, ROS generated by AgNPs can also result in DNA breaks (Piao *et al.*, 2011). DNA damage was also detected in human lung carcinoma cells exposed to AgNPs. The level of DNA adducts was reduced by pre-treatment with the antioxidant NAC, indicating that ROS initiated DNA adduct formation (Foldbjerg *et al.*, 2011).

2. Enzymatic activity

According to the previously mentioned studies, toxic effects decreased by pre-treatment of cells with antioxidants (Trolox and NAC), suggesting a disturbance in the oxidative balance of cells following treatment with AgNPs. It is therefore interesting to study the mechanisms involving antioxidant defence systems in cells. Indeed, during oxidative stress situations, GSH is the major endogenous antioxidant scavenger that is able to bind and reduce ROS. Maintaining a sufficient GSH pool is therefore critical for cell survival. In addition to this non-enzymatic molecule, different antioxidant enzymes also come into action. Enzymes such as SOD, CAT, GR, GP and GST are part of the antioxidant system responsible for the elimination of radicals and molecules produced as a consequence of oxidative stress.

Taking this into account, we aimed at studying the impact of AgNPs on the antioxidant defence system of Caco-2 cells. This is why we studied the evolution of enzymatic activity of certain oxidative stress-related enzymes (CAT, GR, GP and GST).

Unfortunately, the experiments performed during this master's thesis did not allow the detection of any significant changes in enzymatic activity after 3h incubation with 15 µg/ml AgNPs. However, several other studies were able to measure cellular changes even if there is no general consensus on the effects of AgNPs on cellular antioxidant system. Various studies have indicated that cellular levels of GSH are increased after *in vitro* treatment with AgNPs, which may represent a cellular response to the AgNP-mediated oxidative damage (Farkas *et al.*, 2011).

By contrast, other studies indicate that AgNPs induced GSH depletion, suggesting either an inhibition of GSH-synthesising enzymes or an abnormally increased demand for GSH as an electron donor to neutralize ROS by GP and GST enzymes. Furthermore, AgNPs have a strong affinity for thiol groups like those in GSH, which might also be responsible for the observed GSH depletion. It is unclear which mechanism is responsible for the observed depletion of GSH (Rogers *et al.*, 2008; Arora *et al.*, 2008; Piao *et al.*, 2011; Prasad *et al.*, 2013).
The same debate matters for GST, where some studies show a decrease in GST activity whereas others see an increased activity. As a reminder, GST is a family of phase II detoxification enzymes that catalyse the conjugation of GSH to products of oxidative stress. The reduction in GST activity could indicate an overutilisation of existing enzymes to overcome oxidative stress caused by AgNPs (Byoungcheun *et al.*, 2012). However, AgNPs may also trigger the production of enzymes to counteract the severe effects of the particles. Hence, an increased GST content may correlate indicate a depletion of GSH for detoxification processes. However, the correlation between GSH and GST requires further study (Byoungcheun *et al.*, 2012). According to a study on the soil arthropod *Folsomia candida*, GST activity did not change significantly, whereas the GSH pool decreased with increasing concentrations of AgNPs (Sillapawattana *et al.*, 2016). Another study reported that the increased GST activity may also be due to the conjugation of GSH with Ag^+. Induction of GST genes for both AgNP and Ag^+ was reported in the soil invertebrate *E. Fetida* (Ribeiro *et al.*, 2015).
Furthermore, antioxidant enzymes such as SOD and CAT were induced in human hepatoma cells after 24h of AgNP treatment, reflecting cellular coping mechanisms (Kim *et al.*, 2009). The SOD-CAT system provides the first defence against ROS toxicity. SOD catalyses the transformation of superoxide anion in O_2 and H_2O_2 and CAT contributes to convert H_2O_2 to water and oxygen. The previous result is confirmed in a study where AgNPs ingestion by fruit fly larvae activated oxidative stress pathways, leading to significantly higher activities of antioxidant enzyme SOD and CAT in organisms exposed to AgNPs (Ahamed *et al.*, 2010). In another study still involving fruit fly larvae, AgNPs-induced activation of SOD activity was attenuated by administration of vitamin C, a known antioxidant, thus confirming the involvement of oxidative stress in SOD activation (Posgai *et al.*, 2011).

A decreased enzymatic activity of GP and GR enzymes with increasing concentrations of AgNPs has been reported in human liver cell line but also in rainbow trout hepatocytes and erythrocytes (Massarsky *et al.*, 2014; Afifi *et al.*, 2016). Reduced GP activity might be linked to the previously mentioned GSH depletion (Foldbjerg *et al.*, 2011). Since GP eliminates H_2O_2 by consuming reduced GSH, the decrease in its activity may be related to the observed decreased GSH levels. The activity of GR was also reduced, perhaps as a response to the lower GSSG levels caused by the reduced GP activity (Afifi *et al.*, 2016).
However, a study performed on the soil invertebrate *E. Fetida* showed opposite results. The enzymatic activity of GP and GR was increased after exposure to AgNPs. Here again a link was established concerning the activities of GP and GR (Ribeiro *et al.*, 2015).

With regard to all these studies reporting the activity of antioxidant enzymes, we have noticed that there is still much discussion on the subject and that results coming from different studies strongly oppose. It is therefore very difficult to conclude anything since many factors changing the outcomes are involved, such as the organism concerned, the cell type, the concentrations of AgNPs used but also the duration of exposure.

3. HO-1 as Nrf2 gene target

Nrf2 is another defensive pathway that plays an important role in preventing cellular stress through the induction of antioxidant-responsive genes and genes of the phase II detoxifying enzymes such as GST. When the cellular oxidative balance is disturbed by overproduction of ROS, oxidation of Keap-1 cysteine groups occurs, leading to the dissociation of Nrf2, which can then be translocated into the nucleus and ultimately activate target genes (cfr. Part I: 3.4 The Keap1-Nrf2 signalling pathway). Activation of the Nrf2 pathway leads to the generation of cytoprotectors such as HO-1, a known Nrf2 gene target and marker of oxidative stress. HO-1 is considered to be an important component of defence against ROS and its expression is strongly dependent on activation through Nrf2. The HO-1 enzyme is involved in heme catabolism, which counteracts cell death by producing equimolar quantities of Fe^{2+}, biliverdin and carbon monoxide to neutralize ROS.

Since we were able to detect an increased production of ROS after AgNPs exposure, we hypothesized an upregulation of HO-1 through the induction of Nrf2 pathway. Unfortunately, we did not detect a significant increase in HO-1 production after AgNPs or Ag^+ treatments compared to the HBSS control (cfr. Part III: Results: figures 46 and 47). Moreover, the trigonelline (Nrf2 inhibitor) pre-treatment did not cause a decreased HO-1 production. From our results, we should conclude that either the Nrf2 inhibitor did not work, or that in our experimental setup, the production of HO-1 does not depend on the Nrf2 pathway. Other results have shown that trigonelline efficiently decreased tBHQ-induced Nrf2 activity in pancreatic carcinoma cell lines (No *et al.*, 2014).

Furthermore, trigonelline was also able to block the expression of HO-1 in hepatocellular carcinoma cells confirming its ability to act as an Nrf2 inhibitor (Xiaofang *et al.*, 2015). A final possibility could be that AgNPs treatment simply does not induce Nrf2 pathway and the resulting HO-1 production in Caco-2 cells.

A few other studies focused on evaluating the effect of AgNPs exposure on the Nrf2/HO-1 signalling pathway but their results are contradictory. Piao *et al.* showed that a 6h AgNPs (4 µg/ml) treatment decreased the nuclear Nrf2 translocation into the nucleus and transcriptional activity of Nrf2 in human liver cells (Piao *et al.,* 2011b).

In contrast, a stimulation of the expression of HO-1 was observed in AgNPs-treated cervical cancer cells (Miura & Shinohara, 2009). This result is in agreement with the report of Kang *et al*. that demonstrated an activation of the Nrf2/HO-1 signalling pathway in response to AgNPs (10 µg/ml) after 24 h of exposure in human ovarian cancer cell line. They used Nrf2 knockdown cells exposed AgNPs and showed a substantial decrease in cell viability with concomitant increases in apoptosis and DNA damage compared to the control cells. Expression of HO-1 was highly elevated by AgNPs in normal cells, while Nrf2 knockdown cells did not increase HO-1 expression. Interestingly, cobalt protoporphyrin was used as an HO-1 inducer in Nrf2 knockdown cells and was able to prevent AgNPs-mediated cell death, confirming the cytoprotective role of HO-1 against AgNPs (Kang *et al.*, 2012 b).
Similarly, Aueviriyavit *et al.* reported that AgNPs (15 µg/ml) activated the Nrf2/HO-1 signalling pathway in Caco-2 cells after 3h of treatment. In addition, AgNPs significantly depleted the total intracellular GSH level in a dose dependent manner after 24h exposure (AgNPs 5 µg/ml). Furthermore, silencing Nrf2 transcripts significantly reduced the AgNP-induced HO-1 mRNA induction, suggesting a key role for Nrf2 in the control of HO-1 expression (Aueviriyavit *et al.*, 2014). Although, since not all of the induced HO-1 transcript level was attenuated by the Nrf2-knockdown, it might suggest that other transcription factors could be involved in the upregulation of HO-1. Indeed, it has previously been reported that other factors, such as MAPKs and PI3K, are involved in the regulation of HO-1 transcript level (Aueviriyavit *et al.*, 2014). Furthermore, the HO-1 gene contains multiple stress response elements for Nrf2, AP-1 and NF-κB transcription factors that also might be worth investigating (Kang *et al.*, 2012b).
Prasad *et al.* observed transcriptional activation of Nrf2, AP-1 and NF-κB pathways in HepG2 cells after exposure to AgNPs. Among all three pathways, Nrf2 displayed the strongest response elicited by AgNPs. Smaller AgNPs (10 nm) were more potent than larger ones (75 nm) (Prasad *et al.*, 2013).

Finally, a study performed by Kang *et al.* established a link between Nrf2 pathway and GSH levels. They demonstrated that the Nrf2/GSH signalling pathway is activated in response to AgNPs-treated renal epithelial cells, which leads to an increased expression of GSH synthesising enzymes (GCL). As a result, AgNPs increased GSH synthesis in an Nrf2 dependent manner in normal cells whereas AgNPs-treated Nrf2 knockdown cells exhibited a reduction in GSH content and profoundly increased ROS production and DNA damage compared to the control cells. Pre-treatment with NAC in knockdown cells alleviated ROS mediated damage (Kang *et al.* 2012a).

Taken together, these results suggest that the Nrf2-dependent HO-1 upregulation, caused by ROS, plays an important role in the cytoprotective response to AgNP exposure in cells.

4. AgNPs, ROS and inflammation

Oxidative stress due to NPs exposition and inflammation are interrelated by amplification loops (cfr. Part I: 3.5. Interleukins-8 and 6 (IL-8 and IL-6)). ROS modulate inflammatory mediator release through activation of transcription factors such as NF-κB, leading to amplification loops between oxidative stress and inflammation (Foldbjerg *et al.*, 2009; Gaillet & Rouanet, 2015; Liu *et al.*, 2010). Oxidative stress-induced redox signalling is known to involve the activation of redox-sensitive transcription factors like Nrf2, NF-κB and AP-1 contributing to the pro-inflammatory cascade (Reuter *et al*., 2010). The molecular cross-talk between Nrf2 and NF-κB pathways in very complex and remains largely unknown but is probably involved in IL-8 production (Wardyn *et al.*, 2015).

According to previous study at the lab, AgNPs induced IL-8 production on both sides of the culture inserts, especially in the apical compartment. However, IL-8 production could not be attributed to the NF-κB pathway. While some studies confirm that AgNPs did not change (Stępkowski *et al.,* 2014) or even decreased (Satapathy *et al*., 2013) NF-κB expression in cells, many others observed an increase in NF-κB translocation, which could explain IL-8 production. AgNPs activated the NF-κB signalling pathway in HepG2 cells (Prasad *et al*., 2013), human T-lymphocyte cell line (Eom & Choi, 2010) and in human brain cancer cell line (AshaRani *et al*., 2012). The activation of NF-κB by AgNPs results in the transcription of many genes involved in inflammatory response, such as IL-6, IL-8, COX-2 and TNF-α. These pro-inflammatory effects of NPs were dependent on AgNPs size and duration of exposure (Nishanth *et al.*, 2011).

Since the transcription factor Nrf2 is responsive to oxidative stress and induces expression of cytoprotective genes that attenuate tissue injury, Zhang *et al*. postulated that Nrf2 may also regulate chemokine expression. It has already been proven that both IL-6 and IL-8 promoter regions contain a functional antioxidant response element (ARE) that can be targeted by Nrf2 (Zhang *et al.*, 2005; Wruck *et al.*, 2011). Furthermore, they increased Nrf2 expression with an adenoviral construct and detected significantly increased IL-8 mRNA levels and protein secretion. Nrf2 caused only a weak induction of IL-8 transcription, but significantly increased the half-life of IL-8 mRNA (Zhang *et al.,* 2005).

During this thesis we investigated the potential role of the Nrf2 pathway in IL-8 production. Experiments performed on Caco-2 cells were able to detect an increased IL-8 production in AgNPs-treated cells. However, trigonelline (Nrf2 inhibitor) did not have any inhibitory effect on IL-8 production suggesting that IL-8 production was not due to the Nrf2 pathway or that the trigonelline treatment did not work. It may therefore be interesting to study the involvement of other pathways such as AP-1, MAPK, ERK or JNK to explain the increased IL-8 production following treatment with AgNPs (Amruta *et al.*, 2013).

Part V: Conclusion and perspectives

The main objective of this thesis was to deepen the knowledge regarding the effects of AgNPs on intestinal epithelial cells and to determine the potential contribution of Ag^+ in order to participate to the evaluation of the risks associated with an oral exposure to AgNPs. More specifically, we performed different *in vitro* experiments on monocultures of Caco-2 cells to assess the impact of AgNPs and Ag^+ treatments on oxidative stress and the related cellular responses.

These potential effects were studied by performing four main experiments related to the Nrf2 signalling pathway. Indeed, Nrf2 is the major pathway involved in protecting cells from oxidative stress, through the induction of several antioxidant-responsive genes. First of all, the ability of AgNPs and Ag^+ to generate ROS and induce oxidative stress was evaluated by performing an NBT assay on differentiated Caco-2 cells. This assay uses the soluble tetrazolium reagent that, after being absorbed by cells, is reduced by ROS into a blue compound allowing ROS quantification. Secondly, various assays were carried out to determine the impact of AgNPs on the enzymatic activity of several oxidative stress-related enzymes that are known to be induced by Nrf2 (CAT, GR, GP and GST). Thirdly, we studied the impact of AgNPs/Ag^+-induced ROS generation on Nrf2 signalling pathway by performing an ELISA quantification of HO-1, which is an Nrf2 specific gene target. Finally, the potential interaction of Nrf2 signalling pathway and pro-inflammatory response was evaluated after AgNPs treatments. For that purpose we quantified IL-8, a known marker of inflammation, through ELISA.

According to our results, it is suggested that the non cytotoxic AgNPs/Ag^+ concentrations caused a nano-specific increase in ROS production, which is in agreement with similar studies. However, we were not able to detect any significant changes in the tested enzymatic activities after AgNPs treatments. In addition to that, we did not measure any significant effect of AgNPs/Ag^+ on HO-1 production. Nonetheless, those results are contradictory with numerous studies confirming the implication of the Nrf2/HO-1 signalling pathway to explain the cellular responses related to AgNPs-induced ROS production. The last experiment demonstrated a pro-inflammatory effect of AgNPs on Caco-2 cells, revealed by an increased IL-8 production. However, it remains unclear which pathways are involved.

Additional investigation could be done to address the encountered issues and to explore other aspects related to AgNPs. For instance, we could study oxidative stress related enzymes by measuring the mRNA expression levels via qRT-PCR instead of determining enzymatic activity.

Regarding experiments involving the Nrf2 pathway, different approaches should be envisaged:

1. We could inhibit this pathway with the knockdown of Nrf2 transcript levels by siRNA. This can be achieved by transfecting siRNA into Caco-2 cells. We could use this technique to replace the trigonelline (Nrf2 inhibitor) treatment that did not have any inhibitory effect on IL-8 or HO-1 production in our experiments and might lead to the false conclusion that Nrf2 was not involved. Especially since the mechanisms of action of trigonelline are unknown and that we are not certain of its specificity towards Nrf2.
2. Another option to inhibit Nrf2 could be by using the novel and more specific Nrf2 inhibitor, ML385. Indeed, ML385 was identified as a probe molecule that binds specifically to the Neh1 domain of Nrf2, which interferes with the binding of Maf proteins that are essential for downstream target gene expression (Singh *et al.*, 2016).
3. On the other hand, we could try to observe the activation of Nrf2 following AgNPs treatments by analysing its translocation into the nucleus by confocal microscopy. Several attempts have already been made in the lab, without any success.
4. Measuring the expression levels of Nrf2, HO-1 and IL-8 mRNA by qRT-PCR could also be interesting. Regarding IL-8, it could be useful to study the involvement of other pathways such as AP-1, MAPK, ERK or JNK to explain the increased IL-8 production following AgNPs treatments.

Most importantly, we should try to quantify the actual amount of Ag^+ present in the AgNPs solutions that were used, in order to estimate their contribution to the observed responses. This could be achieved by conducting a first ultrafiltration to separate ions from particles, followed by inductively coupled plasma-optical emission spectrometry/ mass spectrometry (ICP-AES/MS) for Ag^+ quantification. The latter technique (ICP-MS) can also be interesting for quantifying AgNPs bound to and taken up by the cells.
Finally, more tests involving Ag^+ treatments should be performed to compare with the AgNPs treatments.

References

- Abreu M., (2010), **Toll-like receptor signalling in the intestinal epithelium: how bacterial recognition shapes intestinal function**, Nature Reviews Immunology volume10, page215, doi:10.1038/nri2728
- Addo N., Thomas T., Begley T., Noonan G., (2015), **Characterisation and potential migration of silver nanoparticles from commercially available polymeric food contact materials**, Food Addit Contam Part A Chem Anal Control Expo Risk Assess, doi: 10.1080/19440049.2015.1029994
- Afifi M., Saddick S., Abu Zinadaa OA., (2016), **Toxicity of silver nanoparticles on the brain of Oreochromis niloticus and Tilapia zillii**, Saudi Journal of Biological Sciences, https://doi.org/10.1016/j.sjbs.2016.06.008
- Ahamed M., Posgai R., Gorey TJ., Nielsen M., Hussain SM., Rowe JJ., (2010), **Silver nanoparticles induced heat shock protein 70, oxidative stress and apoptosis in Drosophila melanogaster**, Toxicol Appl Pharmacol, doi: 10.1016/j.taap.2009.10.016
- Akter M., Sikder M. T., Rahman M. M., Ullah A. K. M. A., Hossain K. F. B., Banik, S., Kurasaki, M. (2017), **A systematic review on silver nanoparticles-induced cytotoxicity: Physicochemical properties and perspectives.**, DOI: 10.1016/j.jare.2017.10.008
- Amruta M., Liying W, Rojanasakul Y., (2013), **Mechanisms of Nanoparticle-Induced Oxidative Stress and Toxicity**, BioMed Research International, Article ID 942916, 15 pages, 2013. https://doi.org/10.1155/2013/942916.
- Araújo F., Sarmento B., (2013), **Towards the characterization of an *in vitro* triple co-culture intestine cell model for permeability studies**, International Journal of Pharmaceutics 458, 128–134, http://dx.doi.org/10.1016/j.ijpharm.2013.10.003
- Arora S., Jain J., Rajwade JM., Paknikar KM., (2008), **Cellular responses induced by silver nanoparticles: *In vitro* studies**. Toxicol. Lett. 179: 93–100., https://doi.org/10.1016/j.toxlet.2008.04.009
- Artursson P, Karlsson J.,(1991), **Correlation between oral drug absorption in humans and apparent drug permeability coefficients in human intestinal epithelial (Caco-2) cells**, Biochem Biophys Res Commun, PMID: 1673839
- Artursson P., (1990), **Epithelial transport of drugs in cell culture. I: A model for studying the passive diffusion of drugs over intestinal absorptive (Caco-2) cells**. J Pharm Sci 79: 476-482.
- AshaRani PV., Low Kah Mun G., Hande MP., Valiyaveettil S., (2009), **Cytotoxicity and genotoxicity of silver nanoparticles in human cells**, ACS Nano, doi: 10.1021/nn800596w
- Aueviriyavit, S., D. Phummiratch and R. Maniratanachote (2014). **Mechanistic study on the biological effects of silver and gold nanoparticles in Caco-2 cells--induction of the Nrf2/HO-1 pathway by high concentrations of silver nanoparticles**. Toxicol Lett 224(1): 73-83.

- Axson J., Stark D., Bondy A., Capracotta S., Maynard A., Philbert M., Bergin I., Ault A., (2015), **Rapid Kinetics of Size and pH-Dependent Dissolution and Aggregation of Silver Nanoparticles in Simulated Gastric Fluid**, J. Phys. Chem. C, DOI: 10.1021/acs.jpcc.5b03634
- Bartz RR., Piantadosi CA., (2010), **Clinical review: oxygen as a signalling molecule**, On line:https://openi.nlm.nih.gov/detailedresult.php?img=PMC3219237_cc9185-2&req=4
- Bergeson L., Hutton C., (2017), **EC Begins Consultation on Revising Recommendation on Definition of Nanomaterial**, Lexology, On line: https://www.lexology.com/library/detail.aspx?g=b335ed42-2304-498d-8c5e-a239cc435d56
- Bevins C., Salzman N., (2011), **Paneth cells, antimicrobial peptides and maintenance of intestinal homeostasis**, Nature Reviews Microbiology volume9, doi:10.1038/nrmicro2546
- Bollong MJ., Yun H., Sherwood L, Woods Ak., Lairson LL., Schultz PG., (2015), **A small molecule inhibits deregulated NRF2 transcriptional activity in cancer**, Chem. Biol, DOI: 10.1021/acschembio.5b00448
- Borowicz H., Kubiak K., Nikolovski G., Niedźwiedź A., (2016), **Impact of Recurrent Airway Obstruction (RAO) on Selected Antioxidants in Horses**, DOI: https://doi.org/10.1515/macvetrev-2016-0074
- Bourlioux, P., B. Koletzko, F. Guarner and V. Braesco (2003). **The intestine and its microflora are partners for the protection of the host: report on the Danone Symposium:The Intelligent Intestine**, held in Paris, June 14, 2002. The American Journal of Clinical Nutrition 78(4):675-683.
- Bouwmeester H., Dekkers S., Noordam M., W. I. Hagens, A. S. Bulder, C. de Heer, S. E. ten Voorde, S. W. Wijnhoven, H. J. Marvin and A. J. Sips, (2009), **Review of health safety aspects of nanotechnologies in food production**, Regul Toxicol Pharmacol 53(1): 52-62. doi: 10.1016/j.yrtph.2008.10.008
- Bouwmeester H., Poortman R., Peters E., Wijma E., Kramer S., Makama K., Puspitaninganindita, Peijnenburg and P. J. M. Hendriksen, (2011), **Characterization of Translocation of Silver Nanoparticles and Effects on Whole- Genome Gene Expression Using an *In Vitro* Intestinal Epithelium Coculture Model**., ACS Nano 5(5): 4091-4103.
- Bove P., Malvindi MA., Kote SS., Bertorelli R., Summa M., Sabella S., (2017), **Dissolution test for risk assessment of nanoparticles: a pilot study**, Nanoscale journal issue 19, DOI:10.1039/C6NR08131B
- Bressan E., Ferroni L., Gardin C., Rigo C., Stocchero M., Vindigni V., Cairns W., Zavan B., (2013), **Silver nanoparticles and mitochondrial interaction**, Int J Dent, doi: 10.1155/2013/312747
- Brown S. , Boyko V., Meyers G. , Voetz M., Wohlleben W., (2013), **Toward Advancing Nano-Object Count Metrology: A Best Practice Framework, Environ Health Perspect**; DOI:10.1289/ehp.1306957
- Bumbudsanpharoke N., Ko S., (2015), **Nano-food packaging: an overview of market, migration research, and safety regulations**, J Food Sci., doi: 10.1111/1750-3841.12861
- Buzea, C., Pacheco, I.I., Robbie, K., (2007), **Nanomaterials and nanoparticles: Sources and toxicity**. Biointerphases 2, MR17. doi:10.1116/1.2815690

- Byoungcheun L., Cuong Ngoc D., Jaegu C., et al., (2012), **Toxicity of Citrate-Capped Silver Nanoparticles in Common Carp (Cyprinus carpio)**, Journal of Biomedicine and Biotechnology, Article ID 262670, 14 pages, 2012. https://doi.org/10.1155/2012/262670.
- Campbell, N., R. J., L. Urry and M. Cain,(2012), Pearson Education.
- Carbone M., Donia D.T., Sabbatella G., Antiochia R., (2016), **Silver nanoparticles in polymeric matrices for fresh food packaging**, Journal of King Saud University - Science, doi: http://dx.doi.org/10.1016/ j.jksus.2016.05.0044
- Chantret I., Barbat A., Dussaulx E., Brattain MG., Zweibaum A., (1988), **Epithelial polarity, villin expression, and enterocytic differentiation of cultured human colon carcinoma cells: a survey of twenty cell lines**, Cancer Res, PMID: 3349466
- Chaudhry Q., Scotte, M., Blackburn J., Ross B., Boxall A., Castle L., Aitken R., and Watkins R., (2008), **Applications and implications of nanotechnologies for the food sector, Food Additives and Contaminants** *25*, 241-258, doi: 10.1080/02652030701744538
- Chen X., Schluesener H.J., (2008), **Nanosilver: A nanoproduct in medical application**, Toxicol. Lett. 176, 1–12. doi:10.1016/j.toxlet.2007.10.004
- Cheng X., Zhang W., Ji Y., Meng J., Guo H., Liu J., Wu X. and Xu H, (2013), **Revealing silver cytotoxicity using Au nanorods/Ag shell nanostructures: disrupting cell membrane and causing apoptosis through oxidative damage**, RSC Advances, DOI:10.1039/C2RA23131J
- Choi AM., Alam J., (1996), **Heme oxygenase-1: function, regulation, and implication of a novel stress-inducible protein in oxidant-induced lung injury**, Am J Respir Cell Mol Biol, DOI: 10.1165/ajrcmb.15.1.8679227
- Ciappellano S.G., (2016) ***In vitro* toxicity assessment of oral nanocarriers**, Adv. Drug Deliv. Rev., http://dx.doi.org/ 10.1016/j.addr.2016.08.007
- Dawei G., Lingying Z., Zhihai H., Haixia Z., Yue G., Wenjuan M., Jie W., Xiuyan Z., Xuefeng Z., Yu Z., Yun Z., Ning G., (2013), **Anti-leukemia activity of PVP-coated silver nanoparticles via generation of reactive oxygen species and release of silver ions**, Biomaterials Volume 34, Issue 32, https://doi.org/10.1016/j.biomaterials.2013.07.015
- des Rieux A., Fievez V., Garinot M., Schneider YJ., Préat V., (2006), **Nanoparticles as potential oral delivery systems of proteins and vaccines: a mechanistic approach**, J Control Release, DOI: 10.1016/j.jconrel.2006.08.013
- des Rieux A., Fievez, V., Theate, I., Mast, J., Preat, V., and Schneider, Y.J. (2007). **An improved *in vitro* model of human intestinal follicle-associated epithelium to study nanoparticle transport by M cells**. European Journal of Pharmaceutical Sciences *30*, 380-391.
- Dreger H., Westphal K., Weller A., Baumann G., Stangl V., Meiners S., Stangl K., (2009), **Nrf2-dependent upregulation of antioxidative enzymes: a novel pathway for proteasome inhibitor-mediated cardioprotection** , Cardiovasc Res, doi: 10.1093/cvr/cvp107
- Durán N., Silveira C., Durán M., Stéfani D., Martinez T., (2015), **Silver nanoparticle protein corona and toxicity: a mini-review**, Journal of Nanobiotechnology, https://doi.org/10.1186/s12951-015-0114-4
- Echegoyen Y., Nerín C., (2013), **Nanoparticle release from nano-silver antimicrobial food containers**, Food Chem Toxicol., doi: 10.1016/j.fct.2013.08.014
- EFSA, (2009), **Scientific opinion of the scientific committee : the potential risks arising from nanoscience and nanotechnologies on food and feed safety**, S. Barlow, A. Chesson, J.D.
- Egerton TA., (2014), **UV-Absorption—The Primary Process in Photocatalysis and Some Practical Consequences, Molecules**, doi:10.3390/molecules191118192

- Eom HJ., Choi J., (2010), **p38 MAPK activation, DNA damage, cell cycle arrest and apoptosis as mechanisms of toxicity of silver nanoparticles in Jurkat T cells**., Environ Sci Technol, doi: 10.1021/es1020668
- Eurell, J.A.C., (2004**), Veterinary histology, Quick look series in veterinary medicine**. Teton NewMedia, Jackson, Wyo.
- European Commission, (2017), **Definition of a nanomaterial**, On line: http://ec.europa.eu/environment/chemicals/nanotech/faq/definition_en.htm
- Fernandez A., Soriano E., Hernandez P., Gavara R., (2010), **Migration of antimicrobial silver from composites of polylactide with silver zeolites**, J Food Sci., doi: 10.1111/j.1750-3841.2010.01549.
- Foldbjerg R., Dang DA., Autrup H., (2011), **Cytotoxicity and genotoxicity of silver nanoparticles in the human lung cancer cell line, A549.,** Arch Toxicol 85(7):743-50, doi: 10.1007/s00204-010-0545-5
- Franklin CC., Backos DS., Mohar I., White CC., Forman HJ., Kavanagh TJ., (2009), **Structure, function and post-translational regulation of the catalytic and modifier subunits of glutamate cysteine ligase**, Mol Aspects Med, doi: 10.1016/j.mam.2008.08.009
- Fröhlich, E. and E. Roblegg (2012), **Models for oral uptake of nanoparticles in consumer products**. Toxicology 291(1-3): 10-17.
- Fuertes G., Soto I., Carrasco R., Vargas M., Sabattin J. and Lagos C., (2016), **Intelligent Packaging Systems: Sensors and Nanosensors to Monitor Food Quality and Safety**, Journal of Sensors, vol. 2016, Article ID 4046061, 8 pages. doi:10.1155/2016/4046061
- Gaillet S., Rouanet JM., (2015), **Silver nanoparticles: Their potential toxic effects after oral exposure and underlying mechanisms** – A review, Food and Chemical Toxicology, https://doi.org/10.1016/j.fct.2014.12.019
- Georgantzopoulou A., Serchi T., Cambier S., Leclercq C., Renaut J., Shao J., Kruszewski M., Lentzen E., Grysan P., Eswara S., Audinot J.-N and Contal S., (2016), **Effects of silver nanoparticles and ions on a co-culture model for the gastrointestinal epithelium**. Particle and Fibre Toxicology 13(1): 1-17.
- Goetz N., Fabricius L., Glaus R., Weitbrecht V., Günther D., Hungerbühler K., (2013), **Migration of silver from commercial plastic food containers and implications for consumer exposure assessment**, Food Addit Contam Part A Chem Anal Control Expo Risk Assess, doi: 10.1080/19440049.2012.762693
- Haase A, Arlinghaus HF, Tentschert J, Jungnickel H, Graf P, Mantion A, Draude F, Galla S, Plendl J, Goetz ME, Masic A, Meier W, Thunemann AF, Taubert A, Luch A., (2011), **Application of laser postionization secondary neutral mass spectrometry/time-of-flight secondary ion mass spectrometry in nanotoxicology: Visualization of nanosilver in human macrophages and cellular responses**. ACS Nano 5: 3059–3068., DOI: 10.1021/nn200163w
- He D., Dorantes J. , Aranda J., Waite TD., (2012), **Silver nanoparticle-algae interactions: oxidative dissolution, reactive oxygen species generation and synergistic toxic effects**, Environ Sci Technol, doi: 10.1021/es300588a
- Hooper L., (2015), **Epithelial cell contributions to intestinal immunity**, Adv Immunol., doi: 10.1016/bs.ai.2014.11.003

- Hsiao IL., Hsieh YK., Wang CF., Chen IC., Huang YJ., (2015), **Trojan-horse mechanism in the cellular uptake of silver nanoparticles verified by direct intra- and extracellular silver speciation analysis**, Environ Sci Technol, doi: 10.1021/es504705p
- Hsin Y.H., Chen C.F., Huang S., Shih T.S., Lai P.S., Chueh P.J.,(2008), **The apoptotic effect of nanosilver is mediated by a ROS- and JNK-dependent mechanism involving the mitochondrial pathway in NIH3T 3 cells**, Toxicol. Lett. 179, doi: 10.1016/j.toxlet.2008.04.015.
- Hu B., Liu X., Zhang C., Zeng X., (2017), **Food macromolecule based nanodelivery systems for enhancing the bioavailability of polyphenols**, J Food Drug Anal, doi: 10.1016/j.jfda.2016.11.004
- Huang, Y., Chen, S., Bing, X., Gao, C., Wang, T., and Yuan, B. (2011), **Nanosilver migrated into food-simulating solutions from commercially available food fresh containers**. Packaging Technology and Science 24, 291-297.
- Imhoff BR., Hansen JM., (2010), **Tert-butylhydroquinone induces mitochondrial oxidative stress causing Nrf2 activation**, Cell Biol Toxicol, doi: 10.1007/s10565-010-9162-6. Epub 2010 Apr 29.
- Jarak I., Carrola J., Barros AS., Gil AM., Pereira ML., Corvo ML., Duarte IF., (2017), **From the Cover: Metabolism Modulation in Different Organs by Silver Nanoparticles: An NMR Metabolomics Study of a Mouse Model.**, Toxicol Sci, doi: 10.1093/toxsci/kfx142
- Javurek A., Suresh D., Spollen WG., Hart M., Hansen SA., Ellersieck M., Bivens N., Givan S., Upendran A., Kannan R., Rosenfeld C., (2017), **Gut Dysbiosis and Neurobehavioral Alterations in Rats Exposed to Silver Nanoparticles**, Scientific Reportsvolume 7, doi:10.1038/s41598-017-02880-0
- Joo M., Kim KH., (2015), **p47phox, a subunit of NADPH oxidase, enhances the function of Nrf2 (INM1P.441)**, The Journal of Immunology, On line: http://www.jimmunol.org/content/194/1_Supplement/56.18
- Kang SJ., Ryoo IG., Lee YJ., Kwak MK., (2012a), **Role of the Nrf2-heme oxygenase-1 pathway in silver nanoparticle-mediated cytotoxicity**, Toxicol Appl Pharmacol, doi: 10.1016/j.taap.2011.10.011.
- Kang SJ., Lee YJ., Lee EK., Kwak MK., (2012b), **Silver nanoparticles-mediated G2/M cycle arrest of renal epithelial cells is associated with NRF2-GSH signalling**, Toxicol Lett, doi: 10.1016/j.toxlet.2012.04.016
- Kansanen E., Kuosmanen SM., Leinonen H., Levonen AL., (2013), **The Keap1-Nrf2 pathway: Mechanisms of activation and dysregulation in cancer**, Redox Biol, doi: 10.1016/j.redox.2012.10.001
- Katouzian I., Jafari S., (2016), **Nano-encapsulation as a promising approach for targeted delivery and controlled release of vitamins**, Trends in Food Science & Technology Volume 53, Pages 34-48, DOI: 10.1016/j.tifs.2016.05.002
- Kim S., Ryu DY., (2013), **Silver nanoparticle-induced oxidative stress, genotoxicity and apoptosis in cultured cells and animal tissues**, J Appl Toxicol., doi: 10.1002/jat.2792
- Kobayashi E., Suzuki T., Yamamoto M., (2013), **Roles Nrf2 Plays in Myeloid Cells and Related Disorders**, Oxidative Medicine and Cellular Longevity Volume 2013 (2013), Article ID 529219, 7 pages, http://dx.doi.org/10.1155/2013/529219

- Köser J., Engelke M., Hoppe M., Nogowski A., Filsera J., Thöminga J., (2017), **Predictability of silver nanoparticle speciation and toxicity in ecotoxicological media**, Environmental Science: Nano, DOI:10.1039/C7EN00026J
- Krejsa CM., Franklin CC., White CC., Ledbetter JA., Schieven GL., Kavanagh TJ., (2010), **Rapid activation of glutamate cysteine ligase following oxidative stress**, J Biol Chem, doi: 10.1074/jbc.M110.116210
- Lanone S., Boczkowski J., (2010), **Les sources de nanoparticules**. Rev. Fr. Allergol. 50, 211–213. doi:10.1016/j.reval.2010.01.039
- Leonard F., Collnot EM., Lehr CM., (2010), **A three-dimensional coculture of enterocytes, monocytes and dendritic cells to model inflamed intestinal mucosa in vitro,** Mol Pharm, doi: 10.1021/mp1000795
- Leydecker S. (2012), **Hello Nanomaterials – Towards Cultural (R)Evolution**, WordPress.com, On line: https://materialsblog.com/2012/05/29/nanomaterials-towards-cultural-revolution/
- Li Y., Qin T., Ingle T., Yan J., He W., Yin J., (2017), **Differential genotoxicity mechanisms of silver nanoparticles and silver ions**, Arch Toxicol, doi: 10.1007/s00204-016-1730-y
- Liu, J., Sonshine, D.A., Shervani, S., and Hurt, R.H., (2010), **Controlled release of biologically active silver from nanosilver surfaces**. ACS Nano 4, 6903-6913.
- Loboda A., Damulewicz M., Pyza E., Jozkowicz A., & Dulak J., (2016), **Role of Nrf2/HO-1 system in development, oxidative stress response and diseases: an evolutionarily conserved mechanism.** Cellular and Molecular Life Sciences, PMCID: PMC4967105
- Luescher S., Urmann C., Butterweck V., (2017), **Effect of Hops Derived Prenylated Phenols on TNF-α Induced Barrier Dysfunction in Intestinal Epithelial Cells.**, J Nat Prod, doi: 10.1021/acs.jnatprod.6b00869
- Mahler GJ., Shuler ML., Glahn RP., (2009), **Characterization of Caco-2 and HT29-MTX cocultures in an *in vitro* digestion/cell culture model used to predict iron bioavailability**, J Nutr Biochem, doi: 10.1016/j.jnutbio.2008.05.006
- Mao BH., Chen ZY., Wang YJ., Yan SJ., (2018), **Silver nanoparticles have lethal and sublethal adverse effects on development and longevity by inducing ROS-mediated stress responses**, Scientific Reportsvolume 8, doi:10.1038/s41598-018-20728-z
- Marieb EN, (2001), **Human Anatomy and Physiology** (The Benjamin/Cummings Series in the Life Sciences) 5th ed, ISBN-13: 978-0805342819
- Martirosyan A., Bazes A., Schneider YJ., (2014), **In vitro toxicity assessment of silver nanoparticles in the presence of phenolic compounds--preventive agents against the harmful effect?**, Nanotoxicology, doi: 10.3109/17435390.2013.812258
- Martirosyan A., Schneider Y.J., (2014), **Engineered nanomaterials in food: implications for food safety and consumer health.** International Journal of Environmental Research and Publich Health 11, 5720-5750.
- Massarsky A., Abrahama R., Nguyen KC., Rippstein , Tayabali AF., *et al.*, (2014), **Nanosilver cytotoxicity in rainbow trout (Oncorhynchus mykiss) erythrocytes and hepatocytes**, Comparative Biochemistry and Physiology Part C: Toxicology & Pharmacology, https://doi.org/10.1016/j.cbpc.2013.09.008
- Massart I., (2016), **Master's thesis : Etude de l'effet des nanoparticules d'argent et des ions argent sur l'inflammation dans un modèle *in vitro* de la barrière intestinale**.

- McShan D., Ray PC., Yu H., (2014), **Molecular toxicity mechanism of nanosilver**, J Food Drug Anal, doi: 10.1016/j.jfda.2014.01.010
- Miura N., Shinohara Y., (2009), **Cytotoxic effect and apoptosis induction by silver nanoparticles in HeLa cells,** Biochemical and Biophysical Research Communications, 390(3), 733-737, 2009, https://doi.org/10.1016/j.bbrc.2009.10.039
- Nel, A., T. Xia, L. Madler and N. Li., (2006), **Toxic potential of materials at the nanolevel**, Science 311(5761): 622-627.
- Nishanth RP., Jyotsna RG., Schlager JJ., Hussain SM., Reddanna P., (2011**), Inflammatory responses of RAW 264.7 macrophages upon exposure to nanoparticles: role of ROS-NFκB signalling pathway**, Nanotoxicology, doi: 10.3109/17435390.2010.541604
- No JH., Kim YB., Song YS., (2014), **Targeting Nrf2 Signalling to Combat Chemoresistance**, J Cancer Prev, doi: 10.15430/JCP.2014.19.2.111
- Osakwe O., (2016), **Preclinical *In Vitro* Studies: Development and Applicability, In book: Social Aspects of Drug Discovery, Development and Commercialization**, pp.129-148, DOI: 10.1016/B978-0-12-802220-7.00006-5
- Ostermeyer AK., Kostigen K., Semprini L, Radniecki T., (2013), **Influence of Bovine Serum Albumin and Alginate on Silver Nanoparticle Dissolution and Toxicity to Nitrosomonas europaea**, Environmental Science & Technology, DOI: 10.1021/es4033106
- Park M., Neigh A., Vermeulen J., de la Fonteyne L., Verharen H., Briede J., Loveren H. and Jong W.,(2011), **The effect of particle size on the cytotoxicity, inflammation, developmental toxicity and genotoxicity of silver nanoparticles**, Biomaterials 9810-9817.
- Park, E.J., Yi, J., Kim, Y., Choi, K., and Park, K., (2010), **Silver nanoparticles induce cytotoxicity by a Trojan-horse type mechanism**. Toxicology *in Vitro* 24, 872-878.
- Pelaseyed T., Bergström JH., Gustafsson JK., Ermund A., Birchenough GM., Schütte A., van der Post S., Svensson F., Rodríguez-Piñeiro AM., Nyström EE., Wising C., Johansson ME., Hansson GC., (2014), **The mucus and mucins of the goblet cells and enterocytes provide the first defence line of the gastrointestinal tract and interact with the immune system**, Immunol Rev, doi: 10.1111/imr.12182
- Piao MJ., Kang KA., Lee IK., Kim HS., Kim S., Choi JY., Choi J., Hyun JW., (2011a), **Silver nanoparticles induce oxidative cell damage in human liver cells through inhibition of reduced glutathione and induction of mitochondria-involved apoptosis**. Toxicol. Lett. 201: 92–100., doi: 10.1016/j.toxlet.2010
- Piao MJ., Kim KC., Choi JY., Choi J., Hyun JW., (2011b) **Silver nanoparticles down-regulate Nrf2-mediated 8-oxoguanine DNA glycosylase 1 through inactivation of extracellular regulated kinase and protein kinase B in human Chang liver cells**, Toxicol Lett, doi: 10.1016/j.toxlet.2011.09.002
- Pinto M., Robine-Léon S., Appay M.-D., Kedinger M., Triado, N., Dussaulx E., Lacroix B., Simon-Assmann P., Haffen K., Fogh J., (1983), **Enterocyte-like differentiation and polarization of the human colon carcinoma cell line Caco-2 in culture**. Biol. Cell 47, 323–330.
- Posgai R., Cipolla-Mcculloch CB., Murphy KR., Hussain SM., Rowe JJ., Nielsen M., (2011), **Differential toxicity of silver and titanium dioxide nanoparticles on Drosophila melanogaster development, reproductive effort, and viability: size, coatings and antioxidants matter**. Chemosphere 85:34–42, DOI: 10.1016/j.chemosphere.2011.06.040

- Powell J., Faria N., Thomas-McKay E., Pele L., (2010), **Origin and fate of dietary nanoparticles and microparticles in the gastrointestinal tract**, Journal of Autoimmunity, 226-233.
- Prasad RY., Mcgee JK., Killius MG., Suarez DA., Blackman CF., DeMarini DM., Simmons SO., (2013) **Investigating oxidative stress and inflammatory responses elicited by silver nanoparticles using high-throughput reporter genes in HepG2 cells: Effect of size, surface coating, and intracellular uptake**. Toxicol. *in Vitro*;27:2013–2021. doi: 10.1016/j.tiv.2013.07.005
- Project on Emerging Nanotechnologies, (2013), **Consumer Products Inventory**. Retrieved [15/08/27], from http://www.nanotechproject.org/cpi
- Qin W., Guan D., Ma R., Yang R., Xing G., Shi H., Tang G., Li J., Lv H., Jiang Y1, (2017), **Effects of trigonelline inhibition of the Nrf2 transcription factor in vitro on Echinococcus granulosus.**, Acta Biochim Biophys Sin, doi: 10.1093/abbs/gmx067
- Rauscher H., Roebben G., Valeria A., Boix A., Calzolai L., Emons H., Gaillard C., Gibson N., Linsinger T., Mech A., Rasmussen K., Sokull-Klüttgen B, Stamm H., (2014), **Towards a review of the EC Recommendation for a definition of the term "nanomaterial",** Part 1: Compilation of information concerning the experience with the definition, JRC Scientific and Policy Report, European Commission doi:10.2788/36237
- Raven, P., G. Johnson, J. Losos and K. Mason, (2014), Biologie. Bruxelles, De Boeck.

- Ravindhranath K., Ramamoorty M., (2017), **Nano aluminum oxides as adsorbents in water remediation methods: A review**, Journal of Chemistry, DOI: 10.7324/RJC.2017.1031762
- Reidy B., Haase A., Luch A., Dawson KA., Lynch I., (2013), **Mechanisms of Silver Nanoparticle Release, Transformation and Toxicity: A Critical Review of Current Knowledge and Recommendations for Future Studies and Applications**, Materials (Basel), doi: 10.3390/ma6062295
- Reuter S., Gupta SC., Chaturvedi MM., Aggarwal BB., (2010), Oxidative stress, inflammation, and cancer: how are they linked? Free Radical Biol Med 49:1603–16
- Ribeiro M., Maria V., Fordsmand J., Amorim M., (2015), **Oxidative Stress Mechanisms Caused by Ag Nanoparticles (NM300K) are Different from Those of AgNO3: Effects in the Soil Invertebrate Enchytraeus crypticus**, Int J Environ Res Public Health, doi: 10.3390/ijerph120809589
- Roger D., Hagen T., (2016), **Nanotechnologies in Food Packaging: an Exploratory Appraisal of Safety and Regulation**, Food Standards Australia New Zealand, On line: http://www.foodstandards.gov.au/publications/Pages/Nanotechnologies-in-Food-Packaging-an-Exploratory-Appraisal-of-Safety-and-Regulation.aspx
- Sambuy Y., De Angelis I., Ranaldi G., Scarino ML., Stammati A., Zucco F., (2005), **The Caco-2 cell line as a model of the intestinal barrier: influence of cell and culture-related factors on Caco-2 cell functional characteristics**, Cell Biol Toxicol., DOI: 10.1007/s10565-005-0085-6
- Satapathy SR. et al., (2013), **Silver-based nanoparticles induce apoptosis in human colon cancer cells mediated through p53**. Nanomedicine (Lond) 8:1307–1322, DOI: 10.2217/nnm.12.176
- SCENIHR (Scientific Committee on Emerging and Newly Identified Health Risks), (2009), Risk **Assessment of Products of Nanotechnologies**, European Commission, On line : http://ec.europa.eu/health/ph_risk/committees/04_scenihr/docs/scenihr_mi_026.pdf

- Sekhon B. S., (2010), **Food nanotechnology – an overview**, Nanotechnology, Science and Applications, 3, 1–15, PMCID: PMC3781769
- Shahan T., (2012), **7 Amazing Ways Animals Use Nanotechnology**, discover magazine. On line: http://discovermagazine.com/galleries/zen-photo/a/amazing-animal-nanostructures
- Shen Y., Zhou M., Yan J., Gong Z., Xiao Y., Zhang C., Du P., Chen Y., (2017), **miR-200b inhibits TNF-α-induced IL-8 secretion and tight junction disruption of intestinal epithelial cells in vitro.**, Am J Physiol Gastrointest Liver Physiol, doi: 10.1152/ajpgi.00316.2016
- Sheng XJ., Tu HJ., Chien WL., Kang KH., Lu DH., Liou HH., Lee MJ., Fu WM., (2017), **Antagonism of proteasome inhibitor-induced heme oxygenase-1 expression by PINK1 mutation**, PLoS One, doi: 10.1371/journal.pone.0183076
- Shroyer N., Kocoshis S., (2011), **Anatomy and Physiology of the Small and Large Intestines, In book: Pediatric Gastrointestinal and Liver Disease**, pp.324-336.e2, DOI: 10.1016/B978-1-4377-0774-8.10031-4
- Siegel D., Kepa JK., Ross D., (2012), **NAD(P)H:Quinone Oxidoreductase 1 (NQO1) Localizes to the Mitotic Spindle in Human Cells**, https://doi.org/10.1371/journal.pone.0044861
- Sillapawattana P., Gruhlke M., Schäffer A., (2016), **Effect of silver nanoparticles on the standard soil arthropod Folsomia candida (Collembola) and the eukaryote model organism Saccharomyces cerevisiae**, Environ Sci Eur, DOI 10.1186/s12302-016-0095-4
- Singh A., Venkannagari S., Kyu HO., Zhang YQ., et al., (2016), **Small molecule inhibitor of NRF2 selectively intervenes therapeutic resistance in KEAP1-deficient NSCLC tumors**, ACS Chem Biol, doi: 10.1021/acschembio.6b00651
- Sinha K., Das J., Pal PB., Sil PC., (2013), **Oxidative stress: the mitochondria-dependent and mitochondria-independent pathways of apoptosis**, Arch Toxicol, doi: 10.1007/s00204-013-1034-4
- Skalska M., Mack H., Massa H., Cripps A., Weinstein S., Gillis D., (2010), **Advantages and limitations of using Caco-2 cells for *in vitro* M cell model**, Griffith university, On line: http://hdl.handle.net/10072/41973
- Smita S., Gupta S., Bartonova A., Dusinska M., Gutleb A., Rahman Q. (2012), **Nanoparticles in the environment: assessment using the causal diagram approach**, Environmental Health201211(Suppl 1):S13 doi : 10.1186/1476-069X-11-S1-S13
- Stępkowski T., Brzóska K., Kruszewski M., (2014), **Silver nanoparticles induced changes in the expression of NF-κB related genes are cell type specific and related to the basal activity of NF-κB**. Toxicol *in Vitro* 28:473–478, doi: 10.1016/j.tiv.2014.01.008
- StoColor Lotusan, (2018), **Self cleaning, innovative exterior paint with the Lotus-effect**, On line: http://www.sto-sea.com/en/company/innovations/sto-lotusan-/sto-color-lotusan.html
- Sun H., Chow EC., Liu S., Du Y., Pang KS.,(2008), **The Caco-2 cell monolayer:usefulness and limitations**, Expert Opin Drug Metab Toxicol, doi: 10.1517/17425255.4.4.395
- Taguchi K., Motohashi H., Yamamoto M., (2011), **Molecular mechanisms of the Keap1–Nrf2 pathway in stress response and cancer evolution**, Genes Cells, doi: 10.1111/j.1365-2443.2010.01473
- Tang J., Xiong L., Wang S., Wang J., Liu L., Li J., Yuan F., Xi T., (2009), **Distribution, translocation and accumulation of silver nanoparticles in rats.**, J Nanosci Nanotechnol, PMID: 19928170
- Trepti S., Shruti S., Pradeep K., Verinder W., (2017), **Application of Nanotechnology in Food Science: Perception and Overview**,Front Microbiol, PMCID: PMC5545585.

- Urban DA., Rodriguez L., Balog S., Kinnear C., Rothen-Rutishauser B., Petri-Fink A., (2016), **Plasmonic nanoparticles and their characterization in physiological fluids, Colloids Surf B Biointerfaces**, doi: 10.1016/j.colsurfb.2015.05.053
- Vance M., Kuiken T., Vejerano P., McGinnis S., Hochella M., Rejeski D., and Hull M., (2015), **Nanotechnology in the real world: Redeveloping the nanomaterial consumer products inventory**. Beilstein Journal of Nanotechnology *6*, 1769-1780. doi: 10.3762/bjnano.6.181.
- Vandenkerckhove J., (2015), **Master's thesis: Silver nanoparticles effects on *in vitro* intestinal inflammation.**
- Verano-Braga T., Miethling-Graff R., Wojdyla K., Rogowska-Wrzesinska A., (2014), **Insights into the cellular response triggered by silver nanoparticles using quantitative proteomics**, ACS Nano 8(3): 2161–2175, doi: 10.1021/nn4050744
- Vredenburg G., Elias NS., Venkataraman H., Hendriks DF., (2014), **Human NAD(P)H:quinone oxidoreductase 1 (NQO1)-mediated inactivation of reactive quinoneimine metabolites of diclofenac and mefenamic acid**, Chem Res Toxicol, doi: 10.1021/tx400431k
- Wardyn JD., Ponsford AH., Sanderson CM., (2015), **Dissecting molecular cross-talk between Nrf2 and NF-κB response pathways**, Biochem Soc Trans, doi: 10.1042/BST20150014
- Wilson G., Hassan I. F., Dix C. J., Williamson I., Shah R., Mackay M. And Artursson P., (1990), **Transport and permeability properties of human Caco-2 cells: an *in vitro* model of the intestinal epithelial cell barrier**. J. Controlled Release 11, 25-40.
- Wruck CJ., Streetz K., Pavic G., Götz ME., Tohidnezhad M., Brandenburg LO., Varoga D., Eickelberg O., Herdegen T., Trautwein C., Cha K., Kan YW., Pufe T., (2011), **Nrf2 Induces Interleukin-6 (IL-6) Expression via an Antioxidant Response Element within the IL-6 Promoter**, J Biol Chem, doi: 10.1074/jbc.M110.162008
- Xiaofang S., Zhanhui O. Ruochan C. Xiaohua N. , (2015), **Activation of the p62-Keap1-NRF2 pathway protects against ferroptosis in hepatocellular carcinoma cells**, Hepatobiliary Malignancies, https://doi.org/10.1002/hep.28251
- Xiong L., Xie J., Song C., Liu J., Zheng J., Liu C., Zhang X., Li P., Wang F., (2015) **The Activation of Nrf2 and Its Downstream Regulated Genes Mediates the Antioxidative Activities of Xueshuan Xinmaining Tablet in Human Umbilical Vein Endothelial Cells**, Evid Based Complement Alternat Med, doi: 10.1155/2015/187265
- Zhang X., Chen X., Song H., Chen HZ., Rovin BH., (2005), **Activation of the Nrf2/antioxidant response pathway increases IL-8 expression**, Eur J Immunol, DOI: 10.1002/eji.200526116
- Zhang XF., Shen W., Gurunathan S., (2016), **Silver Nanoparticle-Mediated Cellular Responses in Various Cell Lines: An *in Vitro* Model**, Int J Mol Sci, doi: 10.3390/ijms17101603
- Zhang XF., Liu ZG., Shen W., Gurunathan S., (2016), **Silver Nanoparticles: Synthesis, Characterization, Properties, Applications, and Therapeutic Approaches**, DOI: 10.3390/ijms17091534

Effects of silver nanoparticles on oxidative stress and Nrf2 pathway in an *in vitro* model of intestinal epithelium cells.

Presented by Audrey Leurquin

Abstract

Considering the very interesting physicochemical properties of nanomaterials, it is not surprising that during the last few years, nanomaterial applications expended exponentially. Among nanoparticles, silver nanoparticles (AgNPs) are the most commonly used in consumer products, mainly because of their antimicrobial properties. AgNPs are already incorporated in many products of the food sector such as food packaging materials, antimicrobial sprays and even dietary supplements. These applications could lead to abnormally high oral exposure for the consumer. Many authors have demonstrated AgNPs toxicity towards various biological systems. Furthermore, there is still a huge lack of knowledge concerning the mechanisms of toxicity related to AgNPs and the contribution of Ag^+ involved in AgNPs toxicity. Therefore, this work was devoted to study AgNPs and Ag^+ effects on oxidative stress and the related cellular responses. In order to do so, monocultures of Caco-2 cells were used. They are indeed a widely used *in vitro* model of the human intestinal epithelium.

First of all, the ability of AgNPs and Ag^+ to generate ROS and induce oxidative stress was evaluated by performing an NBT assay. A significant increase in ROS production was observed for both AgNPs and Ag^+ with a nano-specific effect. The second objective of this thesis was to determine the impact of AgNPs on enzymatic activity of several oxidative stress-related enzymes (CAT, GR, GP and GST). Unfortunately, we were not able to detect any significant changes in these enzymatic activities after 3h incubation with 15 µg/ml AgNPs. Thirdly, we studied the impact of AgNPs/Ag^+-induced ROS generation on Nrf2 signalling pathway by performing an ELISA quantification of HO-1, which is an Nrf2 specific gene target. Nrf2 is a major pathway involved in protecting cells from oxidative stress, through the induction of antioxidant-responsive genes. Surprisingly, we did not measure any significant effect on HO-1 production. Finally, the effect of AgNPs on inflammation was evaluated, along with the potential implication of the Nrf2 signalling pathway. Indeed, preliminary work at the lab indicated that the pro-inflammatory response related to AgNPs was not due to activation of the NF-κB pathway. The alternative Nrf2 pathway was therefore studied to explain the production of the inflammatory marker IL-8 measured by ELISA. According to our results, Nrf2 does not seem to be involved in IL-8 production following AgNPs treatments.

In conclusion, although AgNPs were not cytotoxic at the studied concentrations, we have observed an increased ROS production. Numerous studies confirm our results regarding ROS production, but in contrast to our observations, suggest the implication of the Nrf2/HO-1 signalling pathway to explain the cellular responses related to the AgNPs-induced ROS production.

Keywords: Silver nanoparticles, Caco-2 cells, Oxidative stress, Heme oxygenase-1, Nrf2 pathway, IL-8

Academic year : 2017-2018